The evolution of the precision program: from QCD to SMEFT

Radja Boughezal

Argonne National Laboratory

50 Years of Quantum Chromodynamics

UCLA, September 13, 2023

Big picture motivation

The precision program of HEP

- The ultimate goal of the precision program is to determine the Lagrangian of Nature. So far we have discovered the terms that correspond to the Standard Model.

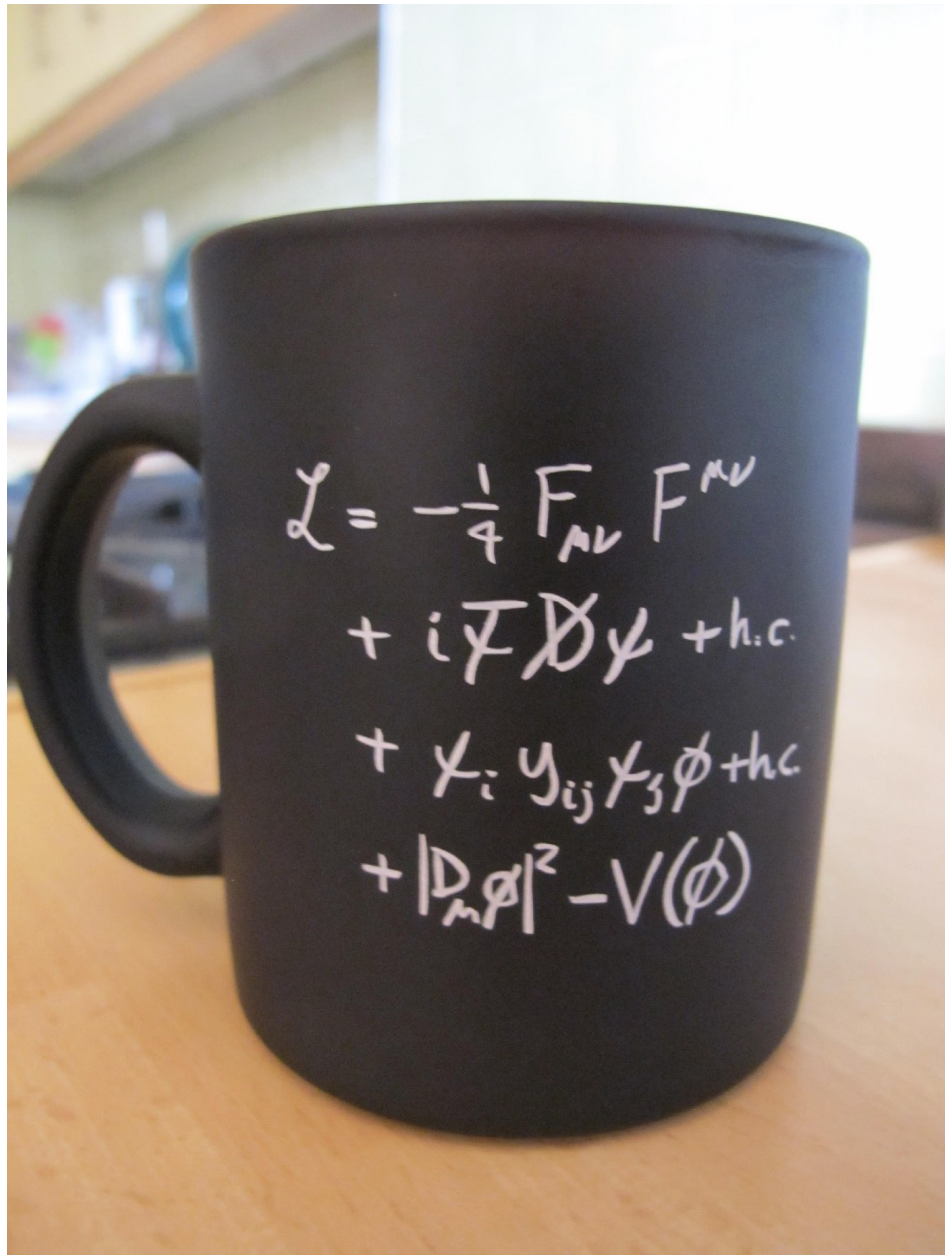

To discover anything beyond these terms that isn't obvious like a resonance peak, we need to understand what the SM predicts very well.

$$\mathcal{L}_{\text{QCD}} = -\frac{1}{4} F_{\mu\nu a} F_a^{\mu\nu} + \sum +i\bar{\psi}_i \left(i\gamma_\mu D^\mu - m_i\right) \psi_i$$

QCD plays an outsized role in this program!

The precision program of HEP

- The ultimate goal of the precision program is to determine the Lagrangian of Nature. So far we have discovered the terms that correspond to the Standard Model.

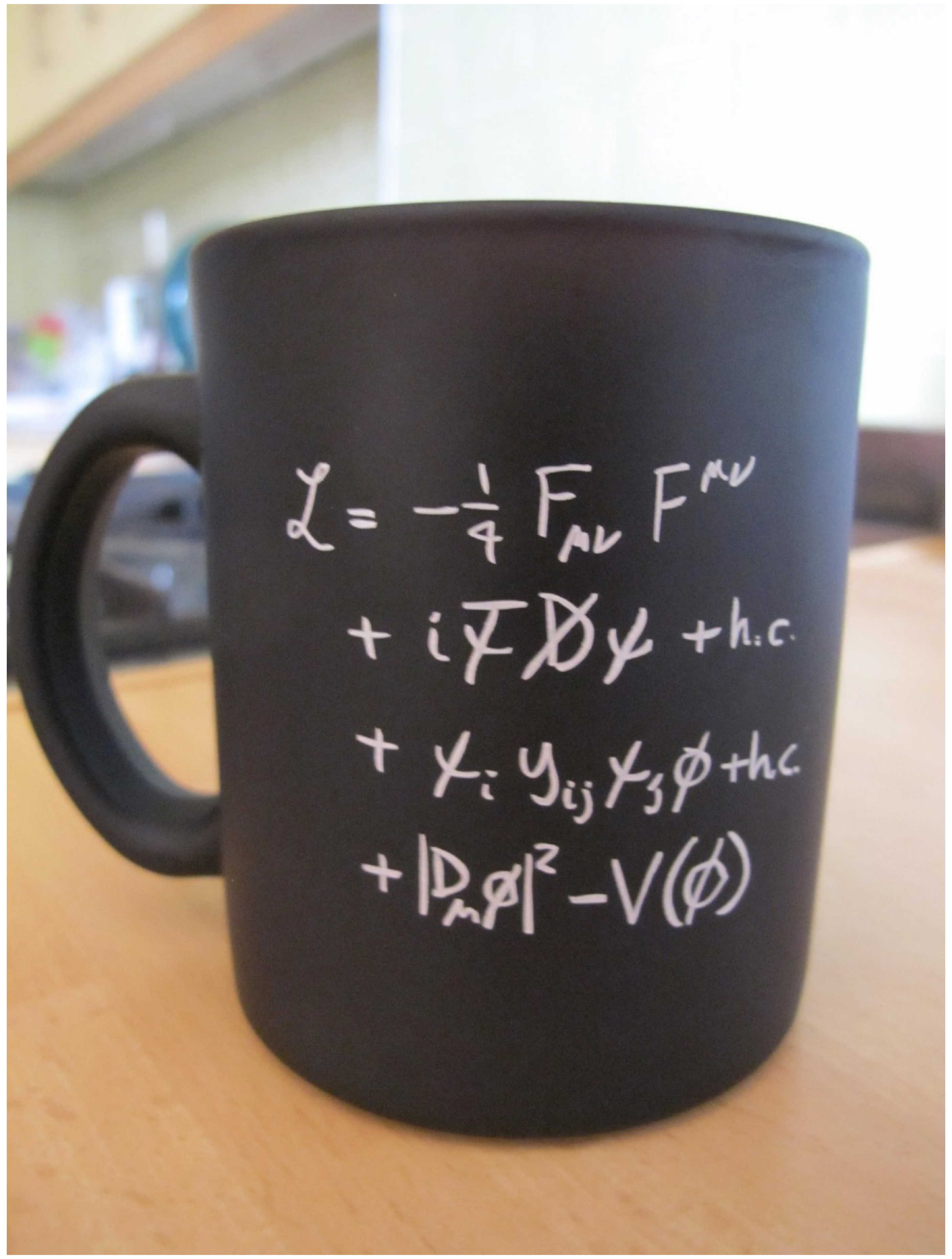

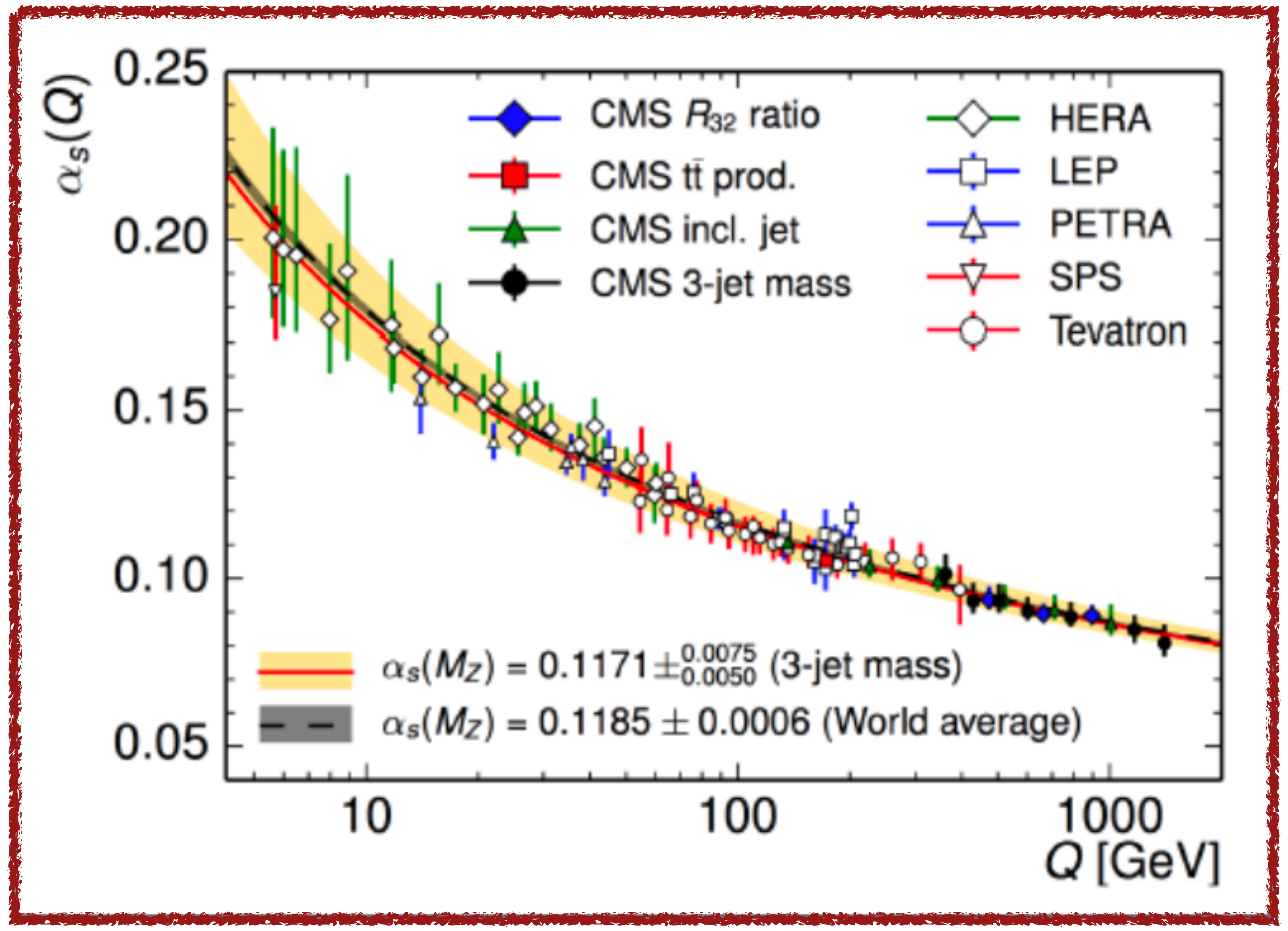

The QCD coupling constant is the strongest of the SM gauge couplings at LHC energies. Perturbative QCD corrections are typically larger than the weak and QED corrections

The precision program of HEP

- The ultimate goal of the precision program is to determine the Lagrangian of Nature. So far we have discovered the terms that correspond to the Standard Model.

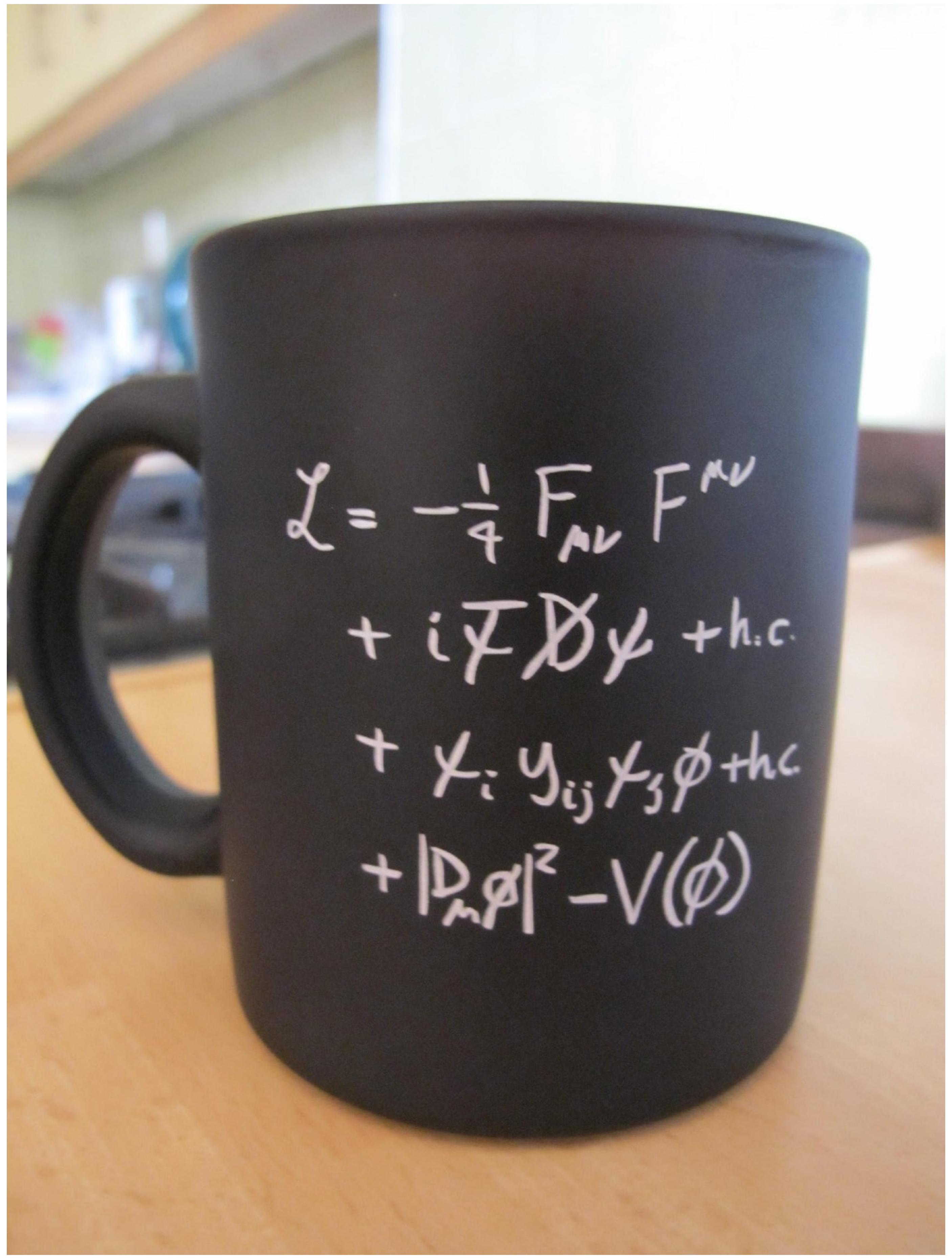

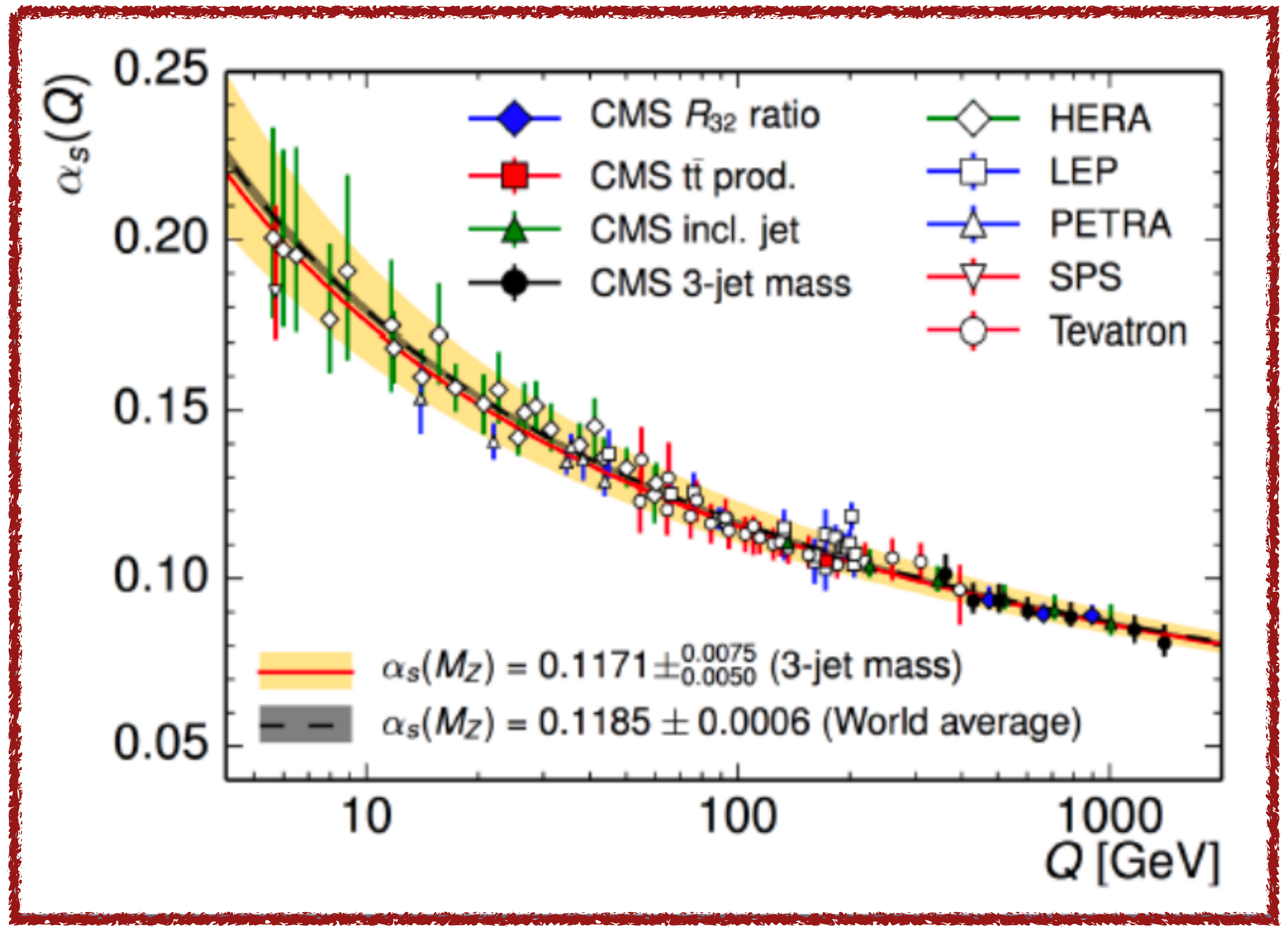

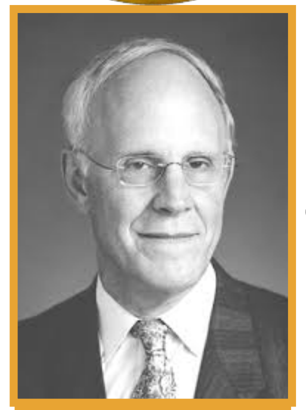
Gross


Politzer

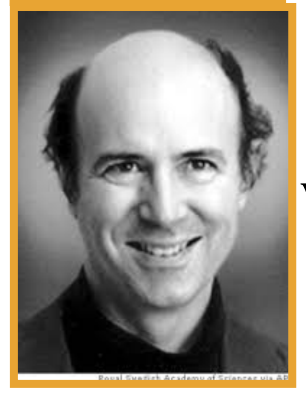
Wilczek

The QCD coupling constant is the strongest of the SM gauge couplings at LHC energies. Perturbative QCD corrections are typically larger than the weak and QED corrections

The precision program of HEP

- The ultimate goal of the precision program is to determine the Lagrangian of Nature. So far we have discovered the terms that correspond to the Standard Model.

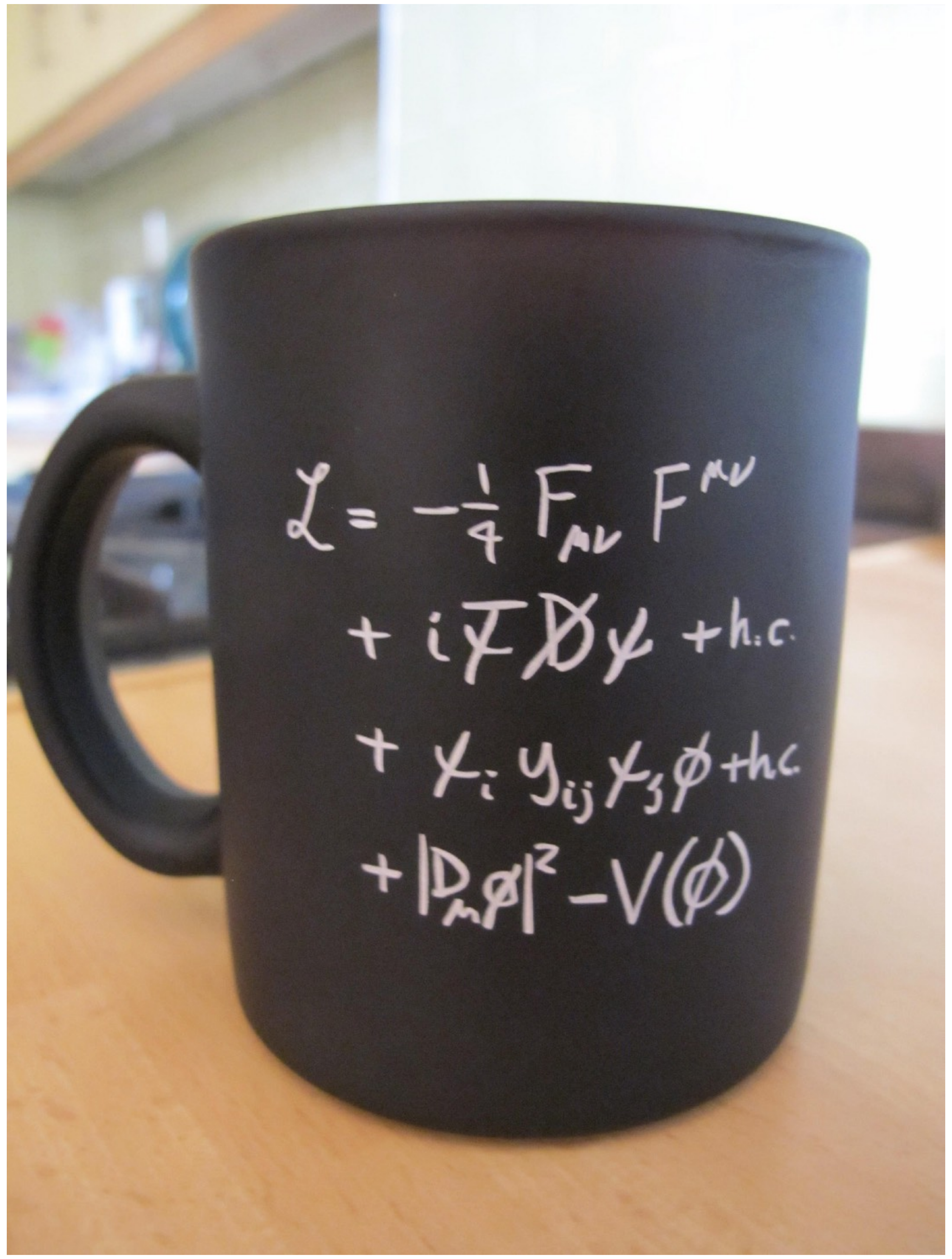

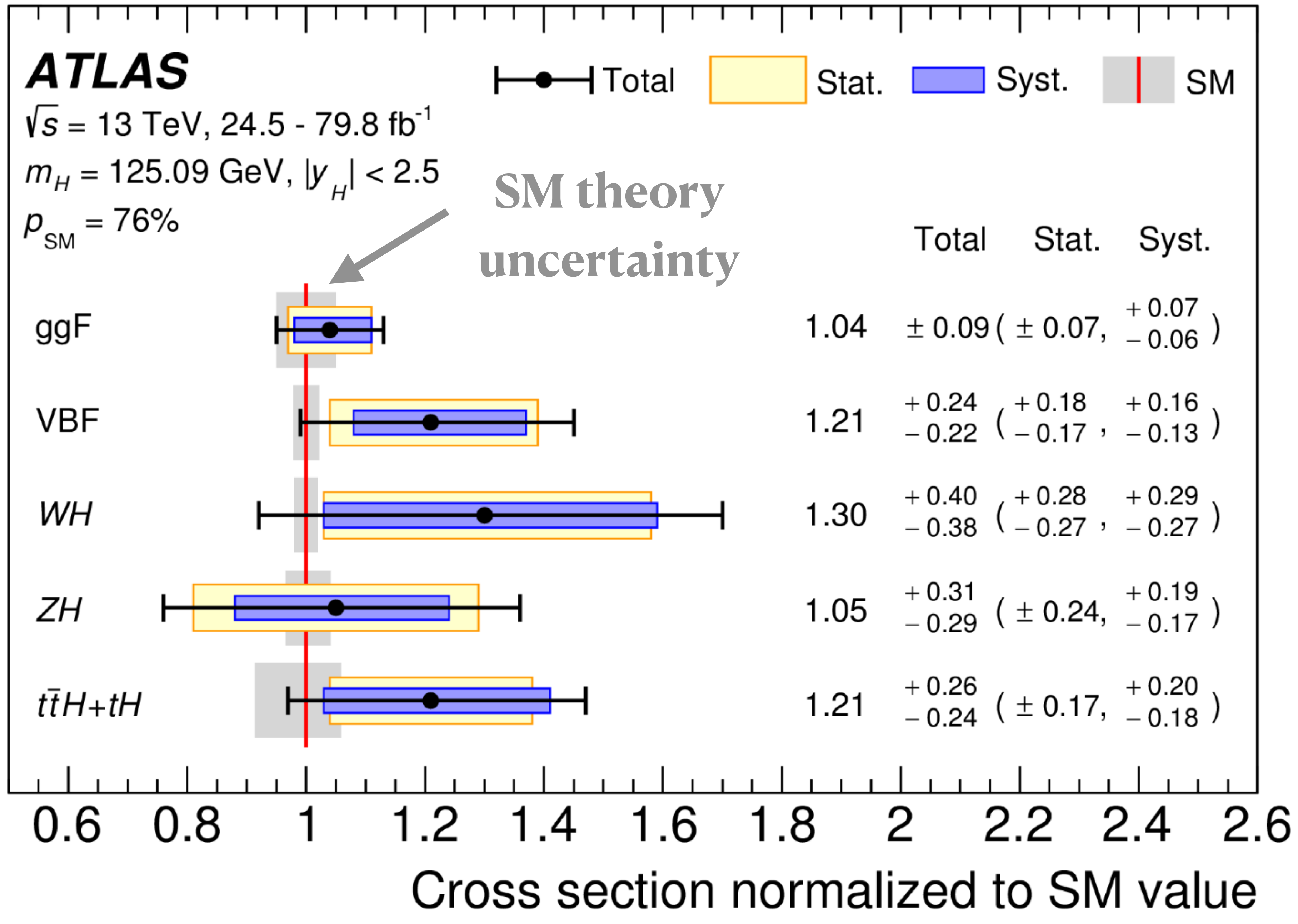

Even with N3LO pQCD predictions (Anastasiou et al (2016)) the theory uncertainties on the gluon-gluon fusion channel are significant!

The precision program of HEP

- The ultimate goal of the precision program is to determine the Lagrangian of Nature. So far we have discovered the terms that correspond to the Standard Model.

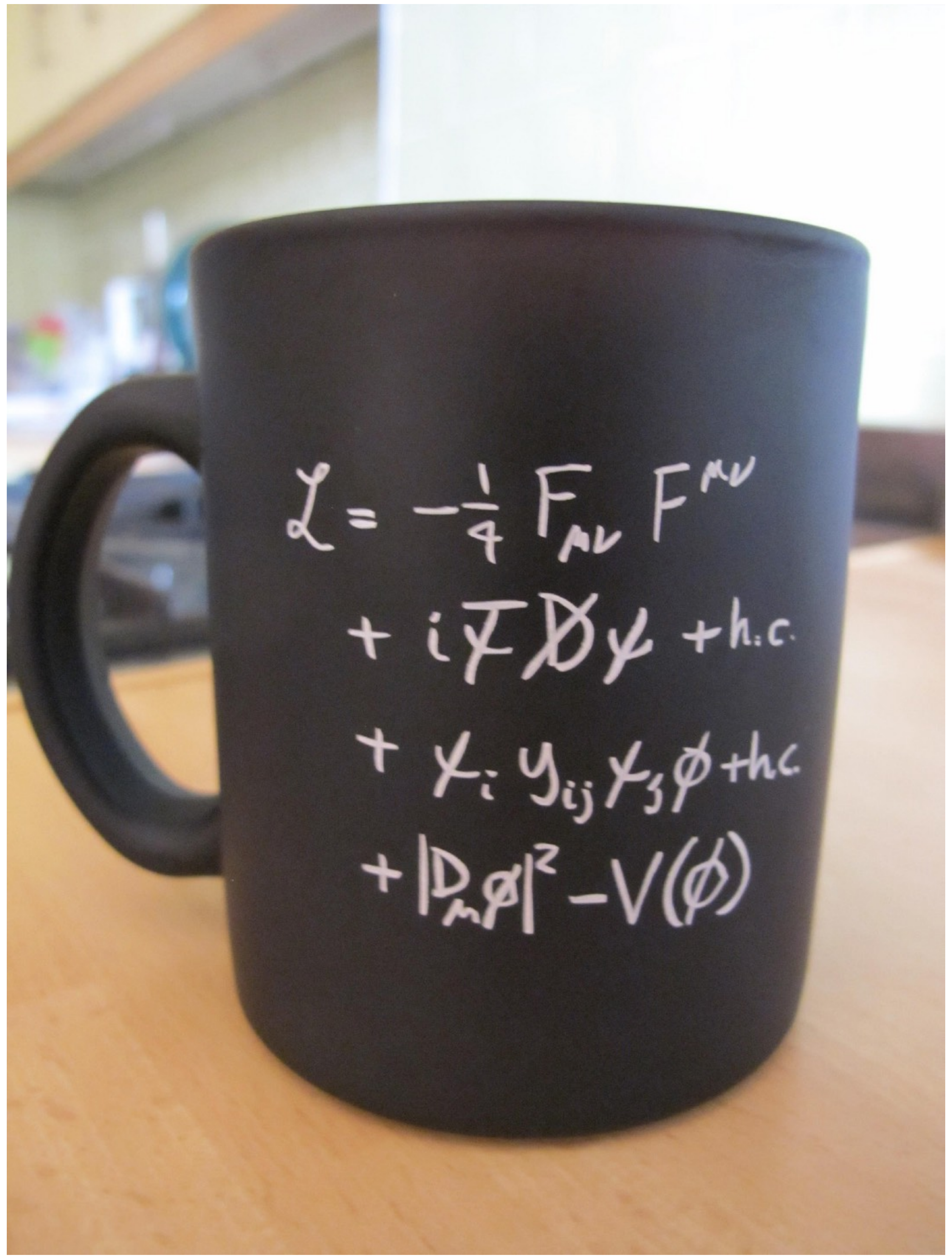

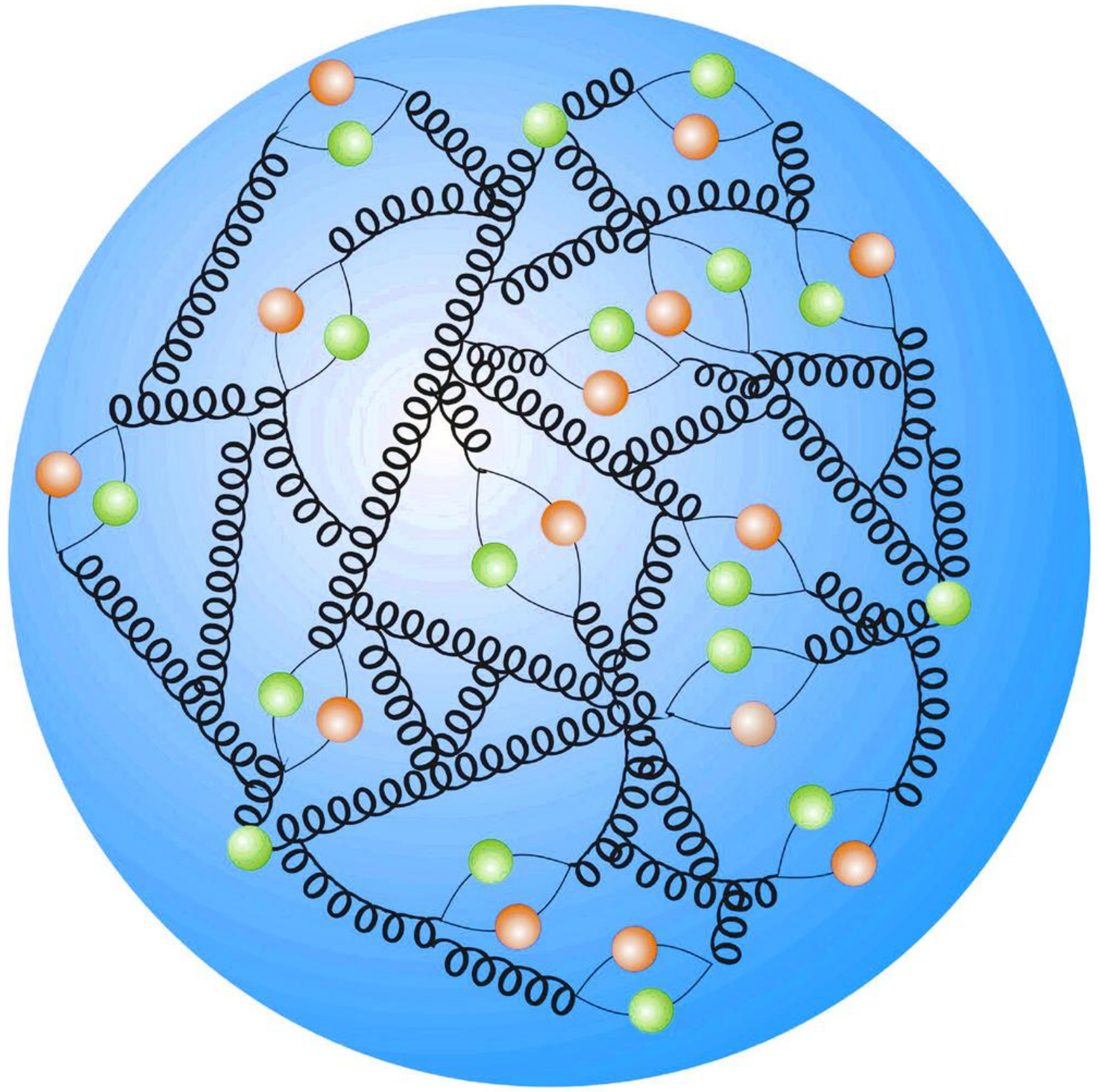

Confinement in QCD binds quarks and gluons into hadrons. Understanding the distribution of these partons in the proton through QCD is a critical component of HEP experiments.

The precision program of HEP

- The ultimate goal of the precision program is to determine the Lagrangian of Nature. So far we have discovered the terms that correspond to the Standard Model.

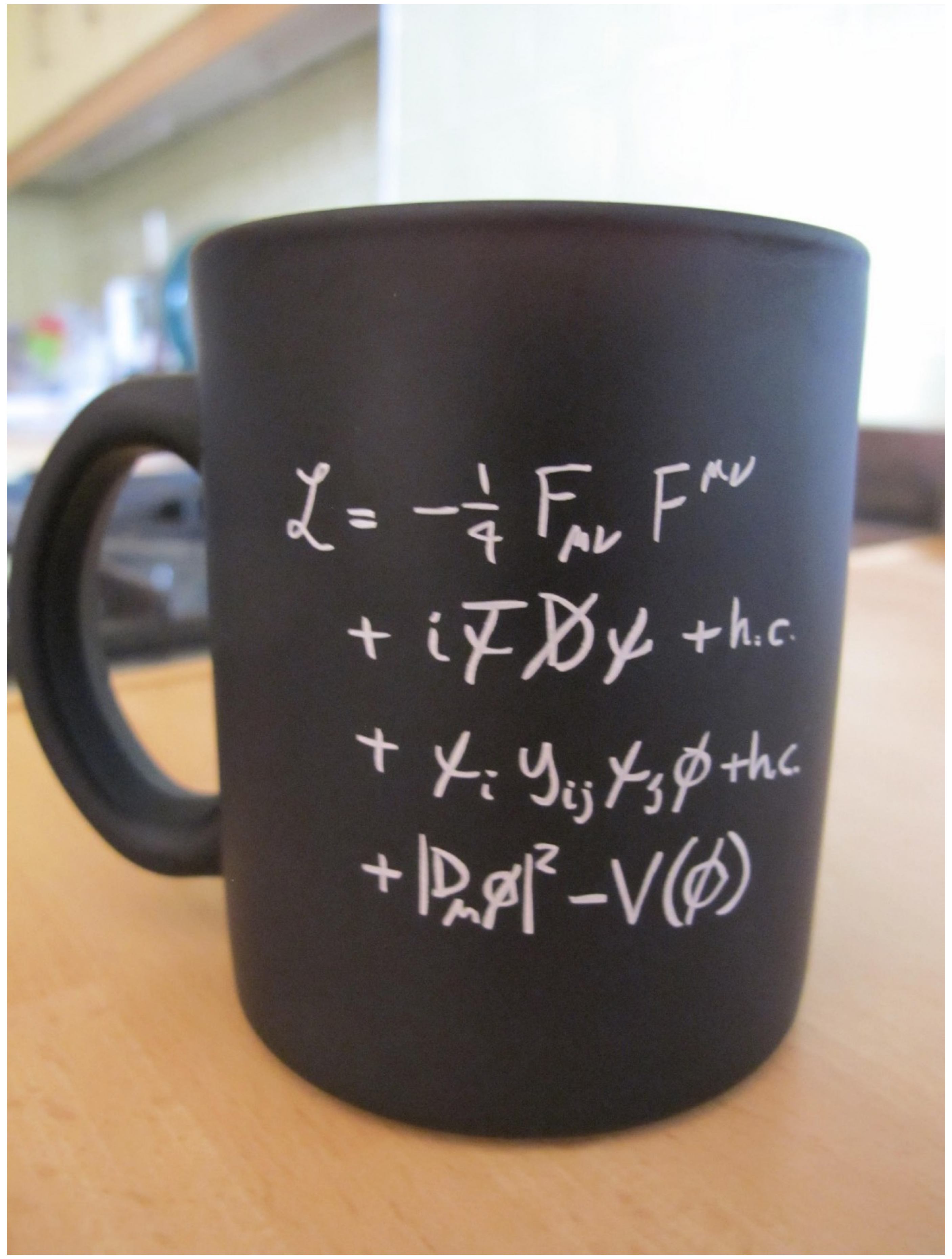

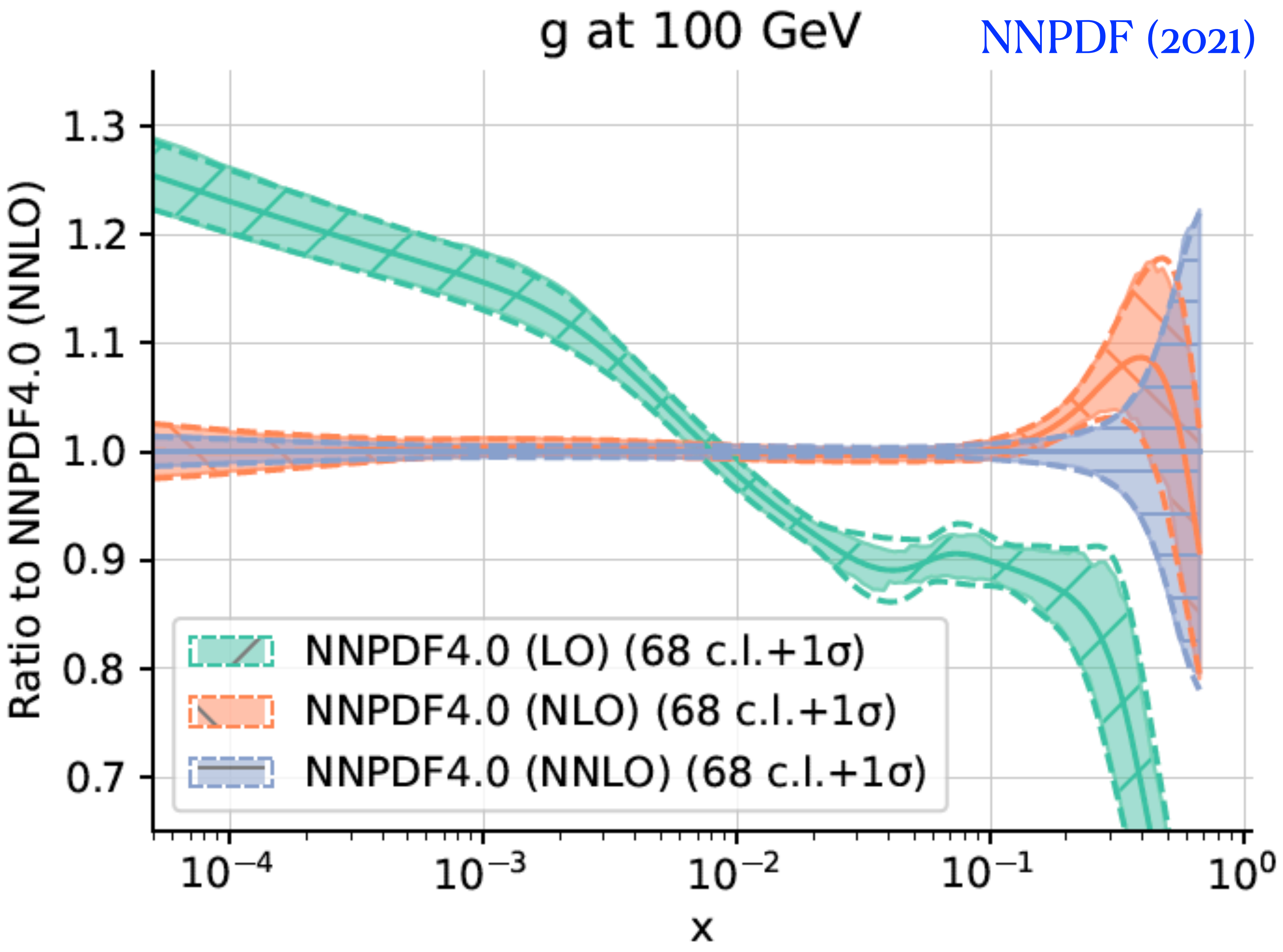

The perturbative precision of PDF extractions has an important influence on high-x parton structure and therefore new physics searches at the LHC and elsewhere.

The precision program of HEP

- The next stage is to learn what solves outstanding problems in Nature (such as dark matter, neutrino masses, the hierarchy problem) in order to add new terms to our Lagrangian. No new particles have been found so far, so the search is conveniently organized using effective field theory.

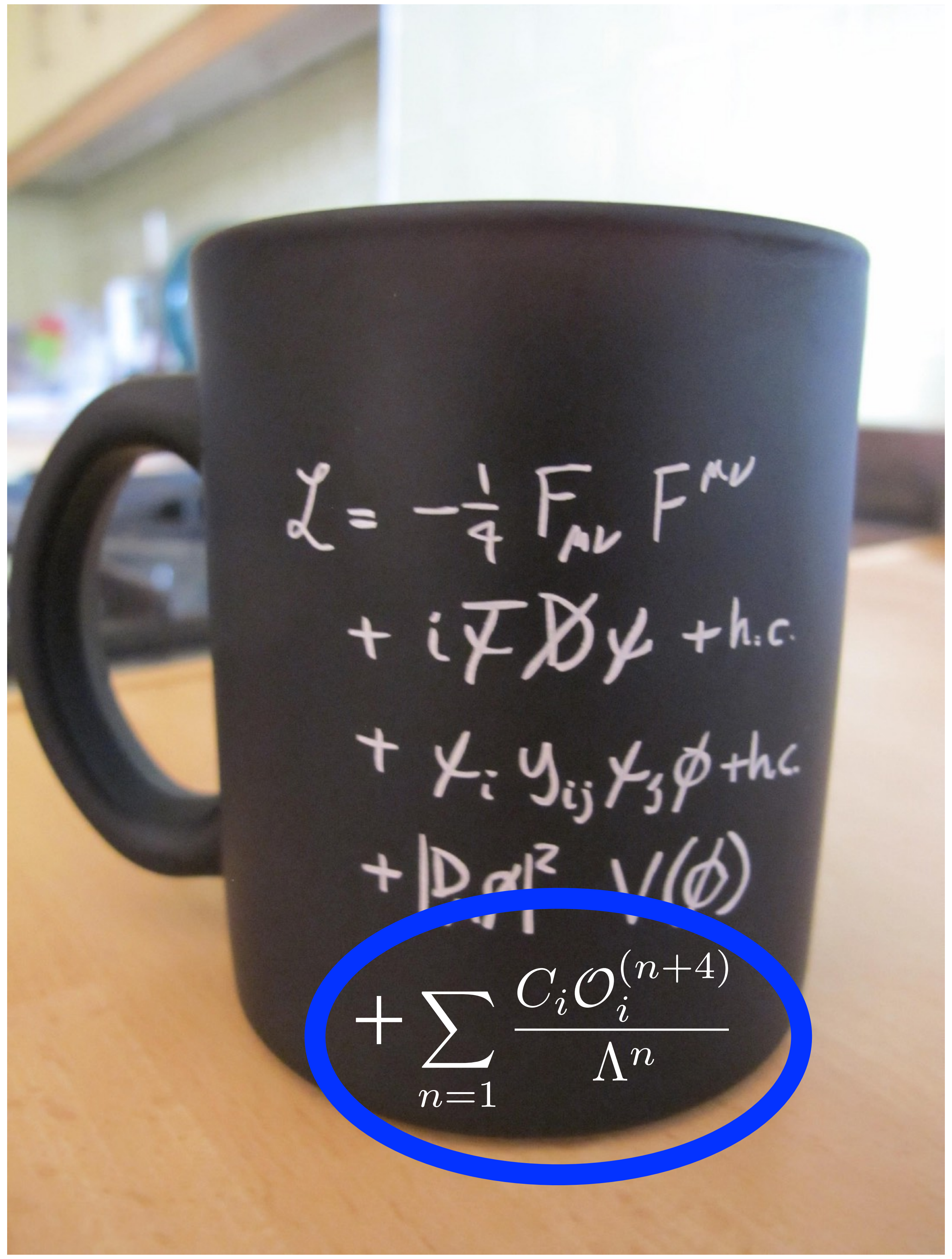

This EFT is an expansion in powers of M/Λ and E/Λ. Λ is the energy scale at which new physics appears. M denotes the SM mass scale, and E the energy of experimental measurements.

Example: $\mathcal{O}_1^{(5)} = (\bar{\tilde{L}}\phi)(\tilde{\phi}^\dagger L)$

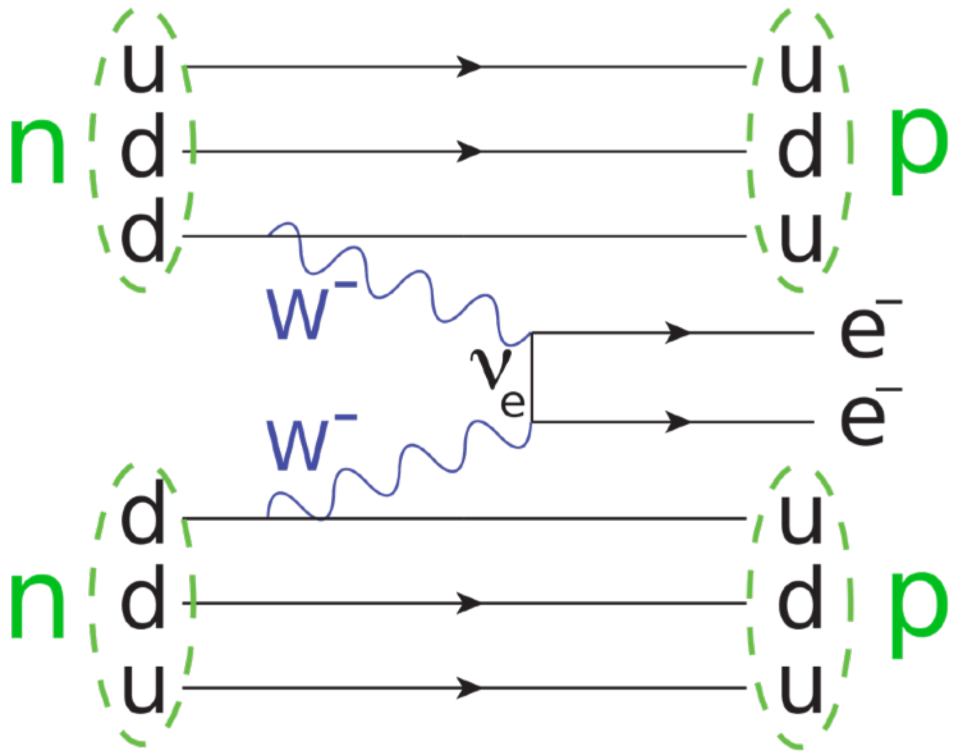

Higgs field, lepton field containing the neutrino. Accommodates neutrino masses; ***predicts*** neutrinoless double beta decay

The precision program of HEP

- The extraordinary success of the LHC and other experimental programs means that predictions in the EFT must be obtained with great precision, like in the SM, in order to properly understand the implications of experimental measurements for possible new terms in the Lagrangian of Nature.
- These considerations lead us to the goals of this talk:

> - Review briefly examples of the precision program in QCD, both its historical successes and current status. The focus will be on perturbative calculations at high orders.
> - Discuss how similar issues of higher-order calculations arise in EFT extensions of the SM, in particular the Standard Model Effective Field Theory (SMEFT).
> - Discuss open questions in the precision study of SMEFT, and summarize new ideas on how to approach them.

Precision SM: QCD in perturbation theory

The foundation: factorization in QCD

- To begin we present our formalism for computing high-precision cross sections, valid both within and beyond the SM.

factorization and renormalization scales

$$\boxed{\sigma(P_1,P_2)=\sum_{i,j}\int dx_1 dx_2 f_{i/h_1}(x_1,\mu_F^2) f_{j/h_2}(x_2,\mu_F^2)\hat{\sigma}_{ij}(p_1,p_2,\alpha_S(\mu_R),Q^2;\mu_F^2,\mu_R^2)+\mathcal{O}\left(\frac{\Lambda_{QCD}}{Q}\right)}$$

Parton distribution functions, universal, non-perturbative

Parton level cross sections, process dependent, perturbative

Power suppressed contributions

- The parton-level cross sections are model dependent but can be computed in perturbation theory. The PDFs are universal, but are non-perturbative and cannot (yet) be computed from first principles. They must be obtained from fits to data.

The foundation: factorization in QCD

- Our focus in this talk will be computing the partonic cross sections to as high an order as possible in the couplings constants (QCD, EW and BSM couplings).

$$\boxed{\hat{\sigma} = \sigma^{\text{Born}} \left(1 + \frac{\alpha_s}{2\pi} \sigma^{(1)} + \left(\frac{\alpha_s}{2\pi} \right)^2 \sigma^{(2)} + \left(\frac{\alpha_s}{2\pi} \right)^3 \sigma^{(3)} + \ldots \right)}$$

Including higher orders in the perturbative expansion improves the accuracy of our prediction, reduces the dependence on non-physical parameters such as μ_F and μ_R, and is needed for a proper description of the experimental data. At least NLO is usually required for a quantitative prediction for collider processes.

The foundation: factorization in QCD

- Our focus in this talk will be computing the partonic cross section to as high an order as possible in the couplings constants (QCD, EW and BSM couplings).

Let's review the importance of the first term, beginning with a historical example

$$\hat{\sigma} = \sigma^{\mathrm{Born}} \left(1 + \frac{\alpha_s}{2\pi} \sigma^{(1)} + \left(\frac{\alpha_s}{2\pi}\right)^2 \sigma^{(2)} + \left(\frac{\alpha_s}{2\pi}\right)^3 \sigma^{(3)} + \dots \right)$$

Including higher orders in the perturbative expansion improves the accuracy of our prediction, reduces the dependence on non-physical parameters such as μ_F and μ_R, and is needed for a proper description of the experimental data. At least NLO is usually required for a quantitative prediction for collider processes.

QCD at NLO: historical example

- An early example that illustrates the incredible importance of perturbative QCD at colliders is the Drell-Yan cross section. A comparison of di-muon invariant mass data from the NA3 experiment (proton-nucleon scattering) at CERN in 1979 showed a discrepancy from the prediction.

LO cross section obtained using old CDHS parametrization of PDFs

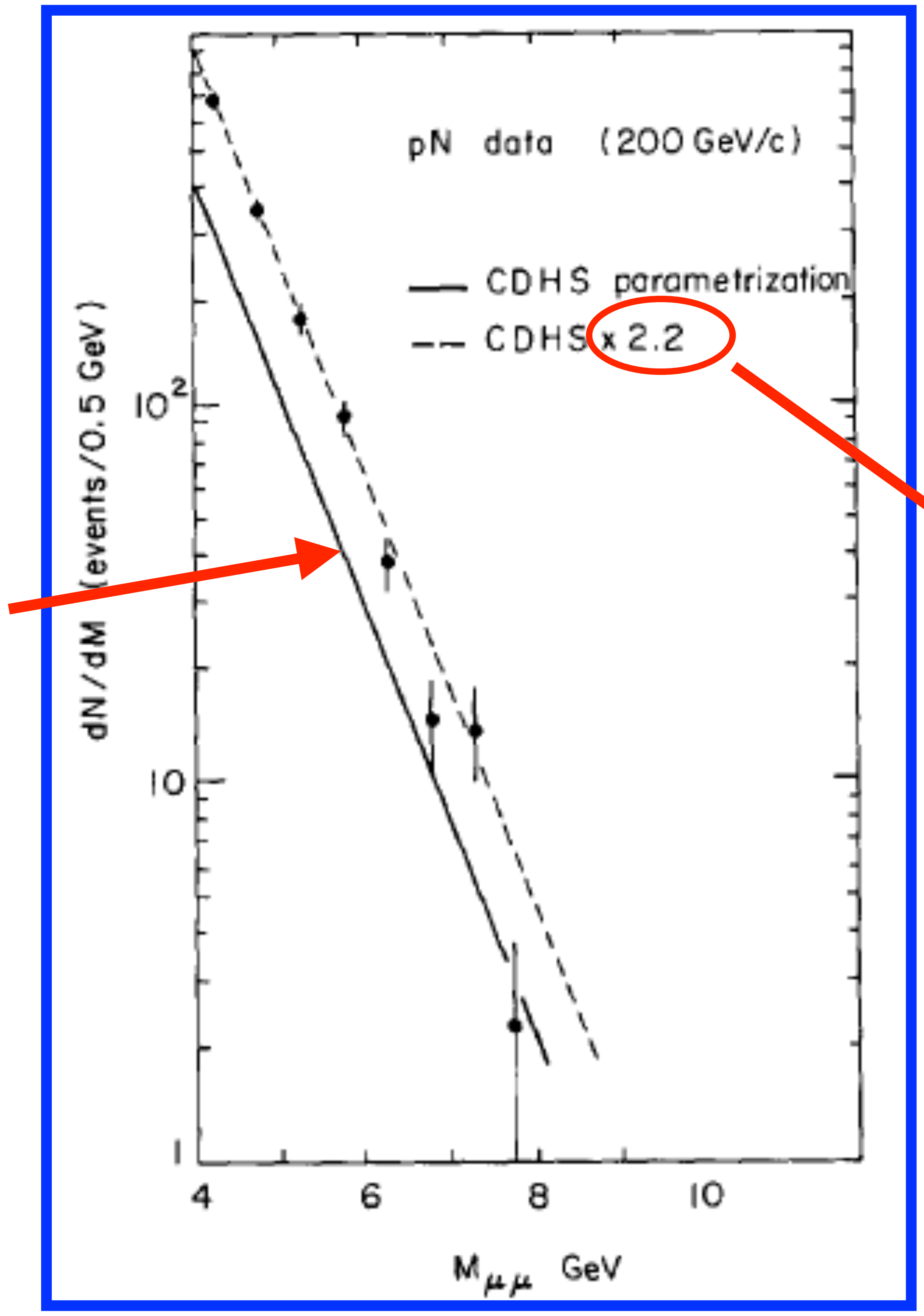

CERN/EP 79-147

In all the channels studied the experimental cross section is significantly larger by a factor of 2.3 ± 0.5 than expected

The first introduction of a “K-factor” to accommodate discrepancies between theory and data

$K = (d^2\sigma/dx_1dx_2)_{exp}/(d^2\sigma/dx_1dx_2)_{DY\ model}$.

Reaction	pN	$\bar{p}N$
K	2.2 ± 0.4	2.4 ± 0.5

QCD at NLO: historical example

- An early example that illustrates the incredible importance of perturbative QCD at colliders is the example of the Drell-Yan cross section.

TOT= sum of all partonic channels @ NLO

$\Delta\sigma =$ pure NLO coefficient

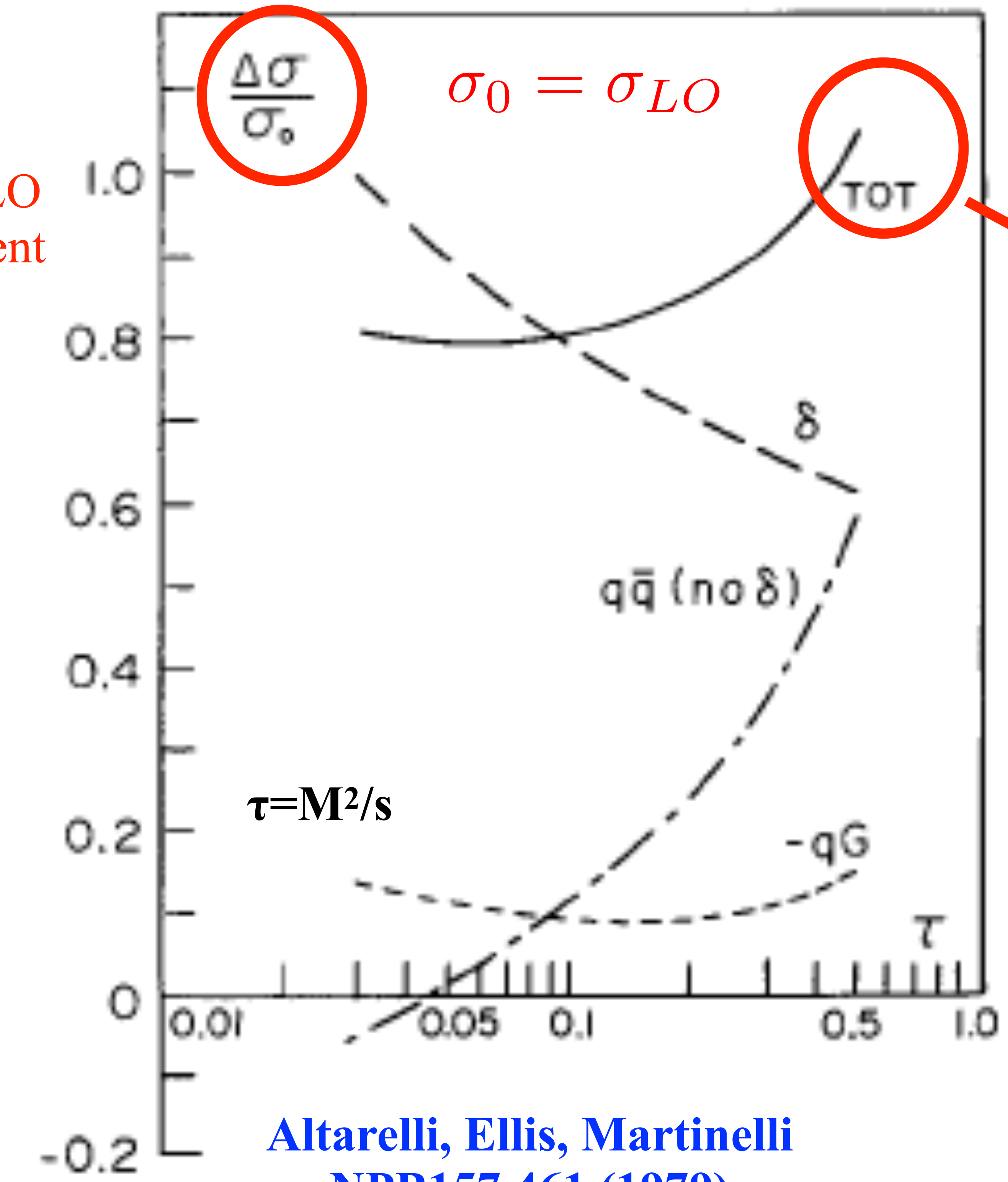

Altarelli, Ellis, Martinelli NPB157 461 (1979)

$$\Delta\sigma_{TOT}/\sigma_0 \sim 0.8 - 1.0$$

$$\sigma_{NLO} = \sigma_0 + \Delta\sigma_{TOT}$$

NLO QCD corrections reach nearly a factor of 2, greatly reducing tension between theory and experiment

Discrepancy resolved by next-to-leading order QCD!

QCD at NLO: today

- Today NLO predictions, in both QCD and EW coupling constants, are available for processes with numerous final state particles. In addition these fixed-order predictions can be combined with parton-shower Monte Carlo programs in order to resum large logarithms in soft and/or collinear regions of jet phase space.

Process		Syntax	Cross section (pb)			
Vector boson +jets			LO 13 TeV		NLO 13 TeV	
a.1	$pp \to W^{\pm}$	`p p > wpm`	$1.375 \pm 0.002 \cdot 10^5$	$^{+15.4\%}_{-16.6\%}$ $^{+2.0\%}_{-1.6\%}$	$1.773 \pm 0.007 \cdot 10^5$	$^{+5.2\%}_{-9.4\%}$ $^{+1.9\%}_{-1.6\%}$
a.2	$pp \to W^{\pm}j$	`p p > wpm j`	$2.045 \pm 0.001 \cdot 10^4$	$^{+19.7\%}_{-17.2\%}$ $^{+1.4\%}_{-1.1\%}$	$2.843 \pm 0.010 \cdot 10^4$	$^{+5.9\%}_{-8.0\%}$ $^{+1.3\%}_{-1.1\%}$
a.3	$pp \to W^{\pm}jj$	`p p > wpm j j`	$6.805 \pm 0.015 \cdot 10^3$	$^{+24.5\%}_{-18.6\%}$ $^{+0.8\%}_{-0.7\%}$	$7.786 \pm 0.030 \cdot 10^3$	$^{+2.4\%}_{-6.0\%}$ $^{+0.9\%}_{-0.8\%}$
a.4	$pp \to W^{\pm}jjj$	`p p > wpm j j j`	$1.821 \pm 0.002 \cdot 10^3$	$^{+41.0\%}_{-27.1\%}$ $^{+0.5\%}_{-0.5\%}$	$2.005 \pm 0.008 \cdot 10^3$	$^{+0.9\%}_{-6.7\%}$ $^{+0.6\%}_{-0.5\%}$
a.5	$pp \to Z$	`p p > z`	$4.248 \pm 0.005 \cdot 10^4$	$^{+14.6\%}_{-15.8\%}$ $^{+2.0\%}_{-1.6\%}$	$5.410 \pm 0.022 \cdot 10^4$	$^{+4.6\%}_{-8.6\%}$ $^{+1.9\%}_{-1.5\%}$
a.6	$pp \to Zj$	`p p > z j`	$7.209 \pm 0.005 \cdot 10^3$	$^{+19.3\%}_{-17.0\%}$ $^{+1.2\%}_{-1.0\%}$	$9.742 \pm 0.035 \cdot 10^3$	$^{+5.8\%}_{-7.8\%}$ $^{+1.2\%}_{-1.0\%}$
a.7	$pp \to Zjj$	`p p > z j j`	$2.348 \pm 0.006 \cdot 10^3$	$^{+24.3\%}_{-18.5\%}$ $^{+0.6\%}_{-0.6\%}$	$2.665 \pm 0.010 \cdot 10^3$	$^{+2.5\%}_{-6.0\%}$ $^{+0.7\%}_{-0.7\%}$
a.8	$pp \to Zjjj$	`p p > z j j j`	$6.314 \pm 0.008 \cdot 10^2$	$^{+40.8\%}_{-27.0\%}$ $^{+0.5\%}_{-0.5\%}$	$6.996 \pm 0.028 \cdot 10^2$	$^{+1.1\%}_{-6.8\%}$ $^{+0.5\%}_{-0.5\%}$
a.9	$pp \to \gamma j$	`p p > a j`	$1.964 \pm 0.001 \cdot 10^4$	$^{+31.2\%}_{-26.0\%}$ $^{+1.7\%}_{-1.8\%}$	$5.218 \pm 0.025 \cdot 10^4$	$^{+24.5\%}_{-21.4\%}$ $^{+1.4\%}_{-1.6\%}$
a.10	$pp \to \gamma jj$	`p p > a j j`	$7.815 \pm 0.008 \cdot 10^3$	$^{+32.8\%}_{-24.2\%}$ $^{+0.9\%}_{-1.2\%}$	$1.004 \pm 0.004 \cdot 10^4$	$^{+5.9\%}_{-10.9\%}$ $^{+0.8\%}_{-1.2\%}$

Alwall et al (2014)

MADGRAPH_aMC@NLO example: NLO cross sections for up to four final-state particles available with automated codes. Up to six final-state particles possible for certain processes with dedicated codes.

QCD at NLO: today

- Today NLO predictions, in both QCD and EW coupling constants, are available for processes with numerous final state particles. In addition these fixed-order predictions can be combined with parton-shower Monte Carlo programs in order to resum large logarithms in soft and/or collinear regions of jet phase space.

State-of-the-art: W+5 jets with BLACKHAT+SHERPA. Absolutely critical to control theoretical uncertainties in W+multijet production, an important SUSY background

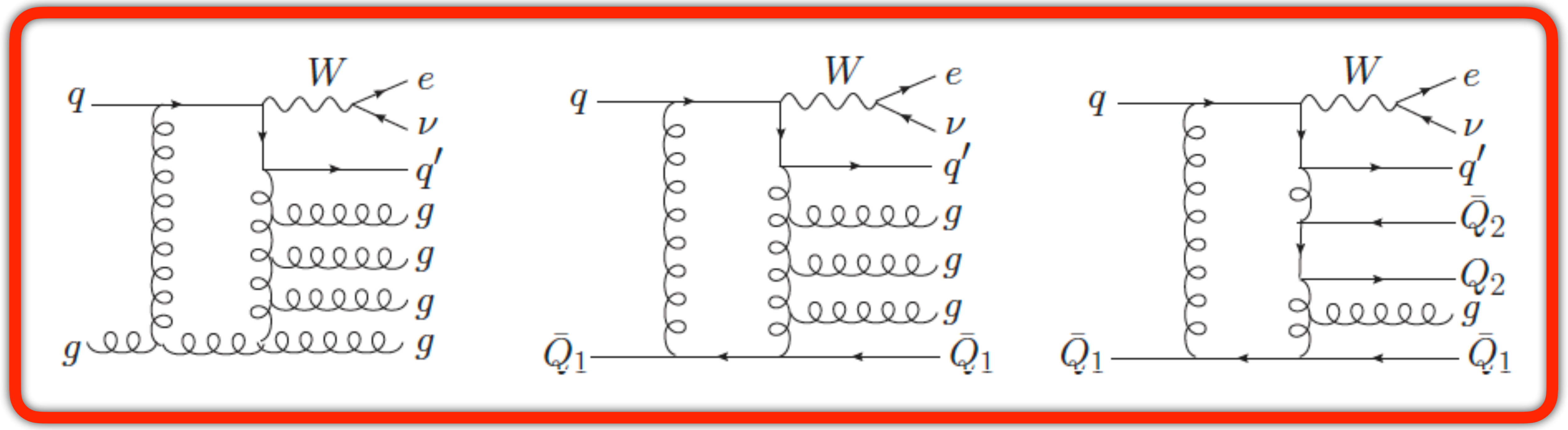

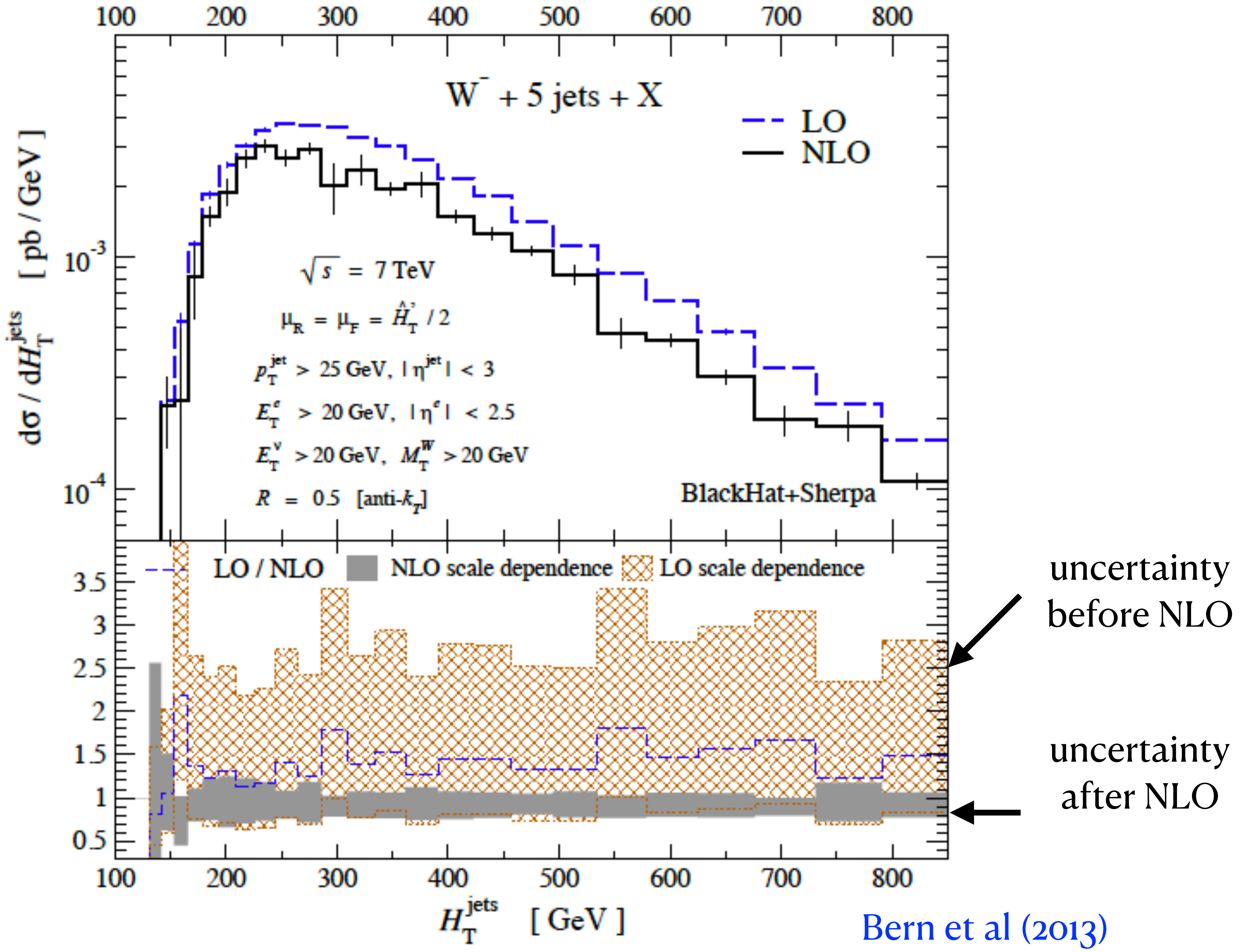

Bern et al (2013)

QCD at NLO: today

- Today NLO predictions, in both QCD and EW coupling constants, are available for processes with numerous final state particles. In addition these fixed-order predictions can be combined with parton-shower Monte Carlo programs in order to resum large logarithms in soft and/or collinear regions of jet phase space.

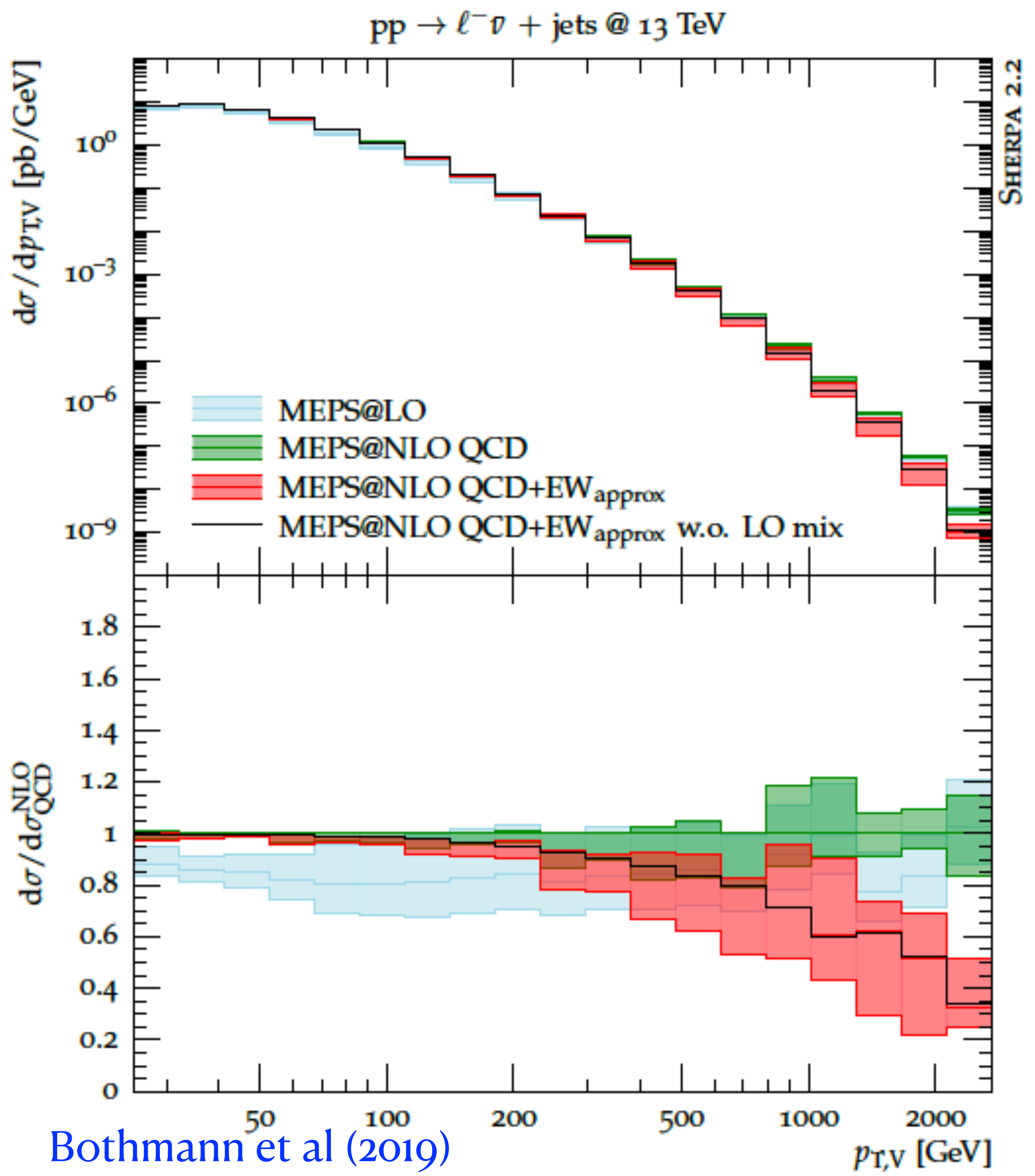

Bothmann et al (2019)

This SHERPA example nicely illustrates the state-of-the-art. The red band combines NLO QCD to W+0,1,2 jets with parton shower predictions, together with NLO electroweak corrections, to get the transverse momentum distribution for W production. This observable is important for the measurements of the W mass.

The SM at NLO is fully ready for current and future experimental data!

QCD at NNLO: historical examples

- The early NNLO corrections were for color-singlet production such as Drell-Yan and Higgs. The observed corrections revealed two trends: NNLO corrections are needed to make the most out of precision measurements at hadron colliders, and the corrections can sometimes be surprisingly large.

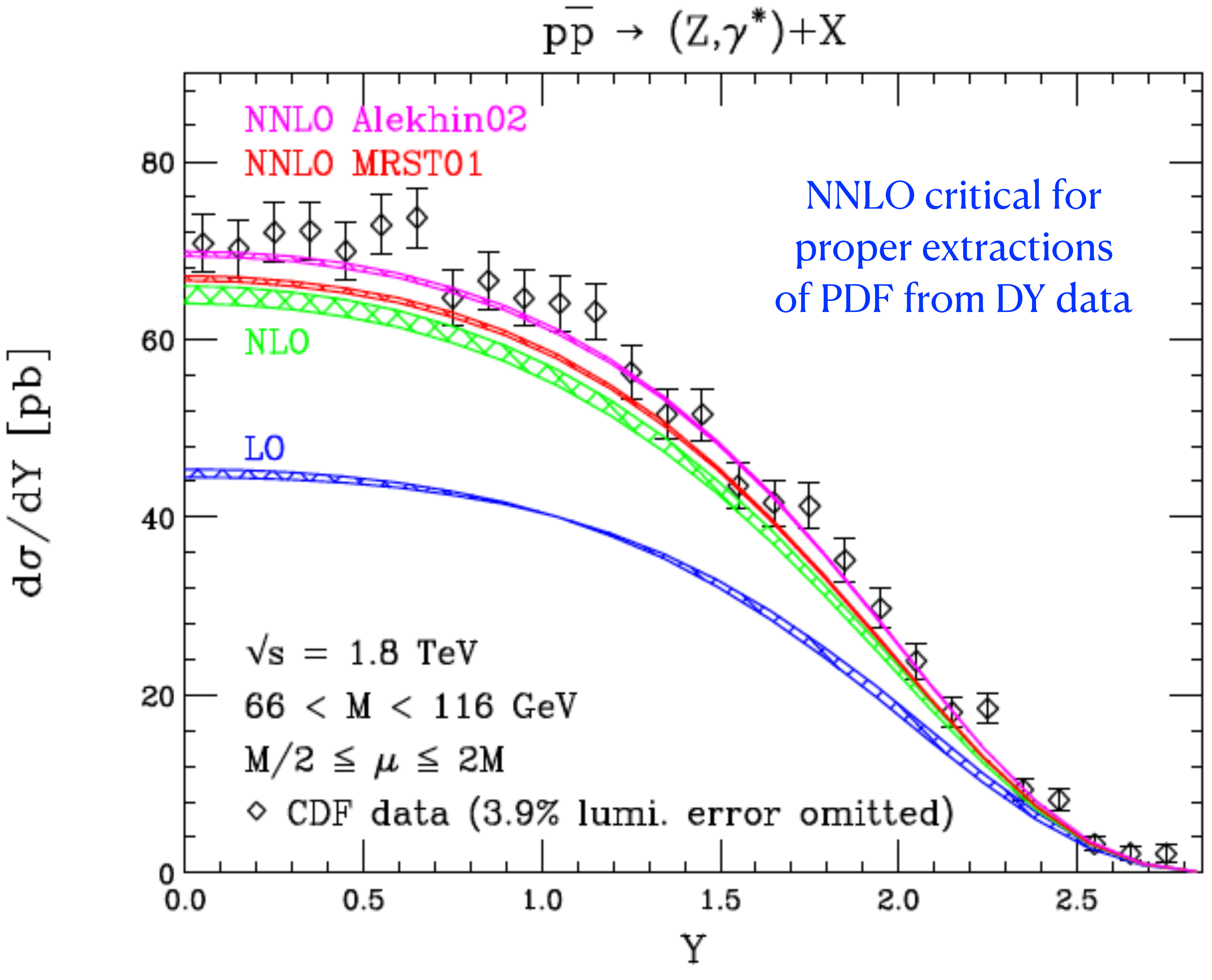

Anastasiou, Dixon, Melnikov, Petriello (2003)

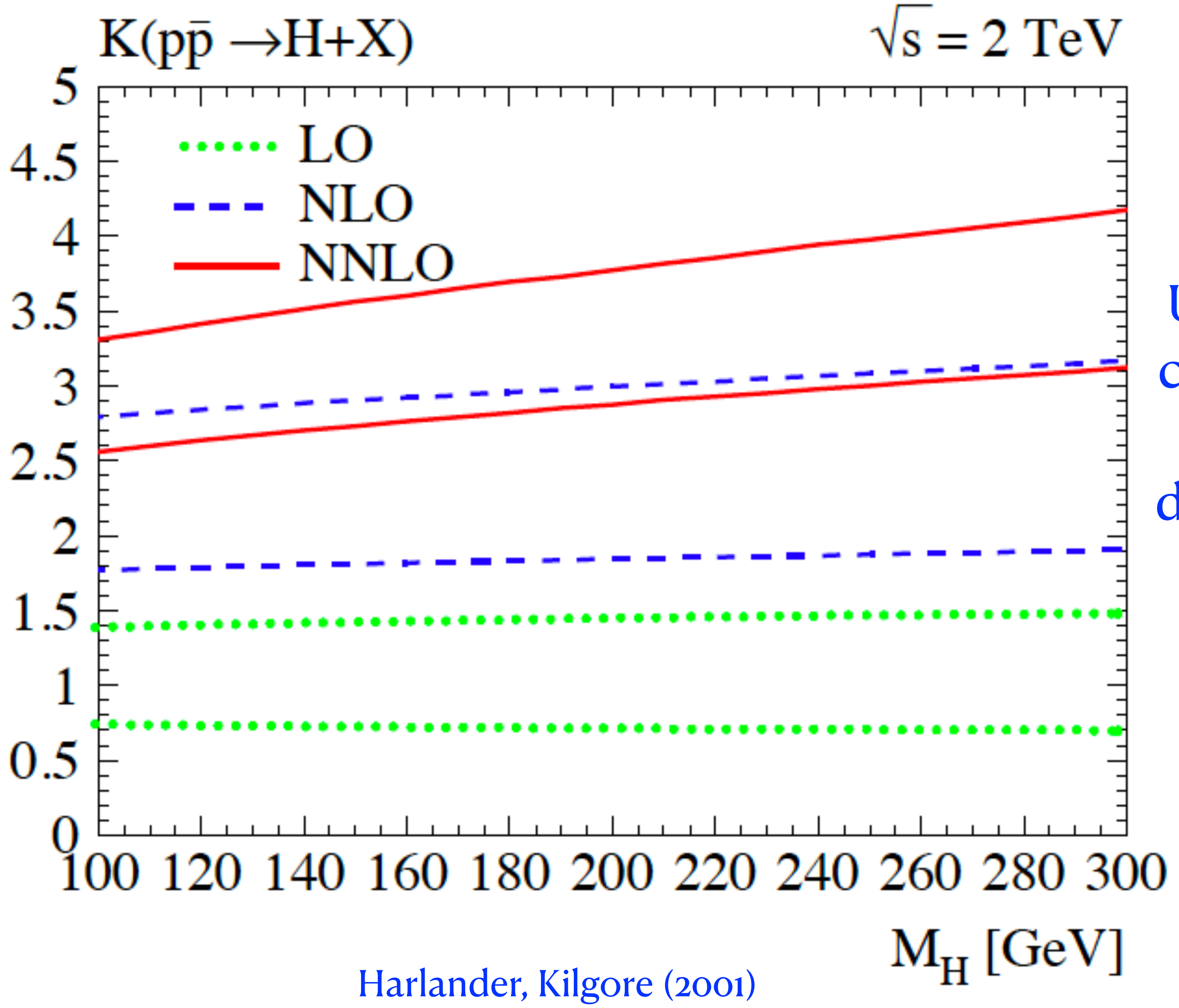

Up to another 75% correction w.r.t. LO from NNLO, depending on mass and scale choice

Harlander, Kilgore (2001)
Anastasiou, Melnikov (2001)

QCD at NNLO: IR subtraction schemes

- The quest to understand how to efficiently organize the cancellation of infrared singularities to facilitate the calculation of more complicated processes took over a decade and led to novel ideas and advances.

Example: Antennae subtraction uses physical processes to construct IR counterterms

Gehrmann, Gehrmann-de Ridder, Glover (2005)

$$X_4^0(i,j,k,l) \sim \frac{|\mathcal{M}_4^0(i,j,k,l)|^2}{|\mathcal{M}_2^0(I,L)|^2}$$

Subtraction term that captures final-state singularity structure of any process with two final-state gluons at tree-level, constructed from H→gg

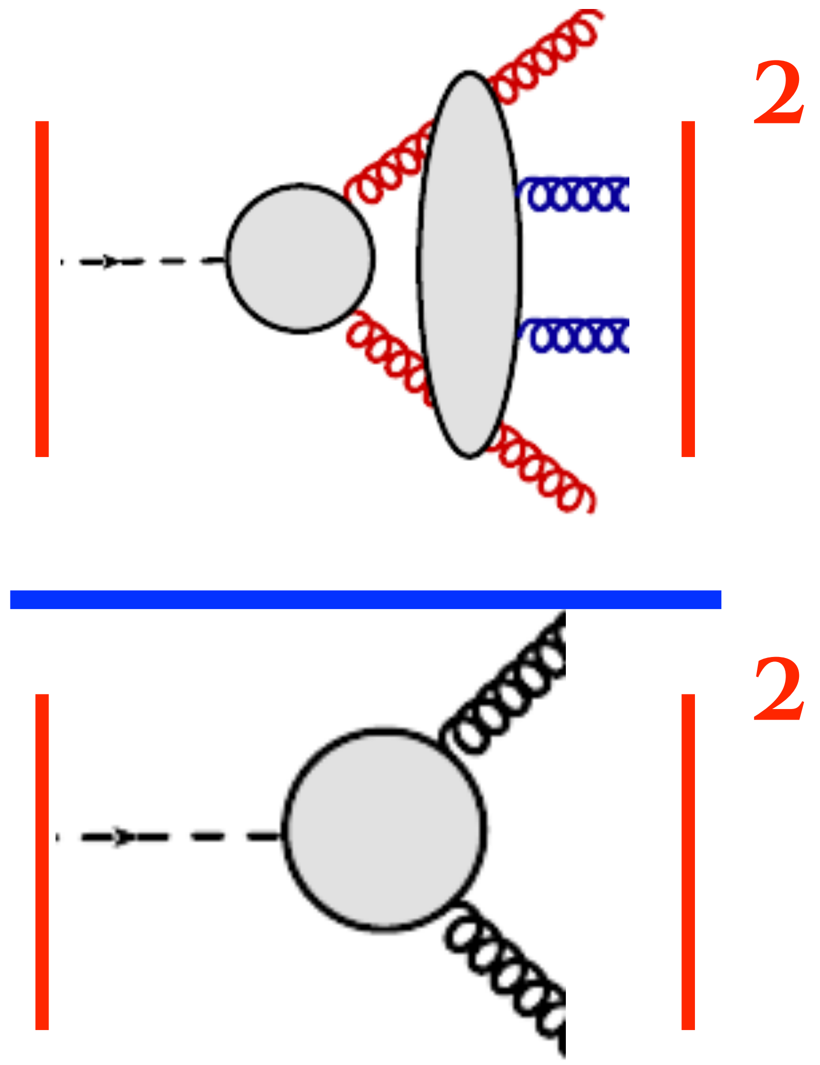

There are several schemes that capture the local singularity structure of arbitrary NNLO final states:

- ColorfulNNLO (Somogyi et al (2005))
- Sector improved residue subtraction (Czakon (2010))
- Projection-to-Born (Cacciari et al (2015))
- Nested soft-collinear subtraction (Caola et al (2017))
- Local analytic sector subtraction (Magnea et al (2018))

QCD at NNLO: IR subtraction schemes

- An influx of ideas from resummation and heavy-quark physics led to new approaches to IR subtraction at NNLO based on factorization and effective field theory. Here is an example that illustrates this type of approach.

RB, Focke, Liu, Petriello; Gaunt, Stahlhofen, Tackmann, Walsh (2015)

$$\boxed{\tau_N = \sum_k \min\{n_i \cdot q_k\}}$$

$$\boxed{\sigma = \int d\tau_N \frac{d\sigma}{d\tau_N}\theta(\tau^{cut} - \tau_N) + \int d\tau_N \frac{d\sigma}{d\tau_N}\theta(\tau_N - \tau^{cut})}$$

N-jettiness, an event shape variable (similar to thrust), first introduced by Stewart et al (2009)

light-like direction of initial state beams and final-state jets

momenta of final-state particles

A simpler effective field theory description is available for this region

Have more than one resolved jet at Born level; **need NLO only!**

Intuition:

$\tau_N \sim 0$: all radiation is either soft, or collinear to a beam/jet

$\tau_N > 0$: at least one additional jet beyond Born level is resolved

- q_T-subtraction (Catani, Grazzini (2007))
- N-jettiness subtraction (RB et al; Gaunt et al (2015))

QCD at NNLO: enabling LHC science

- Numerous example illustrate that NNLO QCD is needed for a precision comparison of the SM with LHC data. In some cases even getting the qualitative behavior correct requires NNLO QCD.

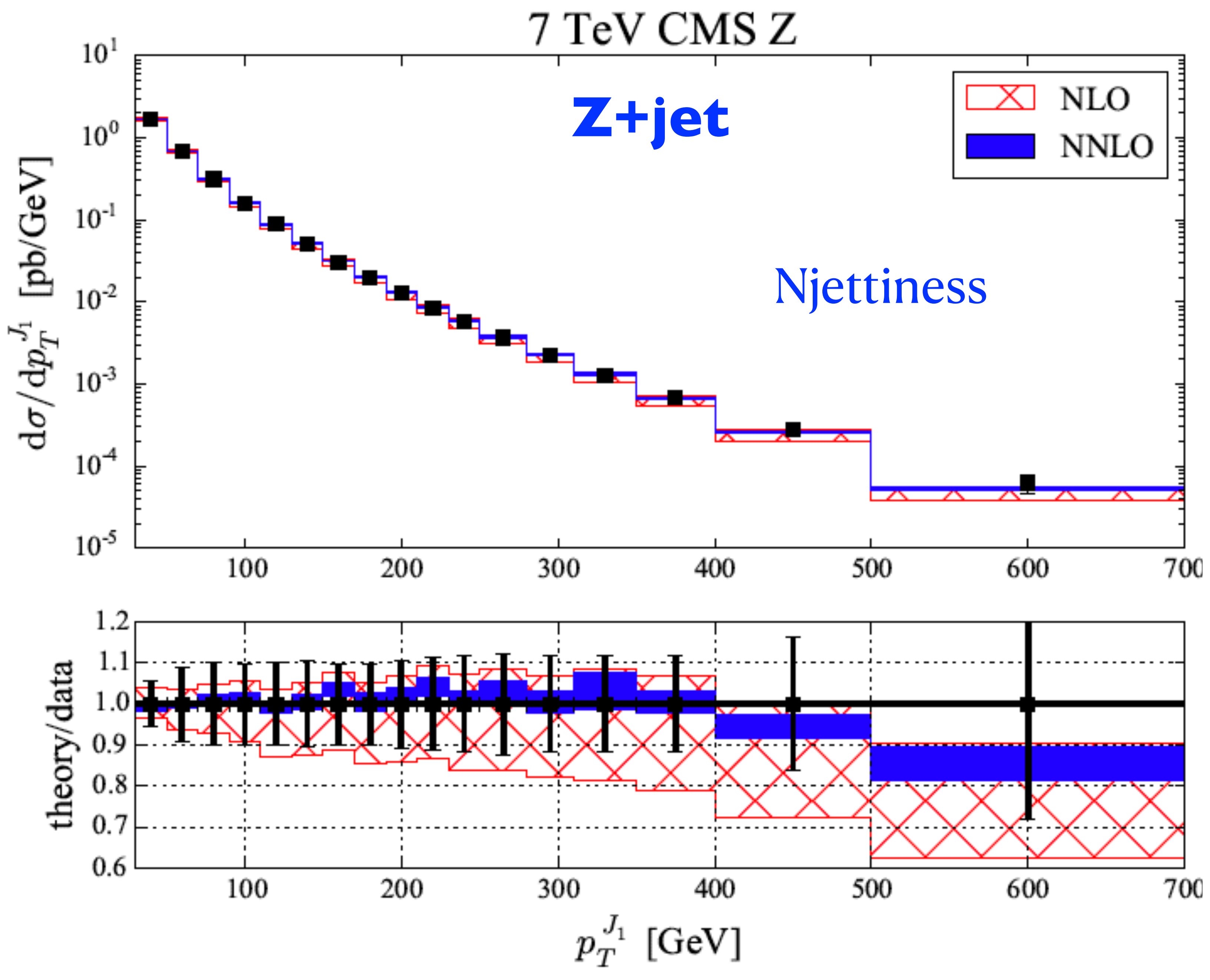

RB et al (2016)

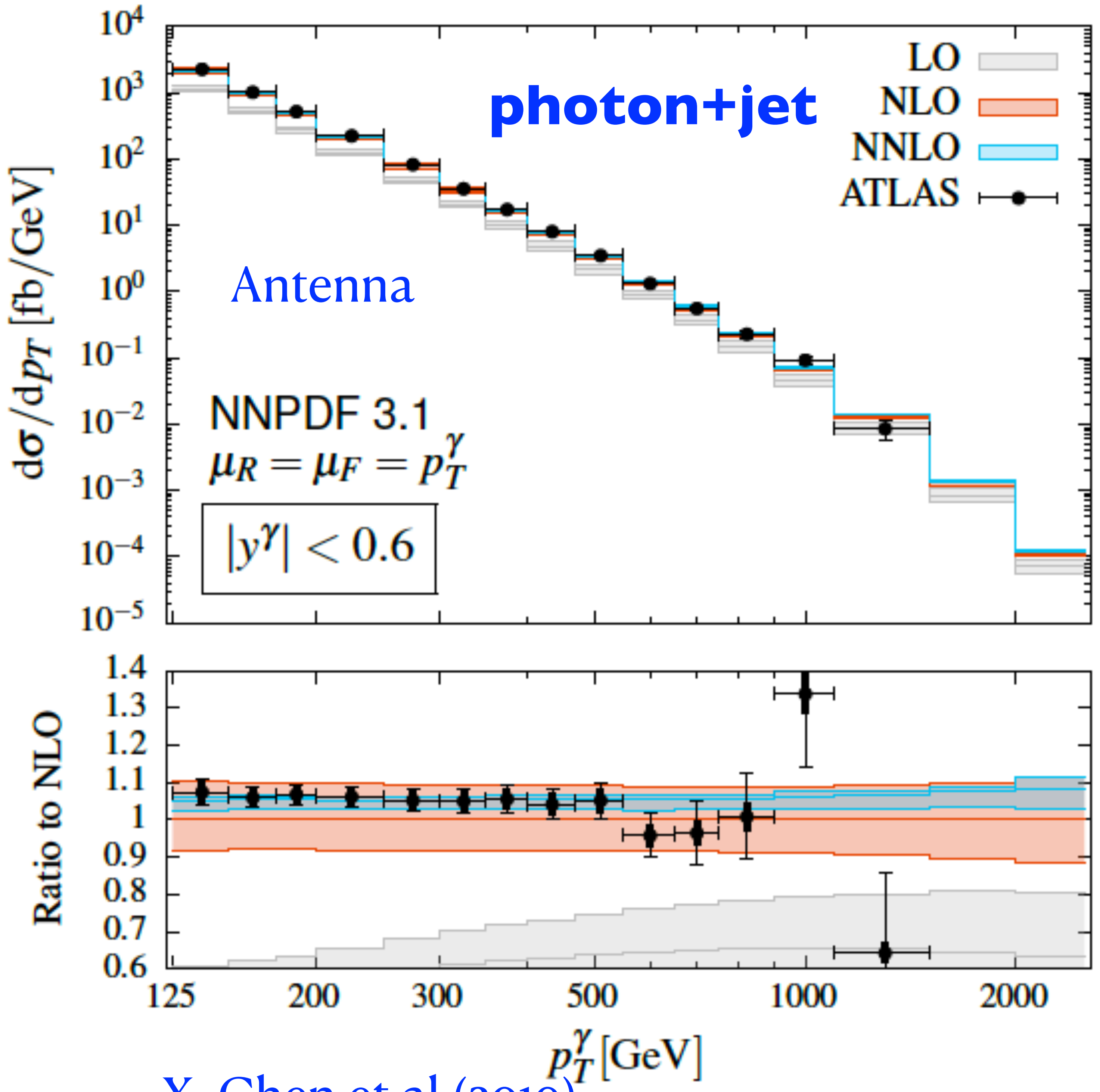

X. Chen et al (2019)

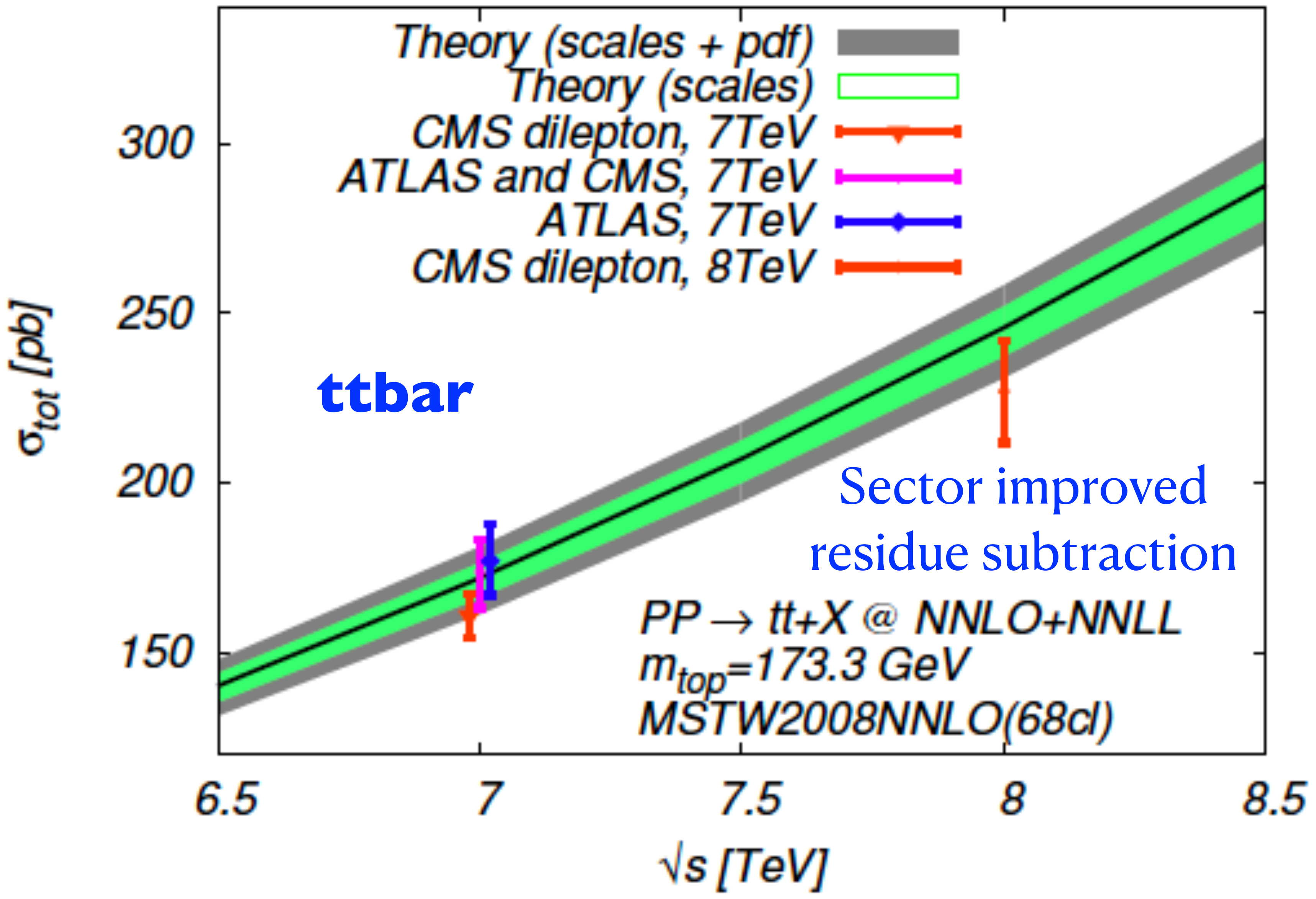

Czakon et al (2013)

QCD today: the current frontier

- The ever-increasing quality of the LHC data, and expected future experimental data, means that innovation in perturbative QCD techniques is still needed. N3LO corrections are available for color-singlet 2→1 processes, the same as NNLO QCD two decades ago.

Duhr, Mistlberger (2021)

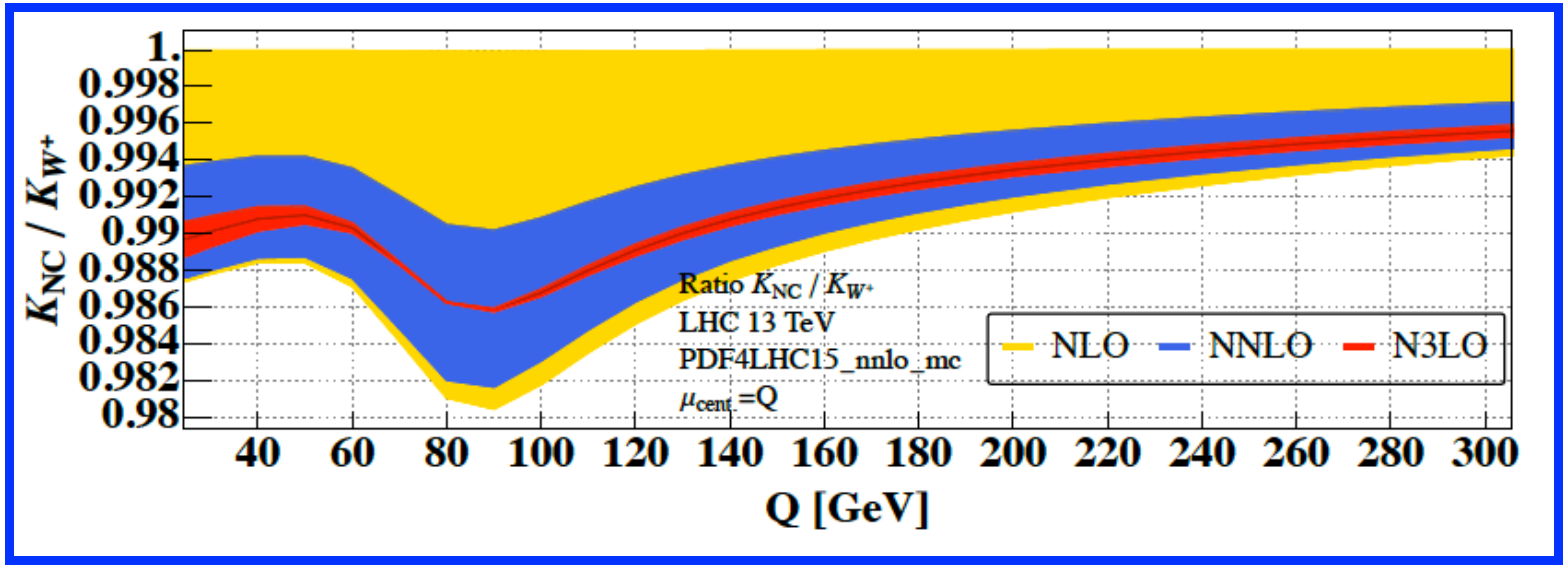

This shows that the ratio of neutral-current to charged-current K-factors is remarkably well-behaved in QCD perturbation theory; there is almost no residual scale dependence, and N3LO is completely contained in NNLO

QCD today: the current frontier

- The ever-increasing quality of the LHC data, and expected future experimental data, means that innovation in perturbative QCD techniques is still needed. N3LO corrections are available for color-singlet 2→1 processes, the same as NNLO QCD two decades ago.

Anastasiou et al (2015)

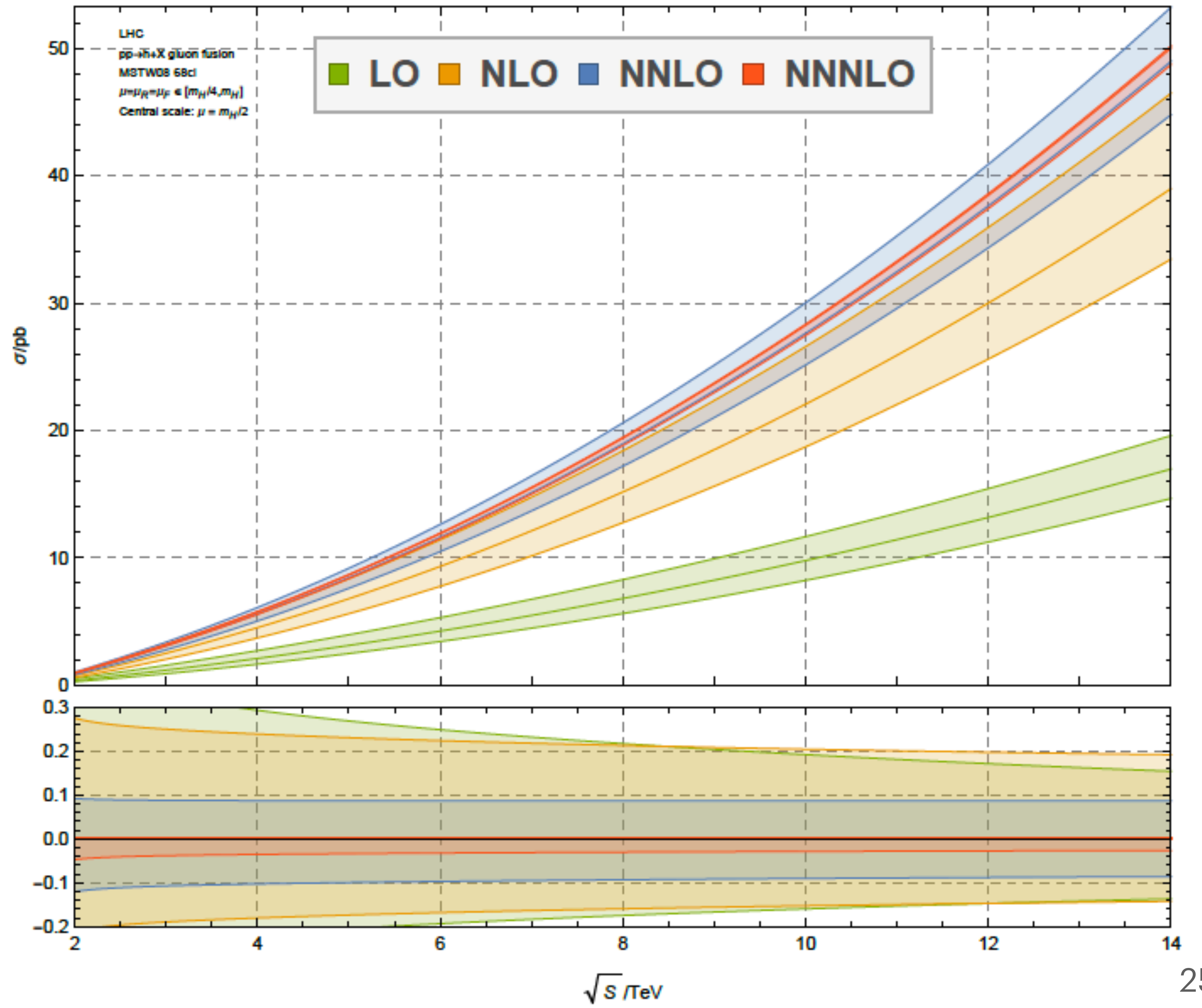

Higgs production in gluon fusion is also known at N3LO. Excellent convergence of the perturbation theory, which will be of prime importance in the continued investigation of Higgs couplings at the HL-LHC

QCD today: the current frontier

- The ever-increasing quality of the LHC data, and expected future experimental data, means that innovation in perturbative QCD techniques is still needed. The first NNLO corrections for 2→3 processes are now appearing.

Czakon, Mitov, Poncelet (2021)

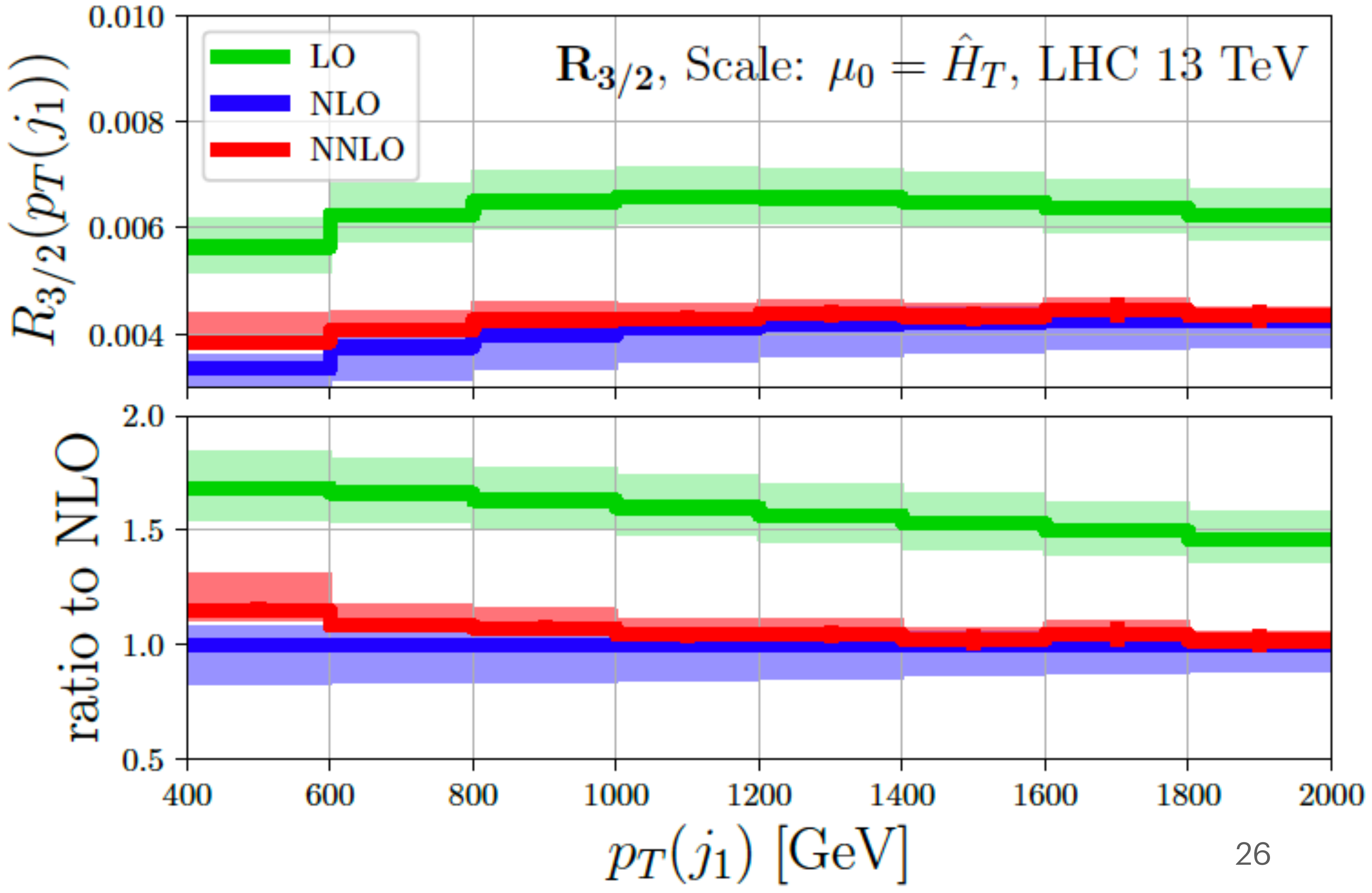

The ratio of 3-jet production over 2-jet production is sensitive to the strong coupling constant. NNLO QCD corrections to 3-jet production changes this ratio by up to 20%, depending on the leading-jet p_T

Precision for new physics: introduction to the SMEFT and open questions

Motivation

What do we learn from the remarkable success of the SM precision program, combined with the null searches so far at the LHC and elsewhere?

- The data suggests (although it doesn't require) a mass gap between the SM and new physics

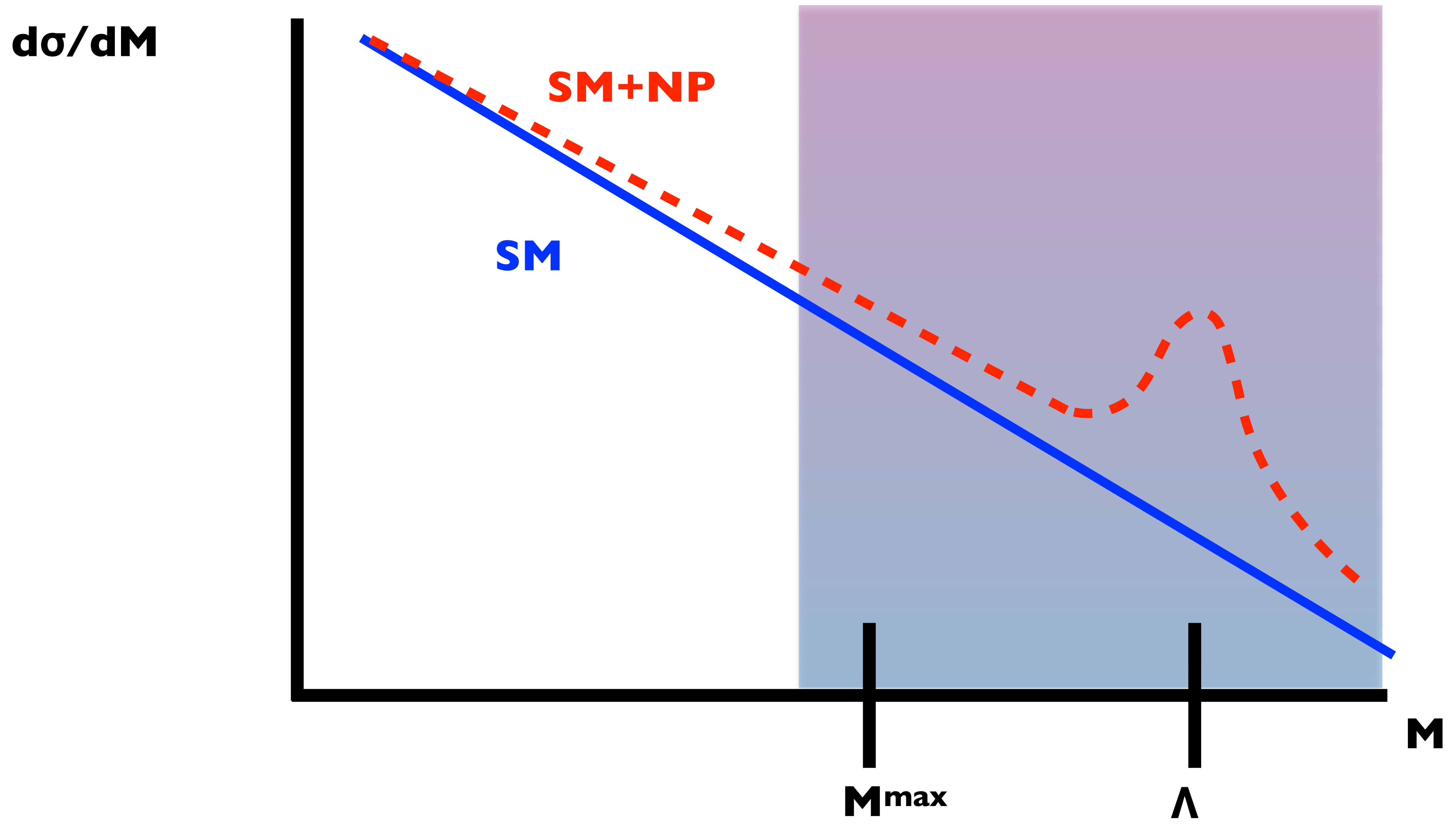

- M^{max} is the maximum energy probed at the LHC and elsewhere
- Λ is the scale where new particles appear

We hope that Λ isn't too far above M^{max}!

Introduction to SMEFT

- An EFT framework that incorporates this point is the Standard Model Effective Field Theory (SMEFT): assume the SM field content and gauge symmetry, and include all possible higher-dimensional operators suppressed by a scale Λ

$$\boxed{\mathcal{L} = \mathcal{L}_{SM} + \frac{1}{\Lambda^2}\sum_i C_6^i(\mu)\underbrace{\mathcal{O}_6^i(\mu)}_{\text{Dimension-6}} + \frac{1}{\Lambda^4}\sum_i C_8^i(\mu)\underbrace{\mathcal{O}_8^i(\mu)}_{\text{Dimension-8}} + \ldots}$$

- $\Lambda \gg E, v$ (Higgs vev) must both be satisfied
- Odd dimensions violate lepton or baryon number; neglected here
- RG running important when comparing experiments at disparate energies

Constructing the SMEFT

- The development of the SMEFT as a fully consistent QFT ready for comparison with experiment, with higher-order corrections and renormalization-group evolution incorporated, is a great success of the past decade.

Pure Gauge interactions

Accommodates a rich phenomenology in all sectors

X^3		φ^6 and $\varphi^4 D^2$		$\psi^2\varphi^3$	
Q_G	$f^{ABC} G_\mu^{A\nu} G_\nu^{B\rho} G_\rho^{C\mu}$	Q_φ	$(\varphi^\dagger\varphi)^3$	$Q_{e\varphi}$	$(\varphi^\dagger\varphi)(\bar l_p e_r \varphi)$
$Q_{\widetilde G}$	$f^{ABC} \widetilde G_\mu^{A\nu} G_\nu^{B\rho} G_\rho^{C\mu}$	$Q_{\varphi\Box}$	$(\varphi^\dagger\varphi)\Box(\varphi^\dagger\varphi)$	$Q_{u\varphi}$	$(\varphi^\dagger\varphi)(\bar q_p u_r \widetilde\varphi)$
Q_W	$\varepsilon^{IJK} W_\mu^{I\nu} W_\nu^{J\rho} W_\rho^{K\mu}$	$Q_{\varphi D}$	$\left(\varphi^\dagger D^\mu\varphi\right)^\star \left(\varphi^\dagger D_\mu\varphi\right)$	$Q_{d\varphi}$	$(\varphi^\dagger\varphi)(\bar q_p d_r \varphi)$
$Q_{\widetilde W}$	$\varepsilon^{IJK} \widetilde W_\mu^{I\nu} W_\nu^{J\rho} W_\rho^{K\mu}$				
$X^2\varphi^2$		$\psi^2 X\varphi$		$\psi^2\varphi^2 D$	
$Q_{\varphi G}$	$\varphi^\dagger\varphi\, G^A_{\mu\nu} G^{A\mu\nu}$	Q_{eW}	$(\bar l_p \sigma^{\mu\nu} e_r)\tau^I \varphi W^I_{\mu\nu}$	$Q_{\varphi l}^{(1)}$	$(\varphi^\dagger i \overleftrightarrow{D}_\mu \varphi)(\bar l_p \gamma^\mu l_r)$
$Q_{\varphi\widetilde G}$	$\varphi^\dagger\varphi\, \widetilde G^A_{\mu\nu} G^{A\mu\nu}$	Q_{eB}	$(\bar l_p \sigma^{\mu\nu} e_r)\varphi B_{\mu\nu}$	$Q_{\varphi l}^{(3)}$	$(\varphi^\dagger i \overleftrightarrow{D}^I_\mu \varphi)(\bar l_p \tau^I \gamma^\mu l_r)$
$Q_{\varphi W}$	$\varphi^\dagger\varphi\, W^I_{\mu\nu} W^{I\mu\nu}$	Q_{uG}	$(\bar q_p \sigma^{\mu\nu} T^A u_r)\widetilde\varphi\, G^A_{\mu\nu}$	$Q_{\varphi e}$	$(\varphi^\dagger i \overleftrightarrow{D}_\mu \varphi)(\bar e_p \gamma^\mu e_r)$
$Q_{\varphi\widetilde W}$	$\varphi^\dagger\varphi\, \widetilde W^I_{\mu\nu} W^{I\mu\nu}$	Q_{uW}	$(\bar q_p \sigma^{\mu\nu} u_r)\tau^I \widetilde\varphi\, W^I_{\mu\nu}$	$Q_{\varphi q}^{(1)}$	$(\varphi^\dagger i \overleftrightarrow{D}_\mu \varphi)(\bar q_p \gamma^\mu q_r)$
$Q_{\varphi B}$	$\varphi^\dagger\varphi\, B_{\mu\nu} B^{\mu\nu}$	Q_{uB}	$(\bar q_p \sigma^{\mu\nu} u_r)\widetilde\varphi\, B_{\mu\nu}$	$Q_{\varphi q}^{(3)}$	$(\varphi^\dagger i \overleftrightarrow{D}^I_\mu \varphi)(\bar q_p \tau^I \gamma^\mu q_r)$
$Q_{\varphi\widetilde B}$	$\varphi^\dagger\varphi\, \widetilde B_{\mu\nu} B^{\mu\nu}$	Q_{dG}	$(\bar q_p \sigma^{\mu\nu} T^A d_r)\varphi\, G^A_{\mu\nu}$	$Q_{\varphi u}$	$(\varphi^\dagger i \overleftrightarrow{D}_\mu \varphi)(\bar u_p \gamma^\mu u_r)$
$Q_{\varphi WB}$	$\varphi^\dagger\tau^I\varphi\, W^I_{\mu\nu} B^{\mu\nu}$	Q_{dW}	$(\bar q_p \sigma^{\mu\nu} d_r)\tau^I \varphi\, W^I_{\mu\nu}$	$Q_{\varphi d}$	$(\varphi^\dagger i \overleftrightarrow{D}_\mu \varphi)(\bar d_p \gamma^\mu d_r)$
$Q_{\varphi\widetilde W B}$	$\varphi^\dagger\tau^I\varphi\, \widetilde W^I_{\mu\nu} B^{\mu\nu}$	Q_{dB}	$(\bar q_p \sigma^{\mu\nu} d_r)\varphi\, B_{\mu\nu}$	$Q_{\varphi ud}$	$i(\widetilde\varphi^\dagger D_\mu\varphi)(\bar u_p \gamma^\mu d_r)$

$(\bar LL)(\bar LL)$		$(\bar RR)(\bar RR)$		$(\bar LL)(\bar RR)$	
Q_{ll}	$(\bar l_p\gamma_\mu l_r)(\bar l_s\gamma^\mu l_t)$	Q_{ee}	$(\bar e_p\gamma_\mu e_r)(\bar e_s\gamma^\mu e_t)$	Q_{le}	$(\bar l_p\gamma_\mu l_r)(\bar e_s\gamma^\mu e_t)$
$Q_{qq}^{(1)}$	$(\bar q_p\gamma_\mu q_r)(\bar q_s\gamma^\mu q_t)$	Q_{uu}	$(\bar u_p\gamma_\mu u_r)(\bar u_s\gamma^\mu u_t)$	Q_{lu}	$(\bar l_p\gamma_\mu l_r)(\bar u_s\gamma^\mu u_t)$
$Q_{qq}^{(3)}$	$(\bar q_p\gamma_\mu \tau^I q_r)(\bar q_s\gamma^\mu \tau^I q_t)$	Q_{dd}	$(\bar d_p\gamma_\mu d_r)(\bar d_s\gamma^\mu d_t)$	Q_{ld}	$(\bar l_p\gamma_\mu l_r)(\bar d_s\gamma^\mu d_t)$
$Q_{lq}^{(1)}$	$(\bar l_p\gamma_\mu l_r)(\bar q_s\gamma^\mu q_t)$	Q_{eu}	$(\bar e_p\gamma_\mu e_r)(\bar u_s\gamma^\mu u_t)$	Q_{qe}	$(\bar q_p\gamma_\mu q_r)(\bar e_s\gamma^\mu e_t)$
$Q_{lq}^{(3)}$	$(\bar l_p\gamma_\mu \tau^I l_r)(\bar q_s\gamma^\mu \tau^I q_t)$	Q_{ed}	$(\bar e_p\gamma_\mu e_r)(\bar d_s\gamma^\mu d_t)$	$Q_{qu}^{(1)}$	$(\bar q_p\gamma_\mu q_r)(\bar u_s\gamma^\mu u_t)$
		$Q_{ud}^{(1)}$	$(\bar u_p\gamma_\mu u_r)(\bar d_s\gamma^\mu d_t)$	$Q_{qu}^{(8)}$	$(\bar q_p\gamma_\mu T^A q_r)(\bar u_s\gamma^\mu T^A u_t)$
		$Q_{ud}^{(8)}$	$(\bar u_p\gamma_\mu T^A u_r)(\bar d_s\gamma^\mu T^A d_t)$	$Q_{qd}^{(1)}$	$(\bar q_p\gamma_\mu q_r)(\bar d_s\gamma^\mu d_t)$
				$Q_{qd}^{(8)}$	$(\bar q_p\gamma_\mu T^A q_r)(\bar d_s\gamma^\mu T^A d_t)$

$(\bar LR)(\bar RL)$ and $(\bar LR)(\bar LR)$		B-violating	
Q_{ledq}	$(\bar l_p^j e_r)(\bar d_s q_t^j)$	Q_{duq}	$\varepsilon^{\alpha\beta\gamma}\varepsilon_{jk}\left[(d_p^\alpha)^T C u_r^\beta\right]\left[(q_s^{\gamma j})^T C l_t^k\right]$
$Q_{quqd}^{(1)}$	$(\bar q_p^j u_r)\varepsilon_{jk}(\bar q_s^k d_t)$	Q_{qqu}	$\varepsilon^{\alpha\beta\gamma}\varepsilon_{jk}\left[(q_p^{\alpha j})^T C q_r^{\beta k}\right]\left[(u_s^\gamma)^T C e_t\right]$
$Q_{quqd}^{(8)}$	$(\bar q_p^j T^A u_r)\varepsilon_{jk}(\bar q_s^k T^A d_t)$	Q_{qqq}	$\varepsilon^{\alpha\beta\gamma}\varepsilon_{jn}\varepsilon_{km}\left[(q_p^{\alpha j})^T C q_r^{\beta k}\right]\left[(q_s^{\gamma m})^T C l_t^n\right]$
$Q_{lequ}^{(1)}$	$(\bar l_p^j e_r)\varepsilon_{jk}(\bar q_s^k u_t)$	Q_{duu}	$\varepsilon^{\alpha\beta\gamma}\left[(d_p^\alpha)^T C u_r^\beta\right]\left[(u_s^\gamma)^T C e_t\right]$
$Q_{lequ}^{(3)}$	$(\bar l_p^j \sigma_{\mu\nu} e_r)\varepsilon_{jk}(\bar q_s^k \sigma^{\mu\nu} u_t)$		

Gauge-Higgs interactions

Fermion-Higgs-gauge interactions

Four-fermion interactions

Baryon-number violating interactions

Dimension-6 basis:

Buchmuller, Wyler (1986);

Grzadkowski et al (2010)

Dimension-6 RG running:

Alonso, Jenkins, Manojar, Trott (2013-2014)

Dimension-8 basis:

Murphy (2020)

Li et al (2020)

Dimension-10,12 bases:

Harlander et al (2023)

Studies of the SMEFT

- SMEFT motivates experimental analyses by identifying new observables to study. For example, the study of SMEFT at dimension-8 reveals an angular structure in Drell-Yan that motivates an extension of the decades-old angular basis used in experimental analyses.

Alioli, RB, Mereghetti, Petriello (2020)

$$\frac{d\sigma}{dm_{ll}^2 dy d\Omega_l} = \frac{3}{16\pi}\frac{d\sigma}{dm_{ll}^2 dy}\Big\{(1+c_\theta^2)+\frac{A_0}{2}(1-3c_\theta^2) + A_1 s_{2\theta}c_\phi + \frac{A_2}{2}s_\theta^2 c_{2\phi} + A_3 s_\theta c_\phi + A_4 c_\theta + A_5 s_\theta^2 s_{2\phi} + A_6 s_{2\theta}s_\phi + A_7 s_\theta s_\phi$$
$$\boxed{+B_3^e s_\theta^3 c_\phi + B_3^o s_\theta^3 s_\phi + B_2^e s_\theta^2 c_\theta c_{2\phi} + B_2^o s_\theta^2 c_\theta s_{2\phi} + \frac{B_1^e}{2}s_\theta(5c_\theta^2-1)c_\phi + \frac{B_1^o}{2}s_\theta(5c_\theta^2-1)s_\phi + \frac{B_0}{2}(5c_\theta^3-3c_\theta)\Big\}}$$

Can probe to the TeV scale at the LHC

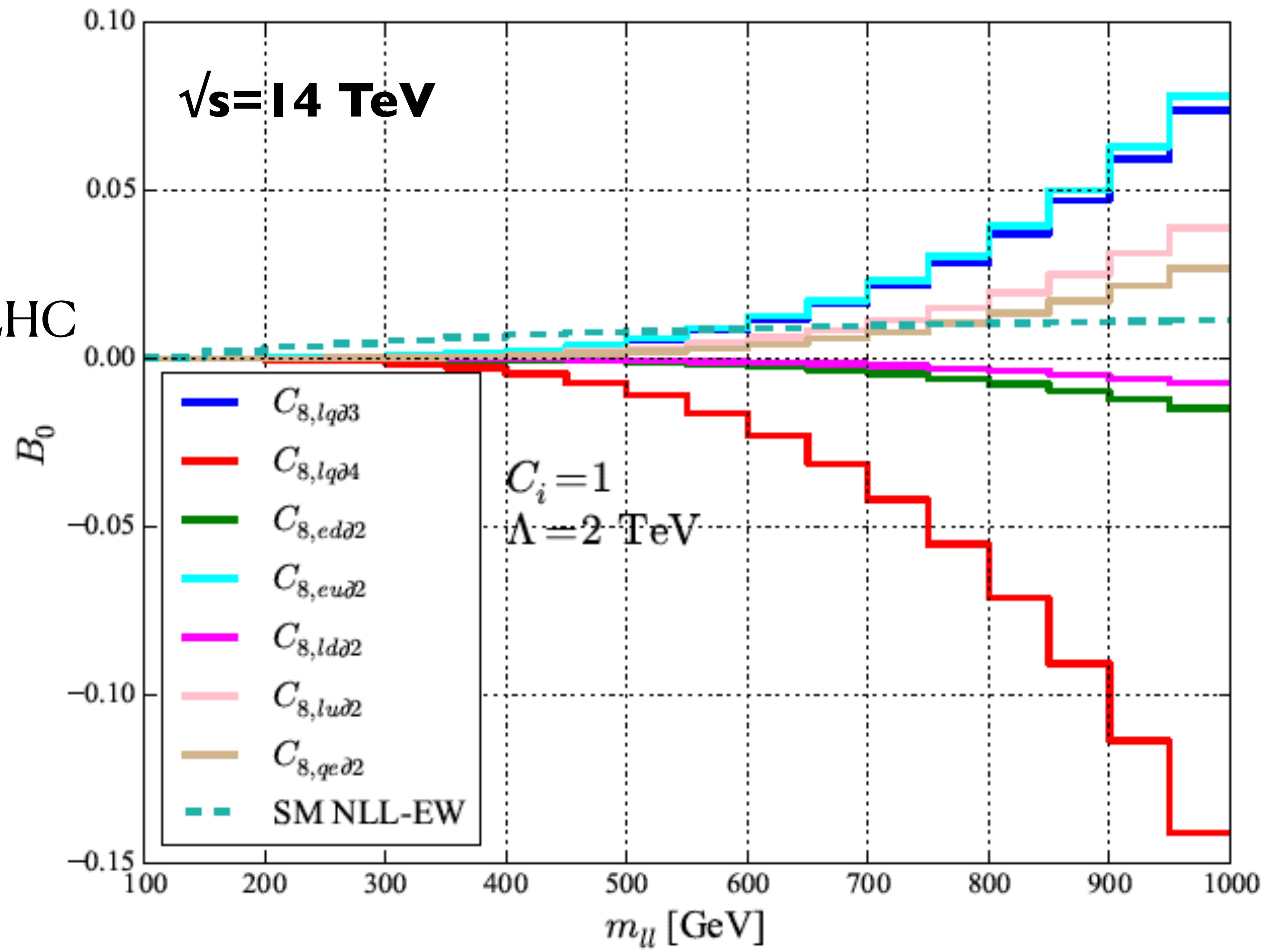

New terms first generated at dimension-8

Studies of the SMEFT

- A rich program exists to search for SMEFT-induced deviations across energy scales. The most natural experiments to look for SMEFT-induced deviations are high-energy ones such as the LHC, since the expansion parameter C^*E^2/Λ^2 is maximized there. Global fits to the available data are pursued by both the experimental and theoretical collaborations.

J. Ellis, Madigan, Mimasu, Sanz, Yu (2020)

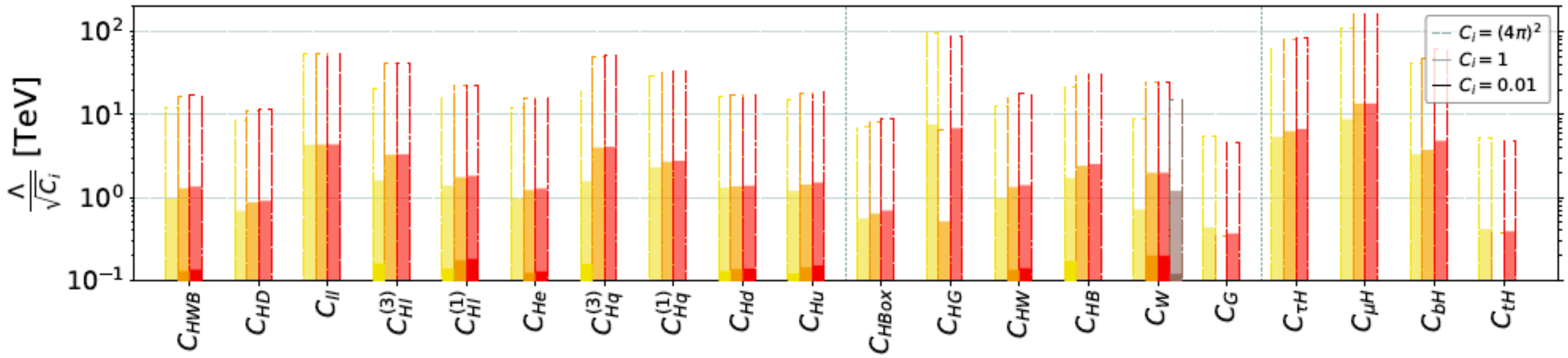

Despite the success of this program many open issues remain to be solved in the interpretation of data within the SMEFT framework

Open question #1

- Many of the questions we confront in QCD play out again in the SMEFT. Do we have control over the SMEFT expansion? We now have the $1/\Lambda$ expansion to control in addition to the expansion in the SM coupling constants.

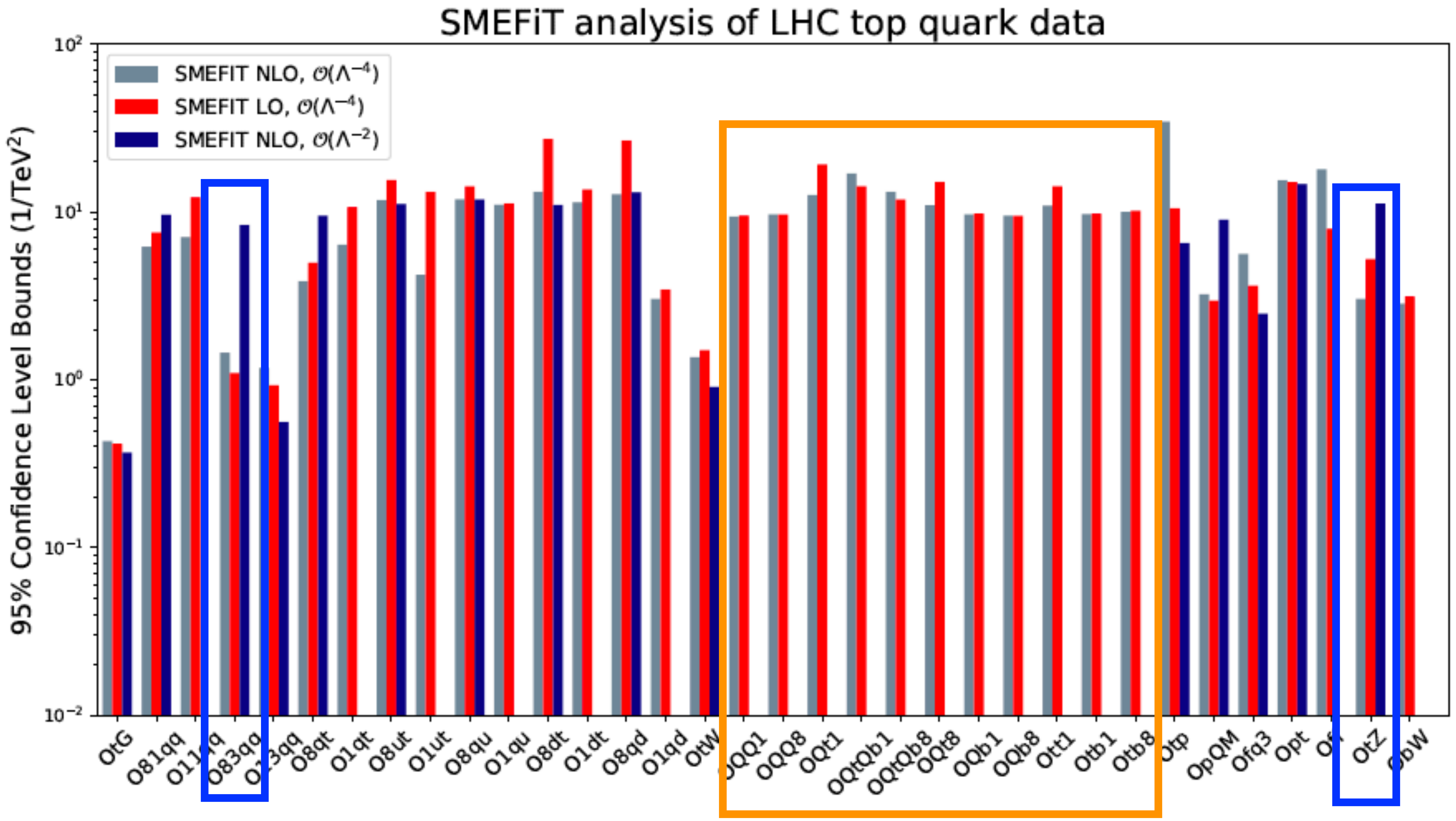

Hartland, Maltoni, Nocera, Rojo, Slade (2019)

Some effects only appear at $O(1/\Lambda^4)$ because the relevant operators don't interfere with the SM

Bounds on others change by an order of magnitude when going from $O(1/\Lambda^2)$ to $O(1/\Lambda^4)$

Open question #2

- Similarly, are dimension-8 terms in the SMEFT important for the data sets that we are considering, and can we distinguish them from dimension-6 effects? Different UV theories can lead to very different patterns of dim-6 and dim-8 terms.

Example 1:

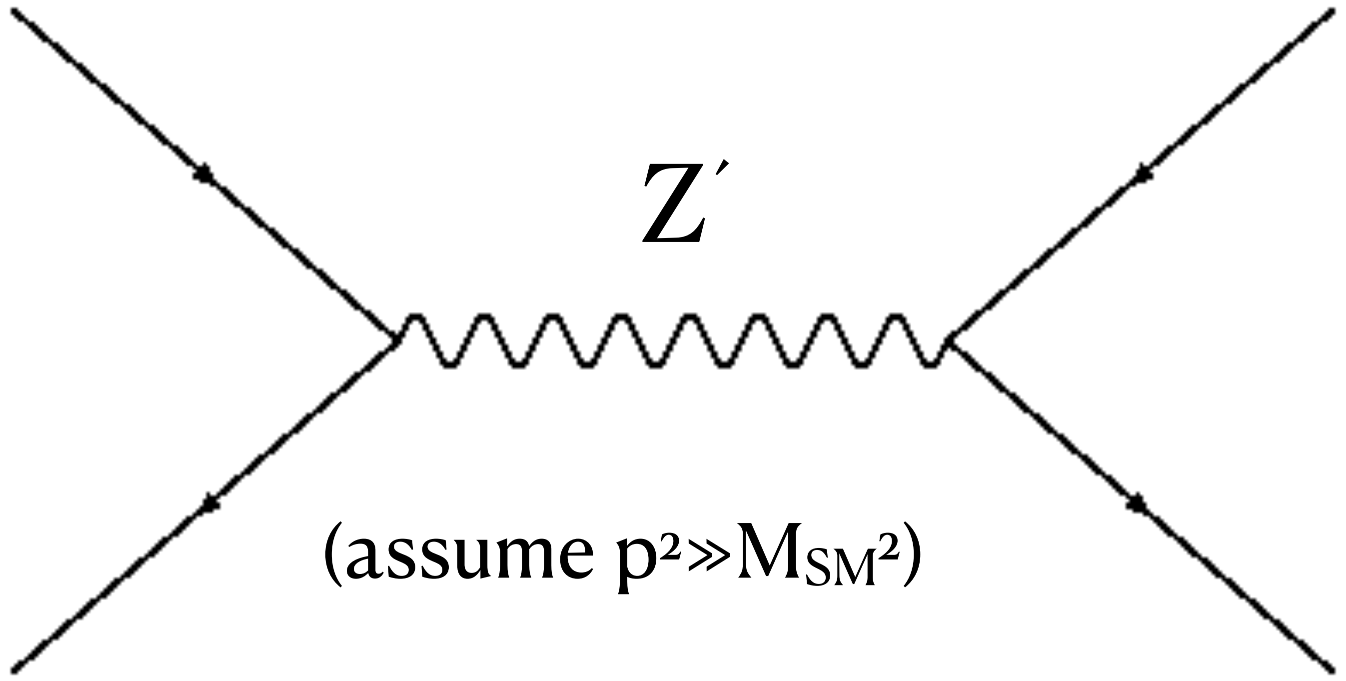

$$\sim -\frac{g_{Z'}^2}{p^2 - M_{Z'}^2} \approx \overset{\text{dim-6}}{\overset{\downarrow}{\frac{g_{Z'}^2}{M_{Z'}^2}}} + \overset{\text{dim-8}}{\overset{\downarrow}{\frac{g_{Z'}^2 p^2}{M_{Z'}^4}}} + \dots$$

$$\boxed{\sigma \sim \underbrace{|\mathcal{M}_{SM}|^2}_{\frac{g_{SM}^4}{p^4}} + \frac{1}{\Lambda^2} \underbrace{2\mathrm{Re}\left[\mathcal{M}_6 \mathcal{M}_{SM}^*\right]}_{\frac{g_{SM}^2 g_{Z'}^2}{p^2 M_{Z'}^2}} + \frac{1}{\Lambda^4}\left\{\underbrace{|\mathcal{M}_6|^2}_{\frac{g_{Z'}^4}{M_{Z'}^4}} + \underbrace{2\mathrm{Re}\left[\mathcal{M}_8 \mathcal{M}_{SM}^*\right]}_{\frac{g_{SM}^2 g_{Z'}^2}{M_{Z'}^4}}\right\}}$$

Open question #2

- Similarly, are dimension-8 terms in the SMEFT important for the data sets that we are considering, and can we distinguish them from dimension-6 effects? Different UV theories can lead to very different patterns of dim-6 and dim-8 terms.

Example 2:

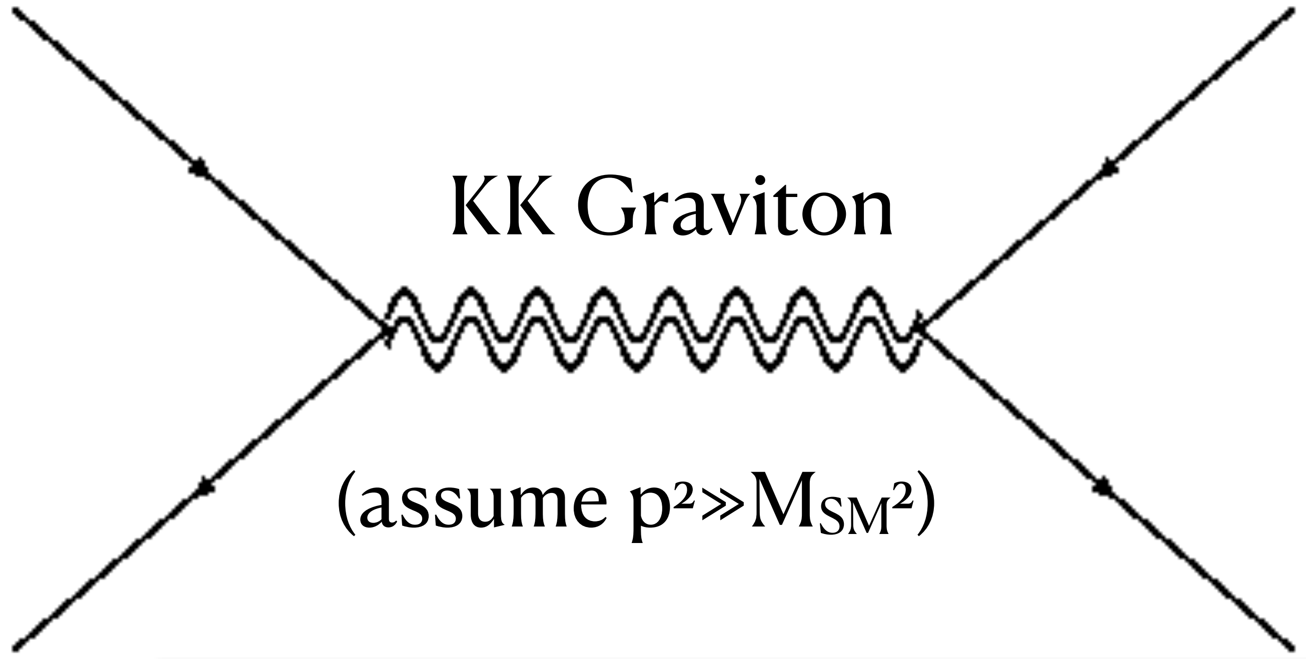

$$\sim \overset{\text{dim-6}}{0} + \overset{\text{dim-8}}{\frac{p^2}{M_S^4}} + \dots$$

Han, Lykken, Zhang (1998)

$$\boxed{\sigma \sim \underbrace{|\mathcal{M}_{SM}|^2}_{\frac{g_{SM}^4}{p^4}} + \frac{1}{\Lambda^2} \underbrace{2\mathrm{Re}\left[\mathcal{M}_6 \mathcal{M}_{SM}^*\right]}_{0} + \frac{1}{\Lambda^4}\left\{\underbrace{|\mathcal{M}_6|^2}_{0} + \underbrace{2\mathrm{Re}\left[\mathcal{M}_8 \mathcal{M}_{SM}^*\right]}_{\frac{g_{SM}^2}{M_S^4}}\right\}}$$

Open question #3

- There are several exciting potential deviations between precision predictions of the SM and experiment. Can EFT guide us to alternative measurements that can shed light on these?

Muon g-2

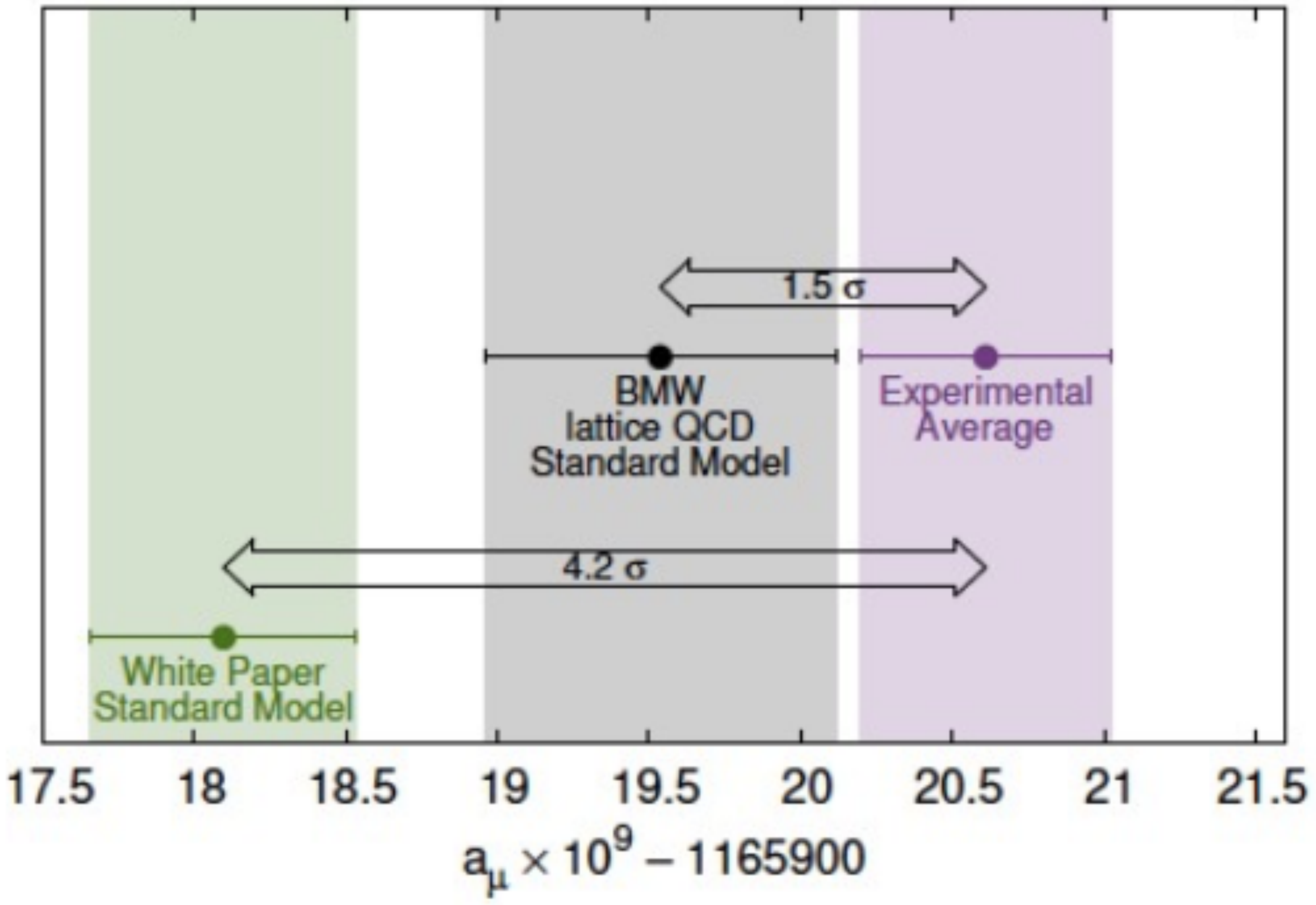

The dipole operators that lead to muon g-2 lead to subleading $1/\Lambda^4$ effects in the Drell-Yan cross section, and are only weakly constrained at the LHC

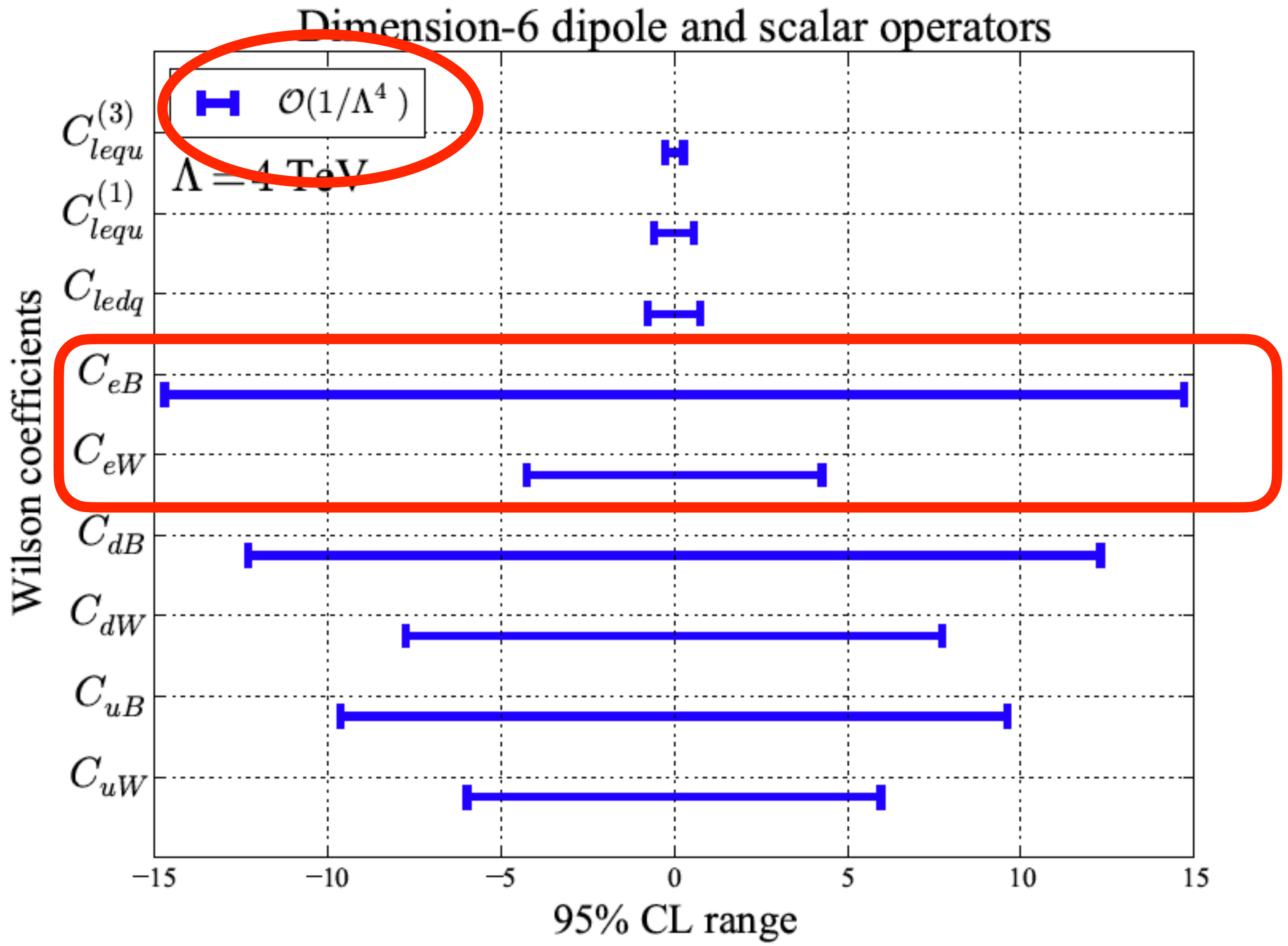

RB, Mereghetti, Petriello (2021)

New ideas in the SMEFT

Sub-leading terms in the SMEFT expansion

- An analysis of the most recent 13 TeV Drell-Yan invariant mass and forward-backward asymmetry data at the LHC illustrates two points: higher-order terms in the SMEFT expansion can have an important impact on fits, and it is important to consider multiple observables.

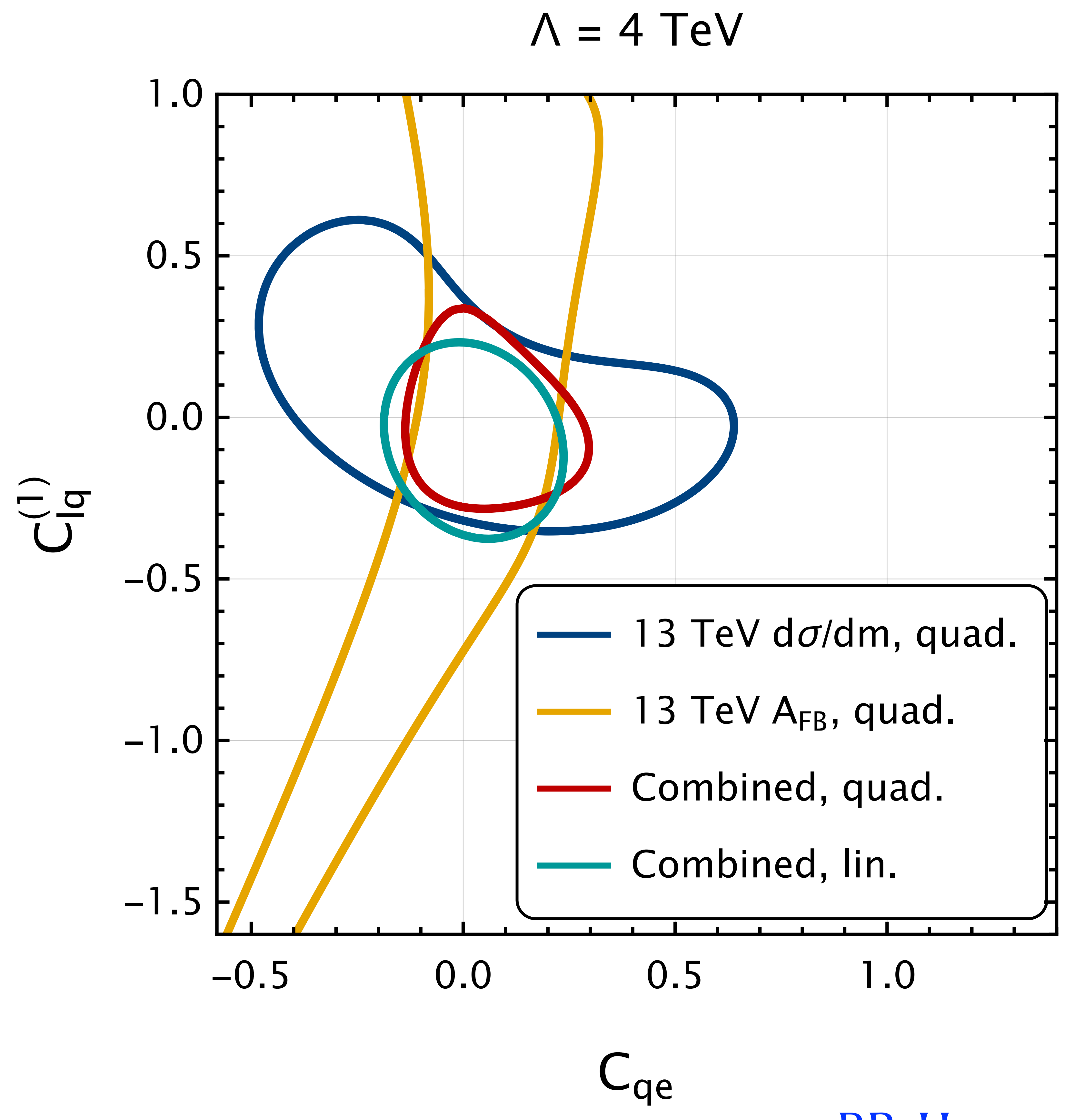

RB, Huang, Petriello (2023)

- Linear combined fit: C/Λ^2 dimension-6 interfered with SM only
- Quadratic combined fit: include $(C/\Lambda^2)^2$ quadratic terms also
- A_{FB} only fit and invariant-mass only fit exhibits degeneracies in the parameter space that are removed when the invariant mass data is included in a combined fit

Question #1 addressed: controlling the impact of higher-order terms in the SMEFT expansion on fits requires considering multiple data sets and observables

Sub-leading terms in the SMEFT expansion

- An analysis of the most recent 13 TeV Drell-Yan invariant mass and forward-backward asymmetry data at the LHC illustrates two points: higher-order terms in the SMEFT expansion have an important impact on fits, and it is important to consider multiple observables.

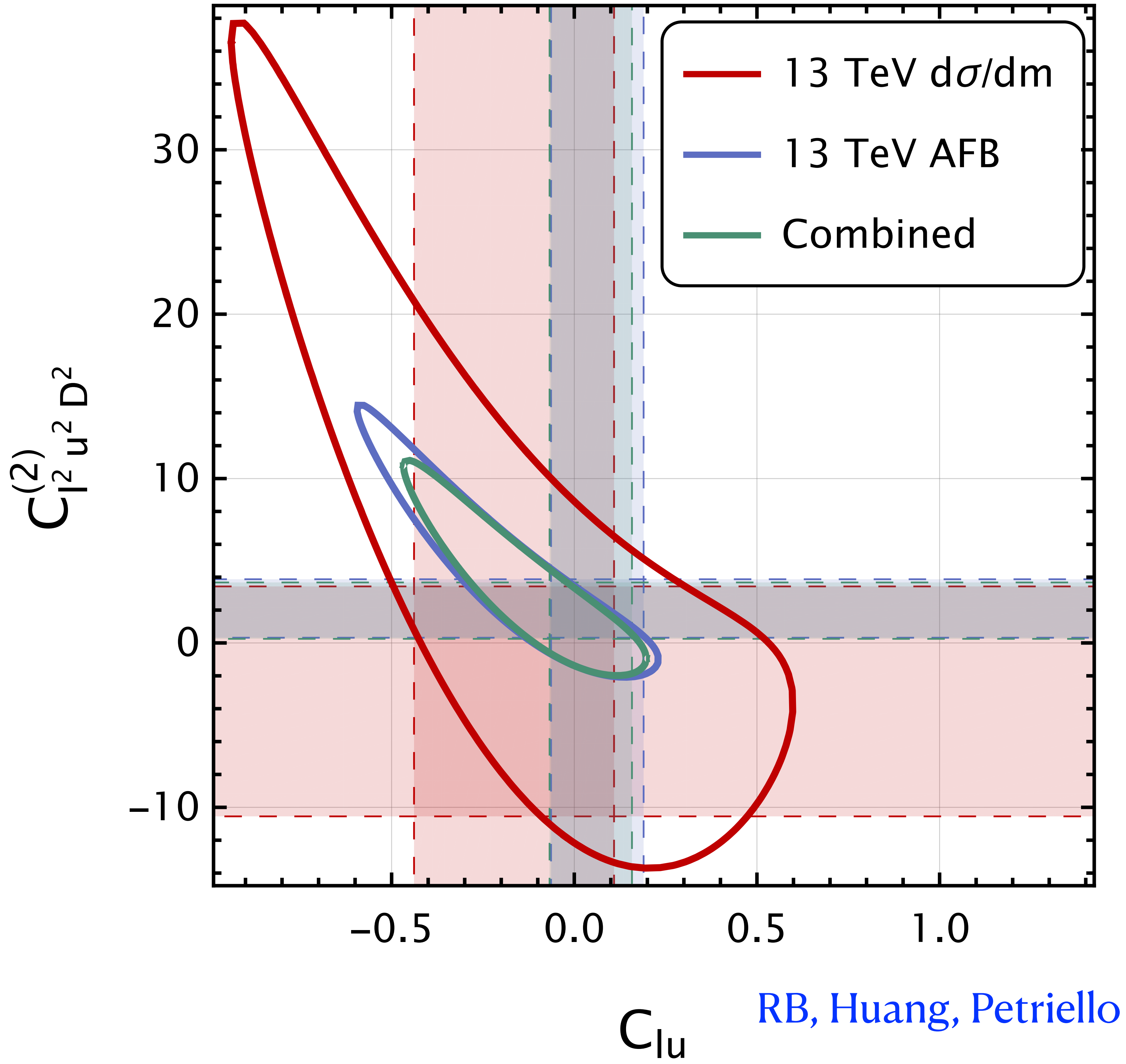

RB, Huang, Petriello (2023)

In some cases combining LHC observables isn't enough; for example, after combining the invariant mass and A_{FB} data there are still degeneracies between dimension-6 operators and their dimension-8 extensions.

Synergy between low and high energy experiments

- High-intensity, low-energy experiments can help disentangle dimension-6 and dimension-8 Wilson coefficients in the EFT. Since the expansion parameter is E^2/Λ^2 these can lead to similar effects at high energies. In low-energy experiments the E^4/Λ^4 dimension-8 terms are negligible, and only dimension-6 is probed.

Example: consider dim-8 extension of semi-leptonic four-fermion operators

Dimension 6		Dimension 8	
$\mathcal{O}_{lq}^{(1)}$	$(\bar{l}\gamma^\mu l)\,(\bar{q}\gamma_\mu q)$	$\mathcal{O}_{l^2q^2D^2}^{(1)}$	$D^\nu\,(\bar{l}\gamma^\mu l)\,D_\nu\,(\bar{q}\gamma_\mu q)$
$\mathcal{O}_{lq}^{(3)}$	$(\bar{l}\gamma^\mu\tau^i l)\,(\bar{q}\gamma_\mu\tau^i q)$	$\mathcal{O}_{l^2q^2D^2}^{(3)}$	$D^\nu\,(\bar{l}\gamma^\mu\tau^i l)\,D_\nu\,(\bar{q}\gamma_\mu\tau^i q)$
$\mathcal{O}_{eu}$	$(\bar{e}\gamma^\mu e)\,(\bar{u}\gamma_\mu u)$	$\mathcal{O}_{e^2u^2D^2}^{(1)}$	$D^\nu\,(\bar{e}\gamma^\mu e)\,D_\nu\,(\bar{u}\gamma_\mu u)$
$\mathcal{O}_{ed}$	$(\bar{e}\gamma^\mu e)\,(\bar{d}\gamma_\mu d)$	$\mathcal{O}_{e^2d^2D^2}^{(1)}$	$D^\nu\,(\bar{e}\gamma^\mu e)\,D_\nu\,(\bar{d}\gamma_\mu d)$
$\mathcal{O}_{lu}$	$(\bar{l}\gamma^\mu l)\,(\bar{u}\gamma_\mu u)$	$\mathcal{O}_{l^2u^2D^2}^{(1)}$	$D^\nu\,(\bar{l}\gamma^\mu l)\,D_\nu\,(\bar{u}\gamma_\mu u)$
$\mathcal{O}_{ld}$	$(\bar{l}\gamma^\mu l)\,(\bar{d}\gamma_\mu d)$	$\mathcal{O}_{l^2d^2D^2}^{(1)}$	$D^\nu\,(\bar{l}\gamma^\mu l)\,D_\nu\,(\bar{d}\gamma_\mu d)$
$\mathcal{O}_{qe}$	$(\bar{q}\gamma^\mu q)\,(\bar{e}\gamma_\mu e)$	$\mathcal{O}_{q^2e^2D^2}^{(1)}$	$D^\nu\,(\bar{q}\gamma^\mu q)\,D_\nu\,(\bar{e}\gamma_\mu e)$

Parity-violating experiments typically organize studies in terms of vector and axial couplings:

$$\mathcal{L}_{PV} = \frac{G_F}{\sqrt{2}}\Big[C_{1u}^6(\bar{e}\gamma^\mu\gamma_5 e)(\bar{u}\gamma_\mu u) + C_{2u}^6(\bar{e}\gamma^\mu e)(\bar{u}\gamma_\mu\gamma_5 u) + \frac{C_{1u}^8}{v^2}D^\nu(\bar{e}\gamma^\mu\gamma_5 e)D_\nu(\bar{u}\gamma_\mu u) + \frac{C_{2u}^8}{v^2}D^\nu(\bar{e}\gamma^\mu e)D_\nu(\bar{u}\gamma_\mu\gamma_5 u) + \ldots\Big]$$

It is simple to derive a linear transformation between this and the usual SMEFT basis.

Synergy between low and high energy experiments

- Future low-energy parity violating measurements will play an important role in global fits of the SMEFT parameter space.

P2: proposed low energy experiment in Mainz. Elastic electron scattering off hydrogen and carbon targets (1802.04759)

Note the elongated LHC ellipse; degeneracy in the structure of the DY cross section leads to this, and it occurs in the high m_{ll} bins where the BSM effects would be largest

Question #2 addressed: dimension-8 effects can be very important at the LHC; low-energy probes will play a critical role in disentangling them in the future program

RB, Petriello, Wiegand (2021)

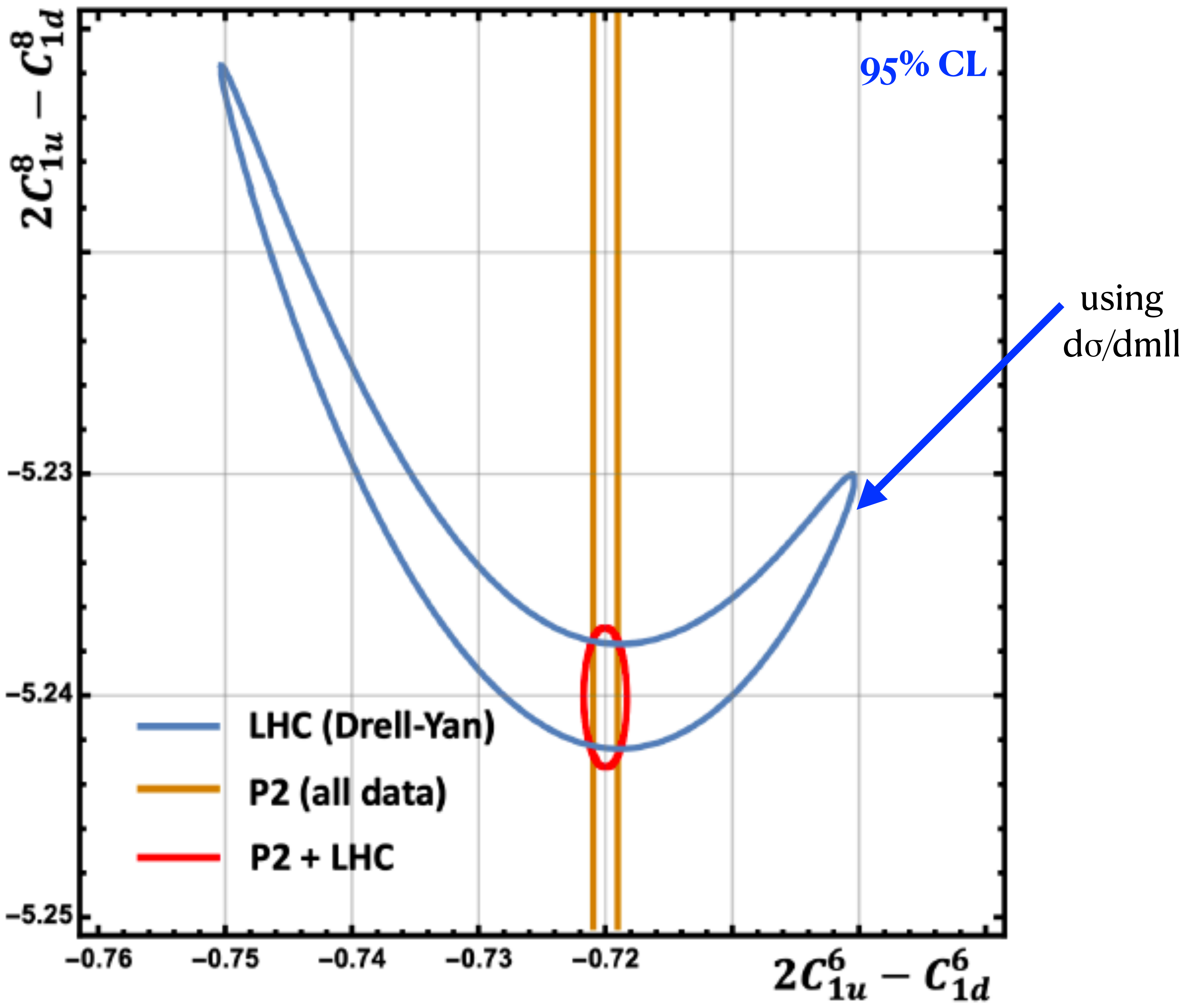

(Near) Future collider experiments

- There will be other experiments turning on within the coming decade. The Electron-Ion Collider (EIC) at BNL will be the first high-energy DIS experiment with the ability to polarize both electron and proton beams, opening a new window onto QCD.

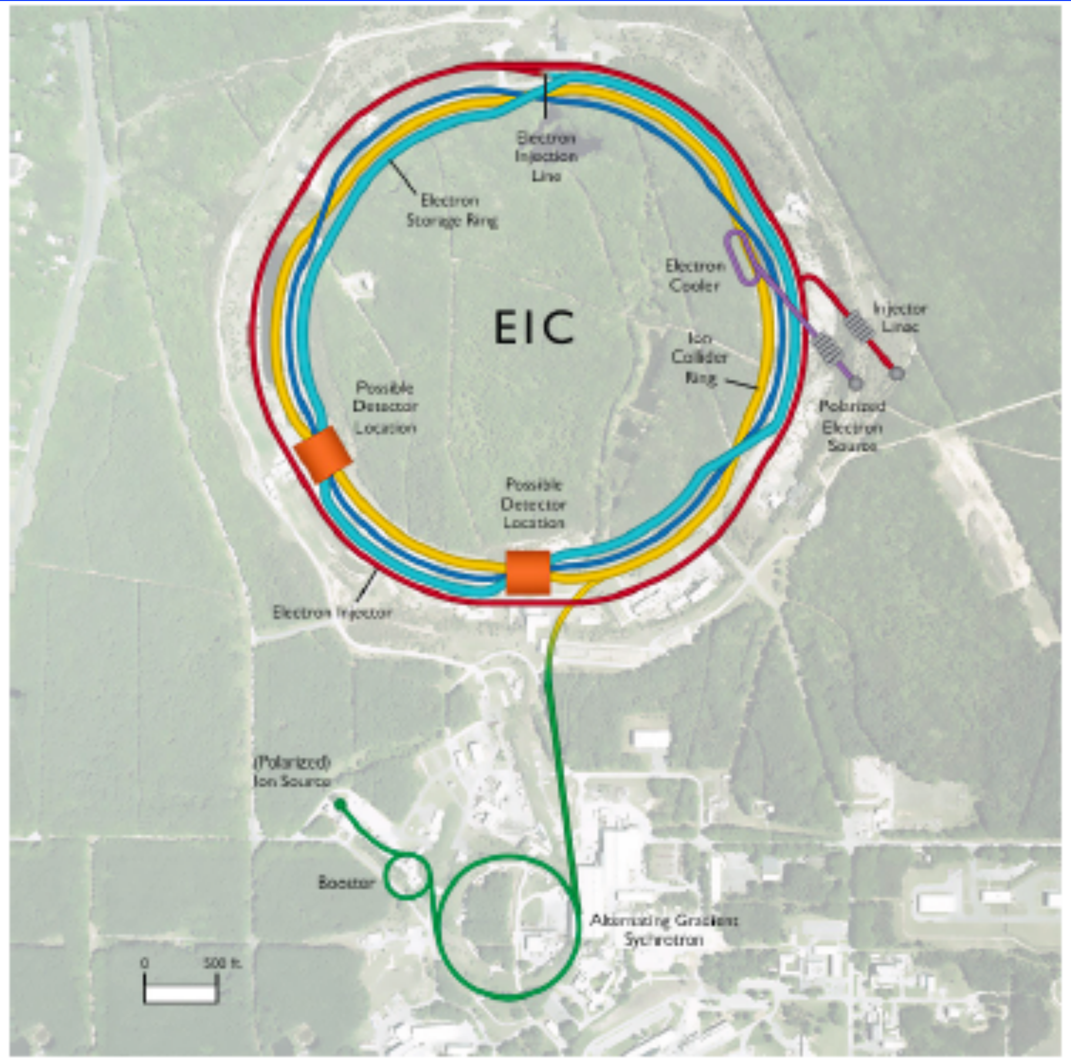

https://www.bnl.gov/eic/

Expected run parameters:

- $\sqrt{s}$~140 GeV
- 70% polarized proton/electron beams
- Luminosity: ≥10 fb^{-1}

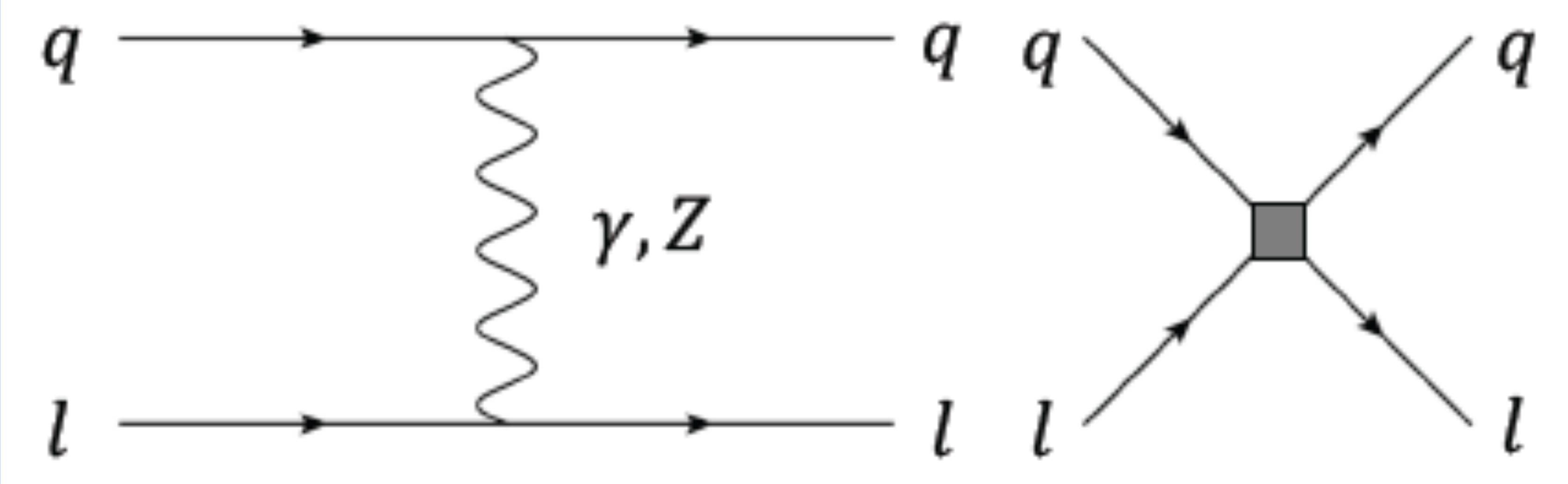

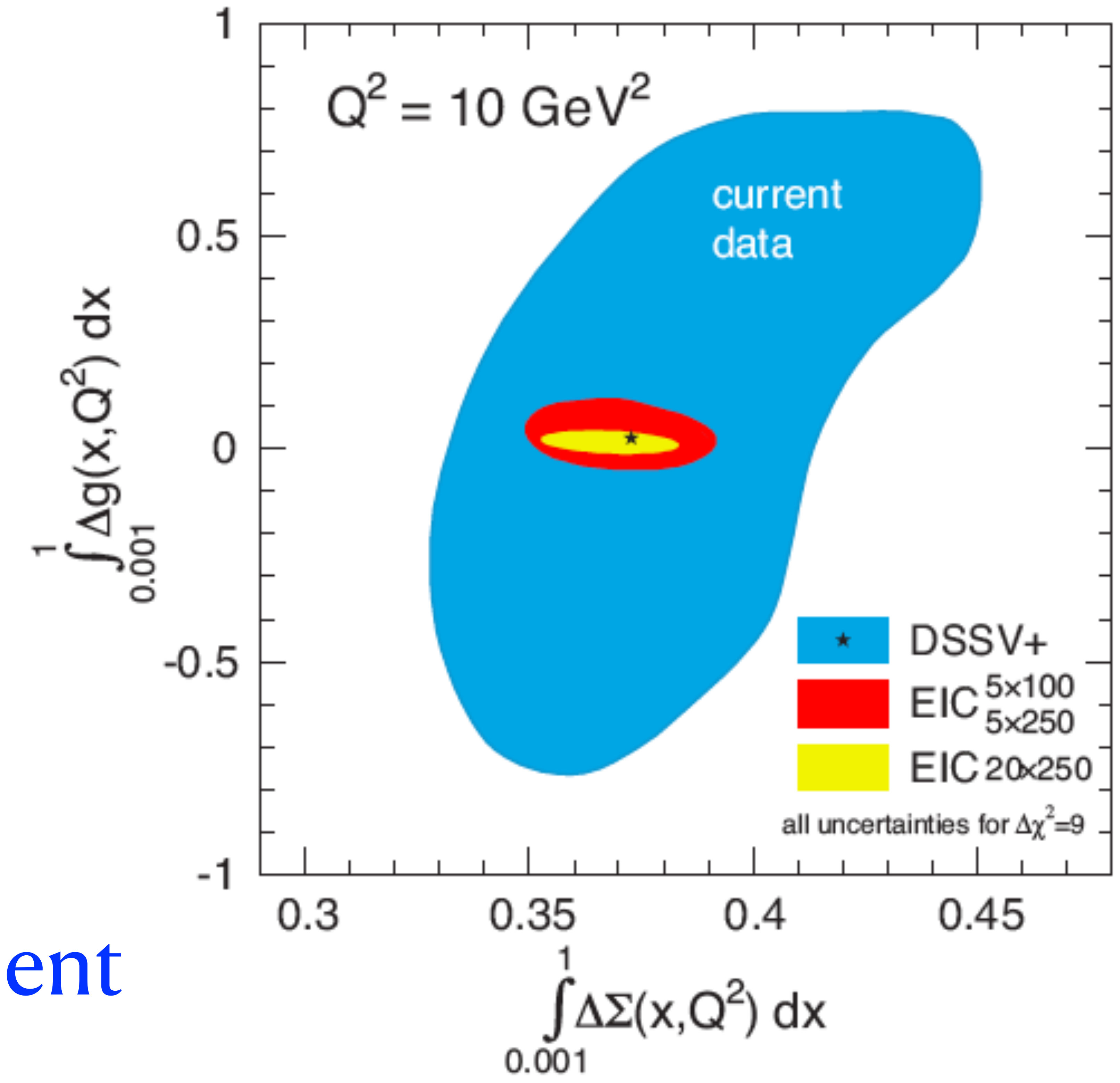

The EIC will provide our first precision measurement of the gluons contribution to the proton spin

(Near) Future collider experiments

- There will be other experiments turning on within the coming decade. The Electron-Ion Collider (EIC) at BNL will be the first high-energy DIS experiment with the ability to polarize both electron and proton beams, opening a new window onto QCD.

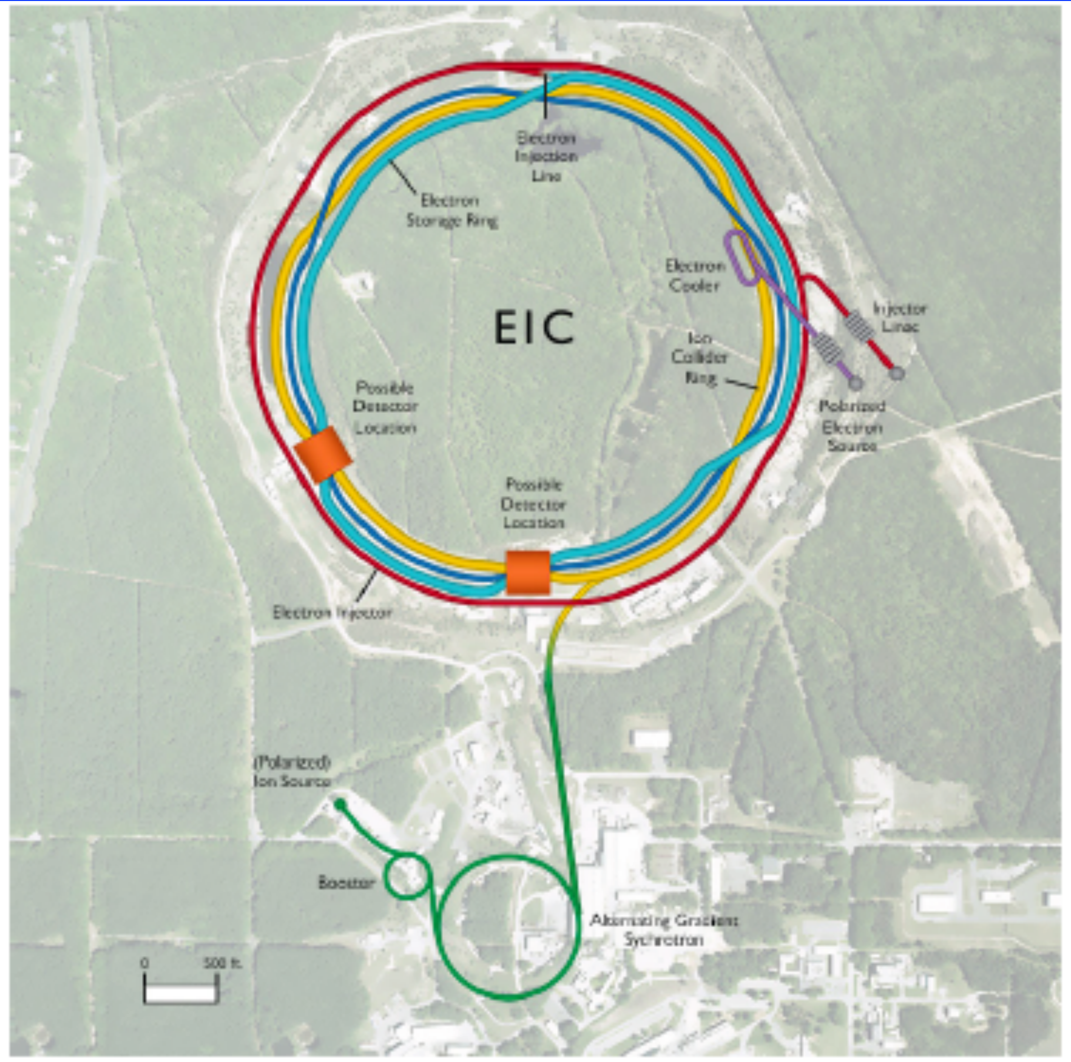

https://www.bnl.gov/eic/

- $\sqrt{s}$~140 GeV
- 70% polarized proton/electron beams
- Luminosity: ≥10 fb^{-1}

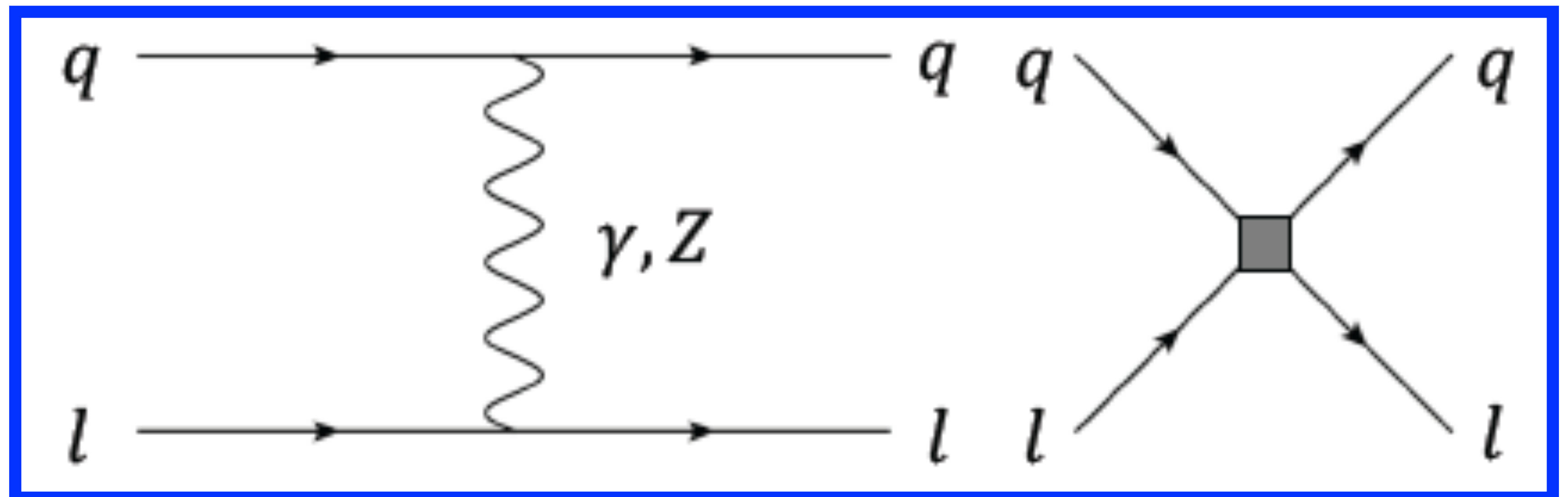

$$\frac{d^2\sigma_u^{\gamma SMEFT}}{dx dQ^2} = -x\frac{Q_u Q^2}{8\pi\alpha}\Big[C_{eu}(1+\lambda_u)(1+\lambda_e) + (C_{lq}^{(1)} - C_{lq}^{(3)})(1-\lambda_u)(1-\lambda_e) + (1-y)^2 C_{lu}(1+\lambda_u)(1-\lambda_e) + (1-y)^2 C_{qe}(1-\lambda_u)(1+\lambda_e)\Big]$$

The ability to polarize both beams opens up new probes of BSM physics complementary to the LHC

(Near) Future collider experiments

- The EIC adds another data set that can remove flat directions that appear when a limited number of data sets are studied, and is complementary to the LHC

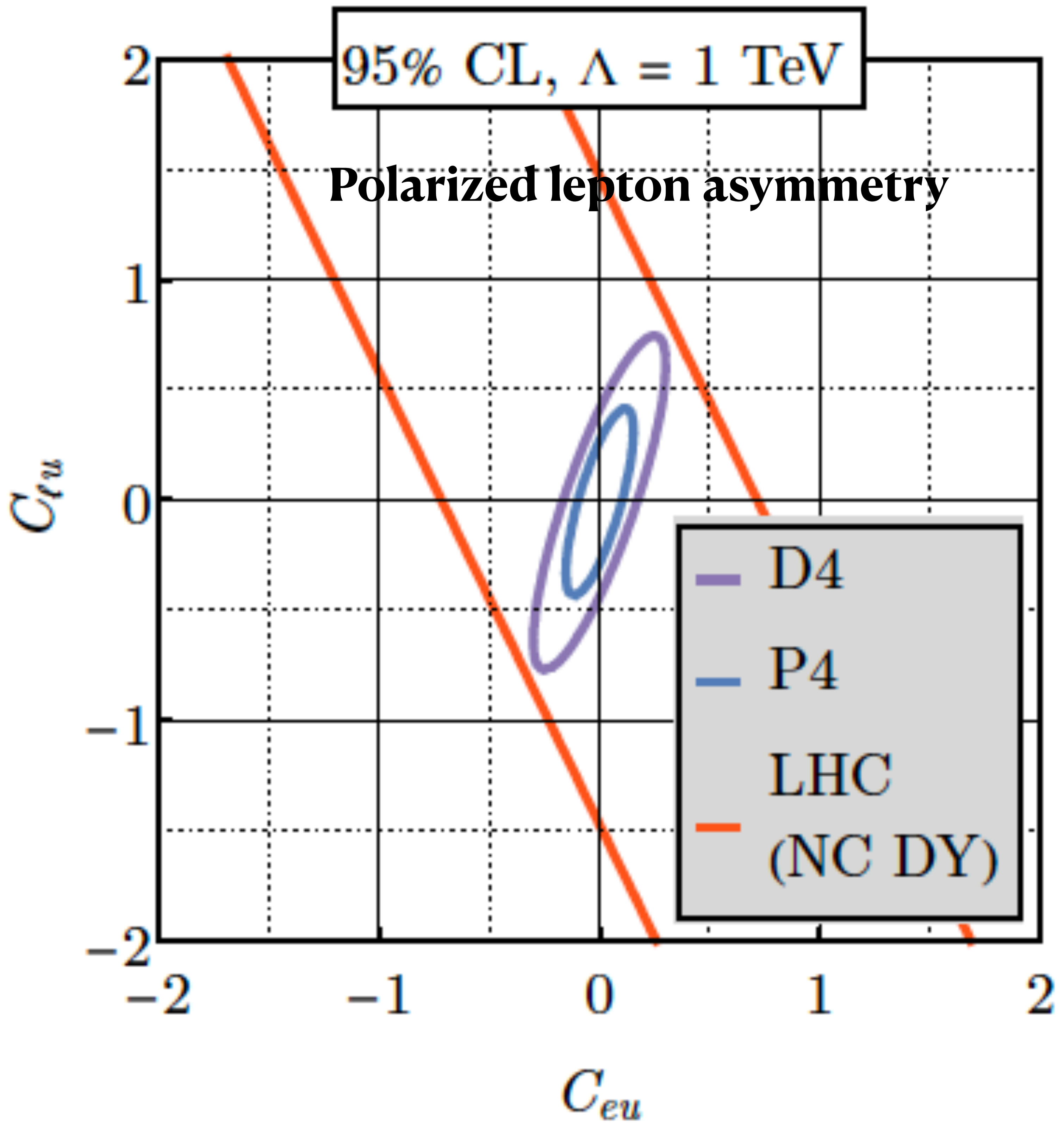

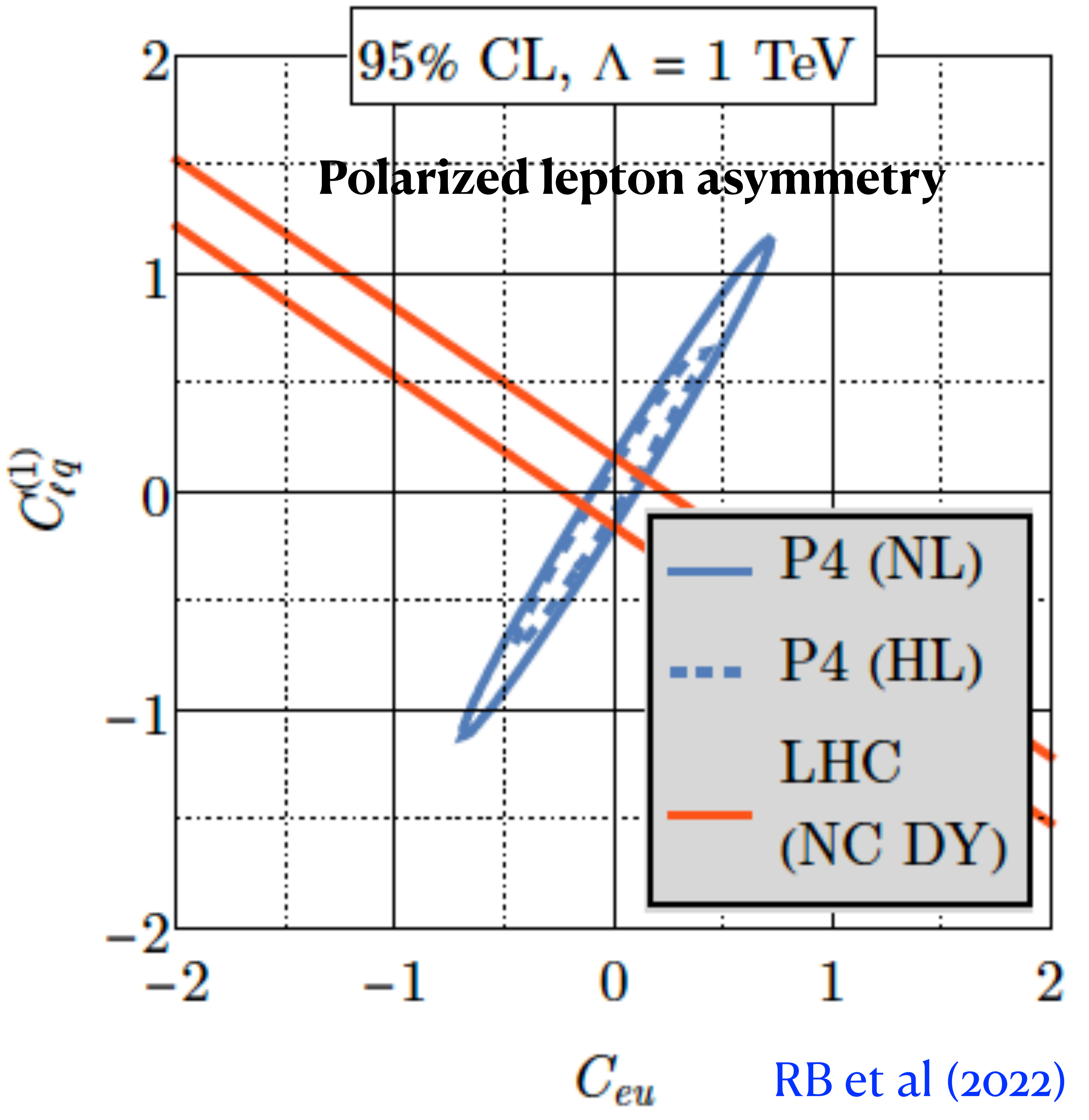

RB et al (2022)

D4: simulated EIC deuteron data

P4: simulated EIC proton data

LHC: invariant mass data only

NL/HL: nominal/high luminosity EIC data

Probes different combinations of Wilson coefficients than the LHC; TeV-scale probes competitive with LHC bounds

Future collider experiments

- Can do even better at a future FCC-eh machine! A fit of the full 17-dimensional parameter space reveals a significant improvement in probes of Z-vertex operators beyond EW precision observables, and a reach approaching 9 TeV in the effective UV scale.

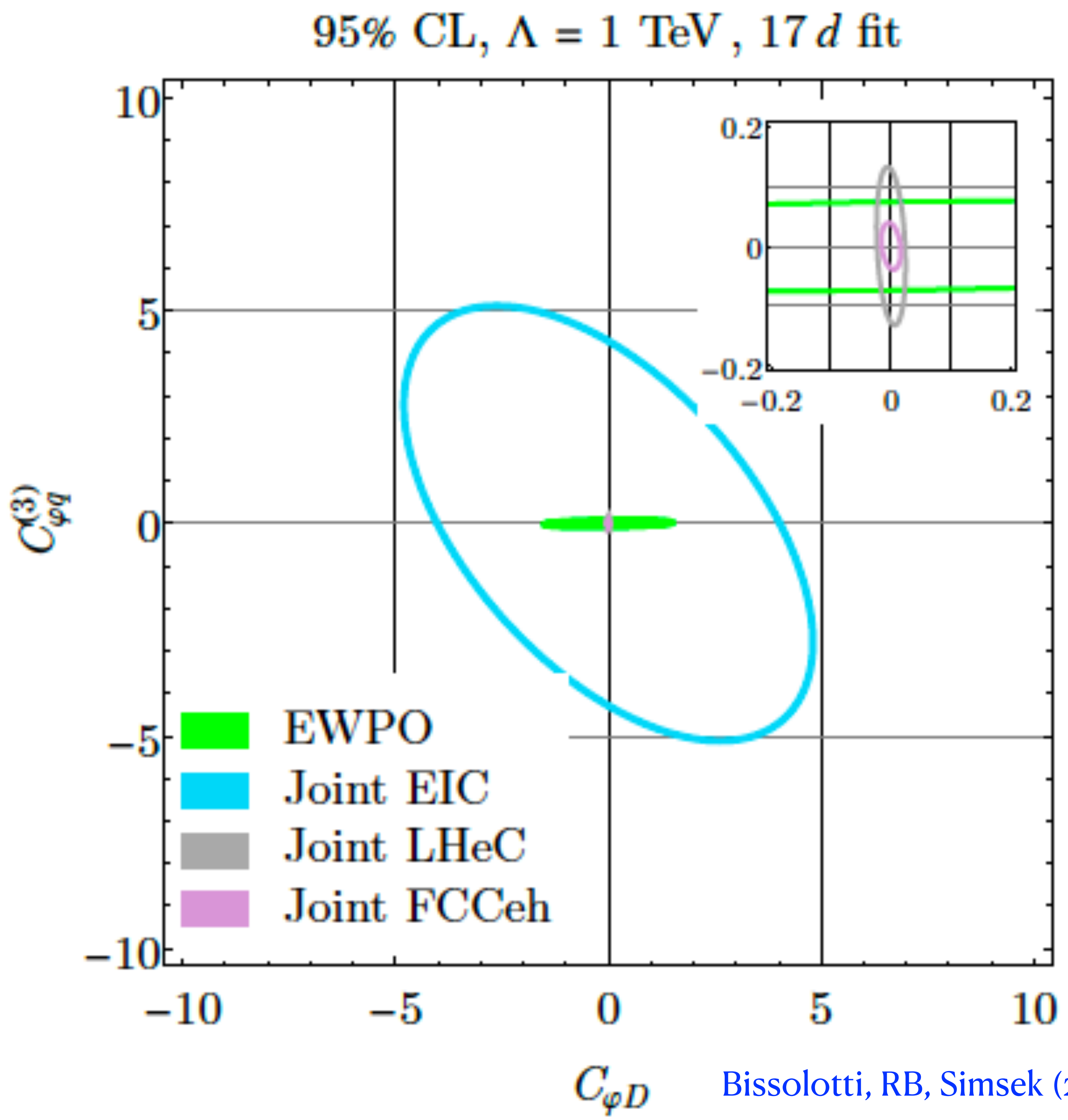

Bissolotti, RB, Simsek (2023)

- The 17-dimensional parameters include all the four fermion operators and vertex corrections to DIS
- NLO QCD corrections also included in this analysis
- The fit is marginalized over the Wilson coefficients not shown
- Both LHeC and FCCeh improve significantly upon EW precision observables constraints.

Transverse spin asymmetries

- New colliders offer new measurement possibilities with new sensitivity to BSM physics. One example of this is the possibility of transverse beam polarization at a future EIC.

Transverse spin asymmetries are defined as the difference of cross sections for positive and negative polarization of a single beam, transverse to the beam direction. In the case of the electron being polarized we have:

$$\boxed{A_{TU} = \frac{\sigma(e^{\uparrow}) - \sigma(e^{\downarrow})}{\sigma(e^{\uparrow}) + \sigma(e^{\downarrow})}}$$

Two mechanisms for producing this asymmetry in the SM: two-photon exchange at the loop level and tree level Z-boson exchange

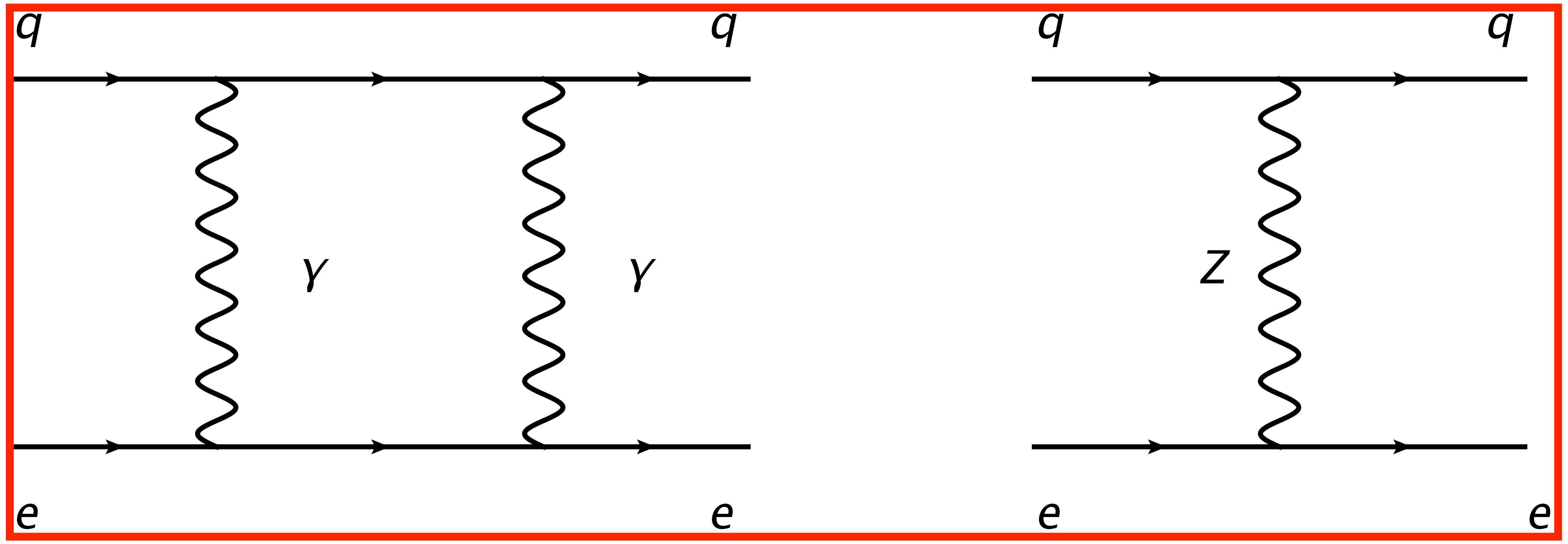

Transverse spin asymmetries

- New colliders offer new measurement possibilities with new sensitivity to BSM physics. One example of this is the possibility of transverse beam polarization at a future EIC.

Transverse spin asymmetries are defined as the difference of cross sections for positive and negative polarization of a single beam, transverse to the beam direction. In the case of the electron being polarized we have:

$$\boxed{A_{TU} = \frac{\sigma(e^{\uparrow}) - \sigma(e^{\downarrow})}{\sigma(e^{\uparrow}) + \sigma(e^{\downarrow})}}$$

Transverse polarization direction:

$$S_T^{\mu} = (0, \cos(\phi), \sin(\phi), 0)$$

$$\boxed{A_{TU}^{\gamma\gamma} = \alpha \frac{m_l}{2Q} \sin(\phi) \frac{y^2\sqrt{1-y}}{1-y+y^2/2} \frac{\sum_q Q_q^3 f_q(x)}{\sum_q Q_q^2 f_q(x)}}$$

Doubly-suppressed by two small quantities

Depends on the transverse-plane azimuthal angle between the initial state lepton polarization and the final-state lepton direction

Transverse spin asymmetries

- New colliders offer new measurement possibilities with new sensitive to BSM physics. One example of this is the possibility of transverse beam polarization at a future EIC.

Transverse spin asymmetries are defined as the difference of cross sections for positive and negative polarization of a single beam, transverse to the beam direction. In the case of the electron being polarized we have:

$$\boxed{A_{TU} = \frac{\sigma(e^{\uparrow}) - \sigma(e^{\downarrow})}{\sigma(e^{\uparrow}) + \sigma(e^{\downarrow})}}$$

Transverse polarization direction:

$$S_T^{\mu} = (0, \cos(\phi), \sin(\phi), 0)$$

RB, de Florian, Petriello, Vogelsang (2023)

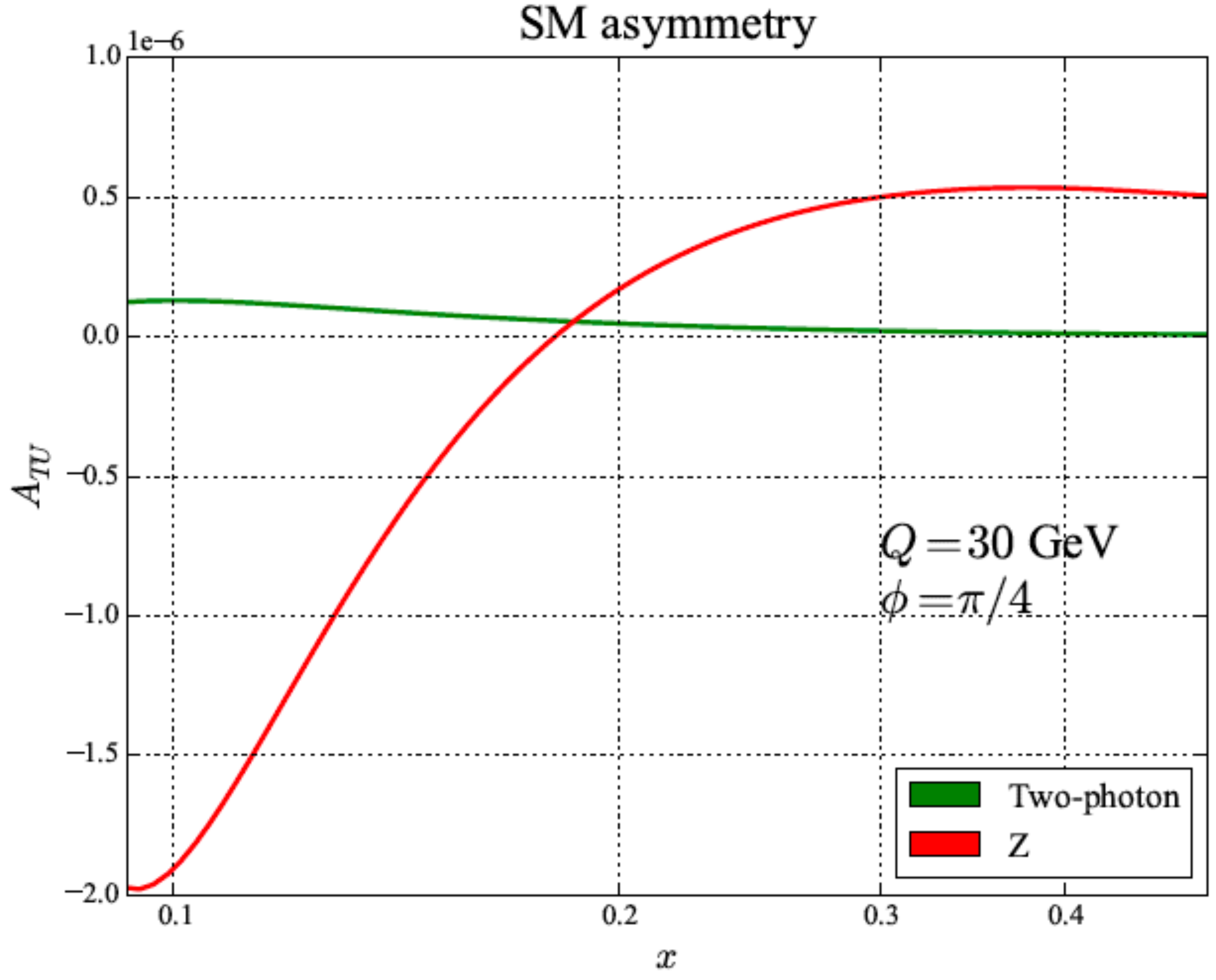

A_{TU}~10^{-6} in the SM; negligibly small and an excellent channel for new physics searches!

Another probe of g-2 new physics

- What kind of new physics can modify the transverse SSAs? We will discuss this in the context of the SMEFT. We will look for SMEFT operators that do not give an explicit lepton mass suppression.

$$\Delta A_{TU}(\phi) = \frac{g_Z}{2\pi\alpha}\frac{Q^3}{M_Z^2}\frac{y\sqrt{1-y}}{1-y+\frac{y^2}{2}}\frac{\sum_q Q_q f_q(x)\left\{g_{aq}\mathrm{Re}[C_{eZ}e^{-i\phi}] - \frac{\mathrm{Re}[C_{e\gamma}e^{-i\phi}]}{s_W c_W}[g_{vq}g_{al}(1-2/y) - g_{aq}g_{vl}]\right\}}{\sum_q Q_q^2 f_q(x)}$$

This asymmetry is sensitive to both the real and imaginary parts of the Wilson coefficients. The real part has a cos(ϕ) dependence and also gives an anomalous magnetic moment contribution, while the imaginary part has sin(ϕ) and also leads to an electric dipole moment.

$$C_{e\gamma} = \frac{v}{\sqrt{2}}[-s_W C_{eW} + c_W C_{eB}]$$
$$C_{eZ} = \frac{v}{\sqrt{2}}[-c_W C_{eW} - s_W C_{eB}]$$

Dipole operators

$$\begin{aligned}
\mathcal{O}_{eW} &= (\bar{l}\sigma^{\mu\nu}e)\tau^I\varphi W^I_{\mu\nu},\\
\mathcal{O}_{eB} &= (\bar{l}\sigma^{\mu\nu}e)\varphi B_{\mu\nu},\\
\mathcal{O}_{uW} &= (\bar{q}\sigma^{\mu\nu}u)\tau^I\varphi W^I_{\mu\nu},\\
\mathcal{O}_{uB} &= (\bar{q}\sigma^{\mu\nu}u)\varphi B_{\mu\nu},\\
\mathcal{O}_{dW} &= (\bar{q}\sigma^{\mu\nu}d)\tau^I\varphi W^I_{\mu\nu},\\
\mathcal{O}_{dB} &= (\bar{q}\sigma^{\mu\nu}d)\varphi B_{\mu\nu}.
\end{aligned}$$

Explicit calculation shows that only dipole operators contribute.

Sensitive to the operators that govern anomalous magnetic and electron dipole moments; can probe them separately; small SM background: an ideal new physics probe!

Numerics at an EIC

- The asymmetries range from 10^{-4} to 10^{-3} for moderate-to-high values of momentum transfers at an EIC, for TeV-scale new physics. The magnitudes for imaginary Wilson coefficients are similar. Our estimates indicate that the EIC can probe TeV-scale new physics affecting dipole operators.

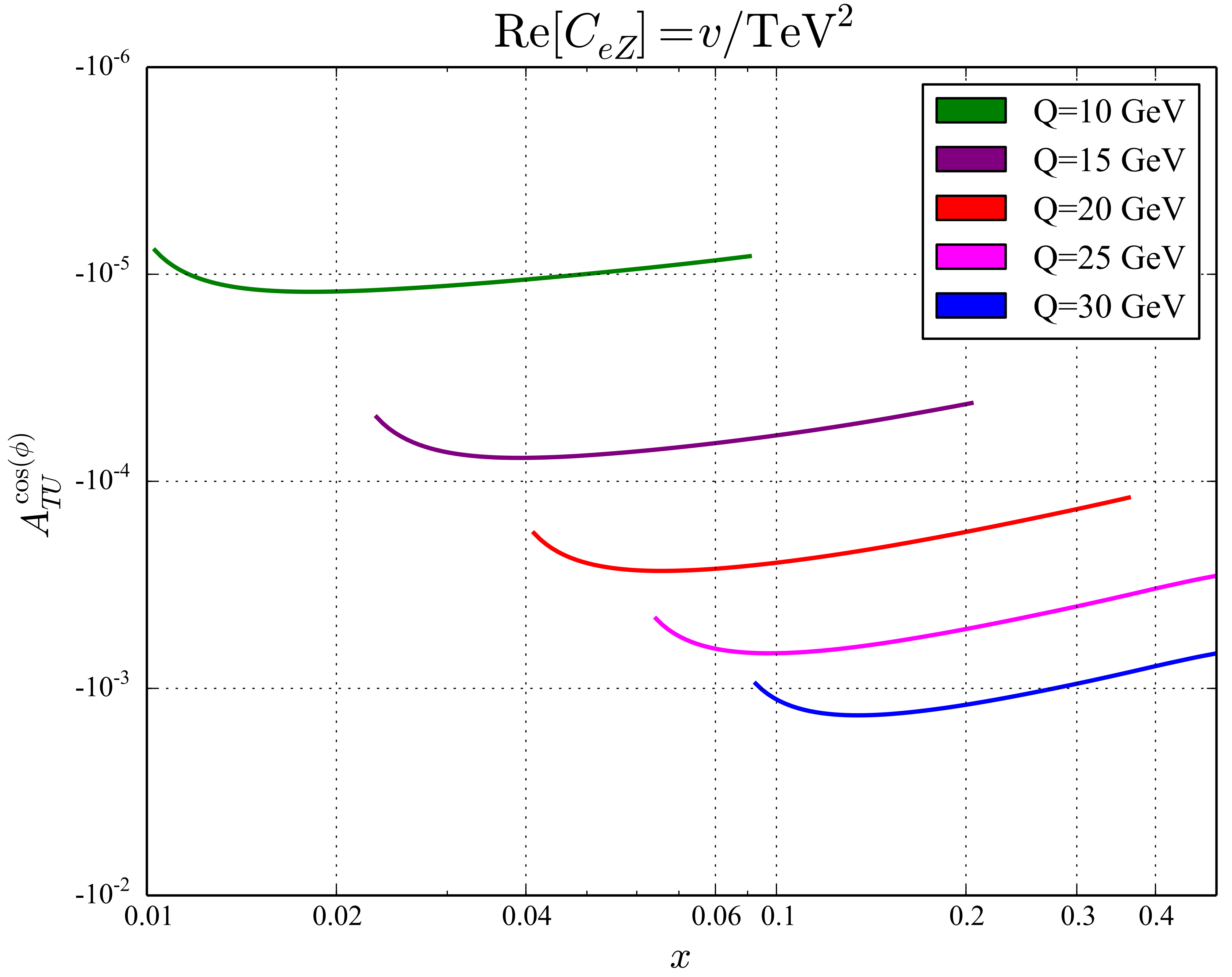

RB, de Florian, Petriello, Vogelsang (2023)

New physics contributions to the electron g-2 take the form:

Aebischer et al (2021)

$$\boxed{(\Delta a_e)^{SMEFT} = \frac{m_e}{m_\mu}\left\{1.4\times 10^{-3} C_{e\gamma} - 1.3\times 10^{-5} C_{eZ}\right\}(250\,\mathrm{GeV})}$$

Assuming C_{ei}=vev/ Λ_{ei}^2, $\Lambda_{e\gamma}$ scales below O(100 TeV) are ruled out; few-TeV Λ_{eZ} scales are allowed

Transverse SSAs at the EIC can probe competitive C_{eZ} scales with the electron g-2

A muon-ion collider

- A proposed upgrade of the EIC involves replacing the electron beam with a high-energy muon beam. This would provide the first step toward a high-energy muon-muon collider. Beam polarization reaching 50% is possible at such a machine (Acosta, Li 2021).

Machine parameters:

- 960 GeV muons x 275 GeV protons, for a CM energy around 1 TeV
- Assume 50% polarization, 50 fb^{-1} of integrated luminosity

Large asymmetries; scales of several TeV should be accessible at a muon-ion collider. We can probe the operators that lead to the muon g-2!

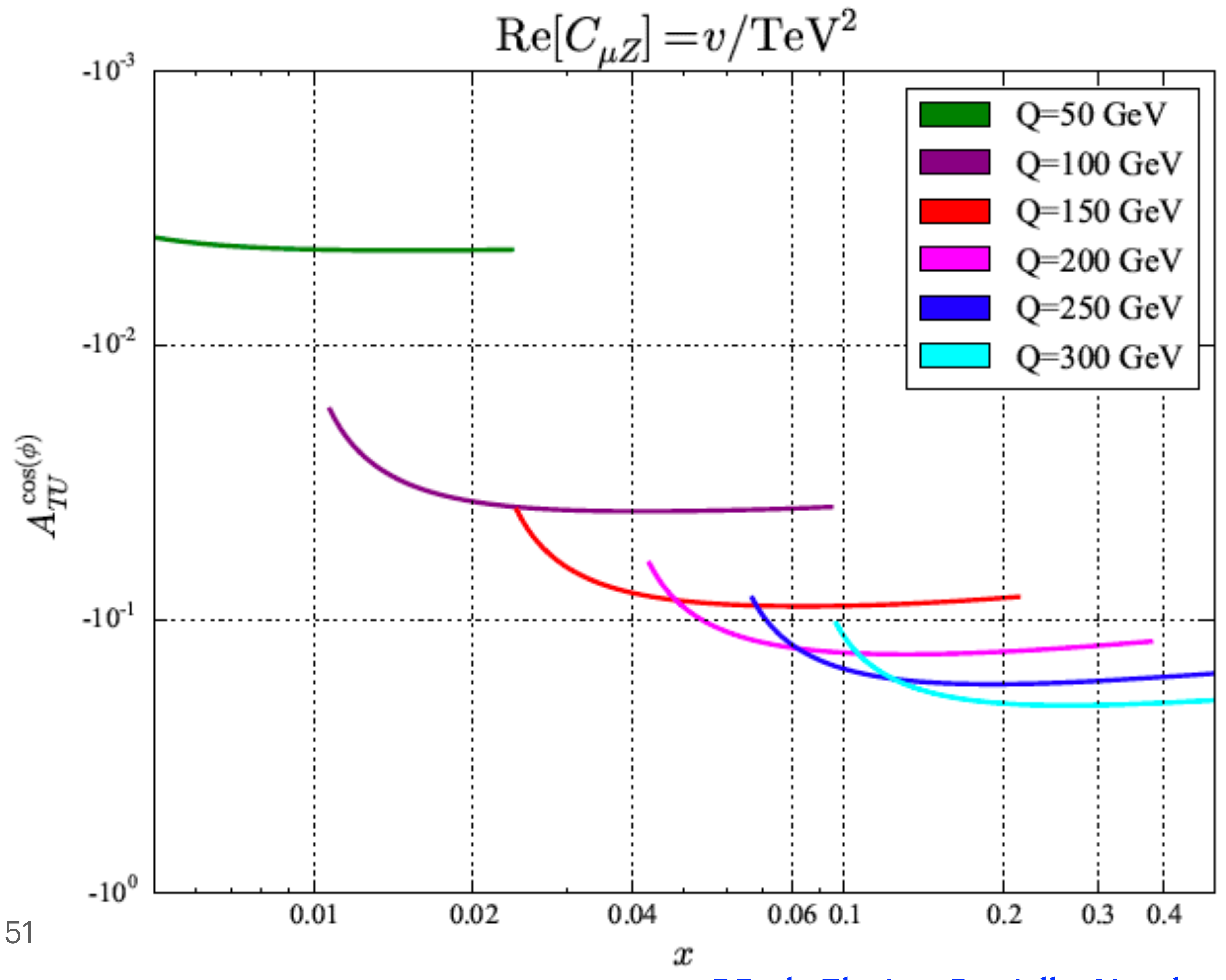

RB, de Florian, Petriello, Vogelsang (2023)

A muon-ion collider

- A proposed upgrade of the EIC involves replacing the electron beam with a high-energy muon beam. This would provide the first step toward a high-energy muon-muon collider. Beam polarization reaching 50% are possible at such a machine (Acosta, Li 2021).

Aebischer et al (2021)

$$\Delta a_\mu^{SMEFT} = 1.1 \times 10^{-3} \left(\frac{\mathrm{Re}[C_{\mu\gamma}]}{1\,\mathrm{TeV}^{-1}}\right) - 1.1 \times 10^{-5} \left(\frac{\mathrm{Re}[C_{\mu Z}]}{1\,\mathrm{TeV}^{-1}}\right)$$

Experiment-theory difference:

$$\Delta a_\mu^{exp-SM} = 251(59) \times 10^{-11}$$

The muon g-2 discrepancy can be explained, for example, by TeV-scale new physics with $C_{\mu\gamma} \approx 0.01 C_{\mu Z}$, which is a loop-factor suppression. Such a scenario is testable at a muon-ion collider!

Question #3 addressed: Transverse SSAs at a muon-ion collider can probe the same parameter space as the muon g-2!

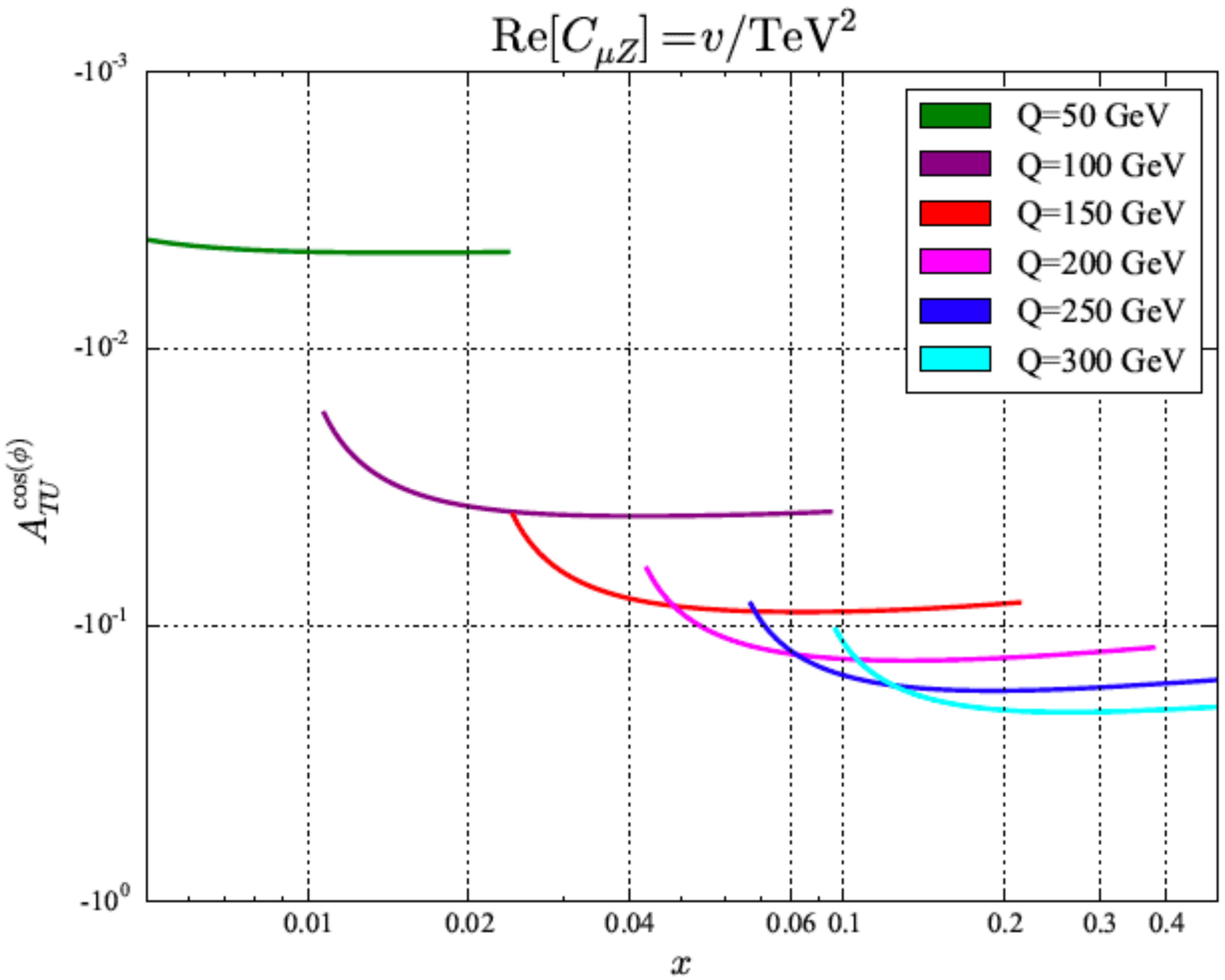

RB, de Florian, Petriello, Vogelsang (2023)

Conclusions

The precision study of QCD has had a profound impact on our understanding of Nature. The lessons we have learned over the decades continue to guide us as we continue our search for the new Standard Model.

May the next 50 years be as successful as the previous ones!